

DISS. ETH No. 20857

**ONLINE CONTROL DEVELOPMENT AND PROCESS
INTENSIFICATION IN CONTINUOUS
CHROMATOGRAPHY (MCSGP)**

A dissertation submitted to
ETH Zurich

For the degree of
Doctor of Sciences

Presented by
MARTIN KRÄTTLI

MSc ETH Chem Bio Eng
ETH Zürich

Born the
20th of April, 1985

Citizen of Untervaz, Graubünden, Switzerland

Accepted on the recommendation of

Prof Dr Massimo Morbidelli (ETH Zurich), examiner
Prof Dr Marco Mazzotti (ETH Zurich), co-examiner

2012

Acknowledgement

This thesis was made possible only through the support of many people and institutions which I would like to thank at this position.

I would like to thank Prof Morbidelli who gave me the opportunity to work on this project in his group. It was a pleasure to work under his supervision and he supported me in finding my way through the PhD, in professional and personal manners. I would also like to thank Prof Mazzotti for taking over the position of the co-examiner.

I am grateful to Guido Ströhlein and Thomas Müller-Späth who supervised me during my work and supported me with fruitful discussions. You helped me a lot by showing me your experience to make the start as a PhD student easier.

I would like to thank my Master students Daniel Baur and Fabian Steinebach and my research project students Patricia Jacomet and Amulya Tata who all contributed significantly to my success. Without your work my thesis would have never reached that scientific level and it was a pleasure for me to work with you.

I would like to thank the Swiss Committee for Technology and Innovation (KTI) and the European Union FW 7 project OPTICO which both funded this work.

I spend a wonderful time in the Morbidelli group; I would like to thank all the group members for that, in particular David Gétaz, Bertrand Guélat, Bertrand de Neuville, Marija Sarenac, Fabio Codari, Bastian Brand and Marco Furlan.

I thank my parents and my siblings who always supported me during all my periods of life.

Thank you, Cécile, for being there all day when I come home and never moving away from my side.

Zusammenfassung

Der Mehrkolonnen-Gegenstrom-Lösungsmittel Gradienten Reinigungsprozess (englische Abkürzung MCSGP) wird in dieser Arbeit weiter untersucht. Der Prozess wurde vor einigen Jahren von Aumann und Morbidelli [1] erstmals erwähnt, die Weiterentwicklung des Prozesses dauert noch an. In dieser Arbeit wurde der MCSGP Prozess für zwei schwierige Trennprobleme eingesetzt, namentlich eine Trennung von Ladungsvarianten von monoklonalen Antikörpern (englische Abkürzung: mAb) und die Aufreinigung von seltenen Erden (englische Abkürzung: REE). Die Ladungsvarianten der drei mAbs Avastin®, Herceptin® und Erbitux® wurden aufgetrennt. Der Fall Herceptin® muss hervorgehoben werden, da für diesen Antikörper die Bio Aktivität der einzelnen Varianten bekannt ist [2], weshalb die spezifische Aktivität eines aufgereinigten Produktes bestimmt werden konnte. Bei allen drei mAbs wurde erfolgreich die Hauptvariante mit diskontinuierlicher Chromatographie und MCSGP angereichert, es wurde in beiden Fällen ein Kationen Tauscher als stationäre Phase verwendet. Die Produktivität konnte für die MCSGP im Gegensatz zur diskontinuierlichen Chromatographie vervierfacht werden. Die Bio Aktivität im Fall von Herceptin® konnte um 30% gesteigert werden. Zusätzlich wurde die Stabilität des MCSGP Prozesses mithilfe von modifiziertem Start-Material getestet, welches mehr Verunreinigungen enthielt. Das Produkt wurde dabei in seiner Qualität nicht signifikant beeinflusst.

Die Trennung von REE wird zu einem immer wichtigeren Problem, da der weltweite Bedarf an REE stetig wächst und gleichzeitig mehrere Produktionsstätten aufgrund von Umweltschäden und zu hohen Kosten geschlossen wurden [3]. Chromatographie war eine wichtige und oft verwendete Trennmethode für REEs, bis sie in den 70er Jahren durch Extraktion ersetzt wurde. Durch die Verwendung des MCSGP Prozesses könnte die Chromatographie wieder wirtschaftlich werden. Zusätzlich wären die umwelttechnischen Bedenken im Falle eines chromatographischen Reinigungsprozesses kleiner als bei Extraktion, was die Produktion von REEs in den westlichen Ländern wieder möglich machen könnte. In dieser Arbeit wurden drei Elemente der Lanthaniden Gruppe (Praesodymium, Cer und Lanthanum) in diskontinuierlicher Chromatographie und mit MCSGP getrennt. Die Trennung war in beiden Fällen erfolgreich, die Produktivität konnte durch den Einsatz von MCSGP um Faktor 5 bis 15 erhöht werden. Leider war die absolute Produktivität aufgrund der tiefen Löslichkeit der REEs in der mobilen Phase aber sehr klein. Um dieses Problem überwinden zu können, könnte eine andere mobile Phase verwendet werden, wie beispielsweise von Hansen und Koautoren vorgeschlagen wurde [4]. Dadurch könnte die Produktivität auf Werte um 1 Kilogramm pro Tag und Liter Kolonnenbett erhöht werden.

Das ursprüngliche Design des MCSGP Prozesses erlaubt eine Trennung in 3 Fraktionen, was für die meisten Prozesse ausreichend ist. In speziellen Fällen sind aber mehrere Substanzen im Gemisch wertvoll und sollten als reines Produkt gesammelt werden. In dieser Arbeit wird ein Aufbau der MCSGP diskutiert, der theoretisch n Fraktionen mit n Säulen auftrennen kann und das Prozess Design dieser Multifraktions MCSGP wird anhand zweier Beispiele erklärt. In den Experimenten wurde die Trennung auf 4 Fraktionen beschränkt, da sonst ein zu grosser Druckabfall über die Säulen entstand. Die

Validierung dieser MCSGP Variante wurde mit einem Protein Modell System und einer mAb Variantentrennung durchgeführt, in beiden Fällen konnte die Ausbeute mit dem MCSGP Prozess im Vergleich zu diskontinuierlicher Chromatographie bei gleicher Reinheit der Produkte gesteigert werden.

Der zyklisch verlaufende MCSGP Prozess kann problemlos für sehr lange Zeiträume in betrieb gehalten werden. Dafür wird ein Kontroll Konzept benötigt um den Prozess stabil zu halten. Zwei verschiedene Controller basierend auf dem empirischen Proportional, Integral und Differential (PID) Konzept wurden in den MCSGP Prozess integriert und getestet. Der erste Controller verwendet als Prozess Information das online gemessene UV Signal der MCSGP Anlage und regelt direkt die Position des Maximums des Signals. Diese sehr schnelle und einfache Kontroll Möglichkeit garantiert dass der Prozess konstant bleibt, kann aber nicht direkt die Reinheit des Produktes regeln, da diese nicht aus dem online UV entnommen werden kann. Entsprechend muss das Design des Prozesses vor dem Einschalten des Controllers von Hand gemacht werden. Der Prozess wurde mit einem Proteinsystem (Lysozym) und einem Peptid (Fibrinopeptide A human) validiert. Der Prozess wurde mit dem Kontroll System eingeschalten gestartet und es wurden Störungen in den Flussraten simuliert. Der Controller reagierte schnell und zuverlässig und konnte sämtliche Störfälle innert 3 – 5 Zyklen meistern. Im zweiten Kontroll Konzept wurde das einfache online UV durch eine automatische HPLC Analyse des Produkts ersetzt, welche direkte Rückschlüsse auf die Reinheit zulässt. Das Konzept basiert auf zwei entkoppelten PID Controllern, welche die beiden Verunreinigungen (Früher eluierend als das Produkt und später eluierend als das Produkt) unabhängig kontrollieren und den gewünschte Reinheitswert einstellen. Dieses Konzept wurde mit zwei Protein Systemen getestet, zum einen ein Modell System und zum anderen der Zellüberstand einer mAb Fermentation. Für beide Systeme wurden Störungen in den Pumpen Flussraten sowie Veränderungen des Grundmaterials künstlich eingeführt, der Controller konnte sämtliche Störungen meistern und kehrte zur gewünschten Reinheit des Produktes zurück.

Abstract

The multi-column countercurrent solvent gradient purification (MCSGP) process is studied in this work. The process was developed some years ago by Aumann and Morbidelli [1], some further process development is still going on. In this work, the process itself was applied for two challenging separation problems; a monoclonal antibody (mAb) charge variant separation and the purification of rare earth elements (REE). The charge variants of three mAbs were separated, namely Avastin®, Herceptin® and Eribix®. Especially Herceptin® should be mentioned, as the bio activity of the charge variants was measured for this mAb in the past [2]. Therefore, the benefit of removing inactive variants could be quantified. All three mAb separations were performed successfully in cation exchange batch chromatography and MCSGP, with MCSGP having an up to 4 fold higher productivity. The activity of the mAb Herceptin® could be increased by 30% in comparison to the original mixture which is available as a therapeutic. Additionally, the stability of the MCSGP process was verified applying feed which was enriched in impurities. It was found that the feed composition was not influencing the product quality significantly.

The separation of REE is becoming an increasingly important challenge, as the demand of REE is increasing worldwide and several production sides have been closed due to environmental concerns and too high costs [3]. In the past, chromatography was an often applied tool for the purification of REE, but was replaced by extraction in the last 40 years. Implementing a continuous chromatographic process as the MCSGP providing higher productivity than batch chromatography the purification of REE based on chromatography could become economically interesting again. In addition, the chromatographic steps could significantly lower the environmental concerns due to milder conditions and thereby reinstate the production of REE in western countries. In this work, three REE species were separated (Praseodymium, Cerium and Lanthanum) applying batch and MCSGP chromatography. The MCSGP process could outperform the batch significantly, improving the productivity by factor 5 to 15. However, the cation exchange chromatography only reached moderate absolute productivities, as the solubility of the REE in the mobile phase was very low. To overcome this problem, a different mobile phase would have to be applied as proposed recently by Hansen et al. [4]. The implementation of this mobile phase could increase the productivity of the MCSGP process to the order of kilograms per day and liter of resin.

MCSGP in its original setup is able to separate three fractions, which is sufficient for most encountered problems. In rare cases where multiple products in a mixture are valuable, the separation of more than three fractions would be beneficial. In this work, the theoretical design of a MCSGP capable of separating n fractions and its design starting from batch chromatography is discussed. In theory, applying a MCSGP process with n columns can separate n fractions as well, in experimental application; the maximum number of fractions was limited to 4 due to pressure drop issues. The four fraction separation was validated applying a model mixture of four proteins and a mAb charge variant separation. In both cases, the yield could be increased applying MCSGP keeping the purity at the same level.

The MCSGP process, which is running on a cyclic base continuously for long time periods, requires an online control concept to stabilize the process. Two different control concepts based on empirical proportional, integral, differential (PID) control were introduced in the frame of this work. The first controller was based on the MCSGP online UV as the feedback information. The goal of the controller is to keep the maximum of the online UV chromatogram, which is normally referring to the product, at a certain position of the process. This method guarantees that the product outlet quality is remaining constant. The drawback of this very simple control concept is the missing information on the actual purity of the product. Therefore, the tuning of the MCSGP process has to be performed offline, the controller is just assisting in keeping the process stable. The controller was validated experimentally applying a protein system (Lysozyme) and a peptide (Fibrinopeptide A human). The process startup was guided to steady state and during steady state operation; various disturbances in the flow rates of system pumps were introduced. The controller was reacting reliable and fast, restoring the product quality within 3 - 5 cycles guaranteeing stable operation. In the second control concept, the feedback was replaced with an at-line HPLC analysis of the product stream, allowing to directly controlling the purity. The control concept relied on two decoupled PID controller, one controlling the early eluting, and one controlling the late eluting impurities. The controller was tested with two protein systems, a model separation and a mAb supernatant capture. In both cases, a purity requirement similar to the purity reached with batch chromatography was set. The controller was able to guide the process from different starting points to this desired purity constraints and was able to reject disturbances in flow rates and the feed composition.

Contents

Acknowledgement	III
Zusammenfassung	IV
Abstract	VI
1. Introduction	1
1.1. Chromatographic separation	1
1.2. Countercurrent chromatography	2
1.3. PID control	4
2. Increasing the Activity of Monoclonal Antibody Therapeutics by Continuous Chromatography (MCSGP)	7
2.1. Introduction	7
2.1.1. mAb variants	7
2.1.2. Purification of mAb variants	8
2.2. Materials and methods	9
2.2.1. Monoclonal antibody products	9
2.2.2. Analytics	12
2.2.3. Stationary phases, buffers and hardware	12
2.2.4. Four- and three-column MCSGP process	14
2.2.5. Modeling	15
2.2.6. Performance parameter definition	16
2.3. Results and discussion	18
2.3.1. Operation of the batch gradient process	18
2.3.2. Operation of the MCSGP process	20
2.3.3. Comparison of mAb variant purifications in batch and MCSGP mode	22
2.3.4. Robustness to feed variations	24
2.3.5. Improvement of the bioactivity of Trastuzumab	26
2.4. Conclusion and outlook	28
2.5. Remark	29
3. Multifraction separation in Continuous Chromatography (MCSGP)	30
3.1. Introduction	30
3.2. The multi fraction MCSGP process	31
3.2.1. From three to four fraction MCSGP	31
3.2.2. From four to n- fraction MCSGP with $n > 4$	35
3.2.3. Design equations	36
3.3. Materials and methods	39
3.3.1. Protein model mixture	39

3.3.2.	Monoclonal antibody.....	41
3.3.3.	Stationary phases, buffers and hardware	42
3.4.	Results and discussion.....	44
3.4.1.	Purification of the protein model mixture.....	44
3.4.2.	Monoclonal antibody variant separation.....	47
3.5.	Conclusion	49
3.6.	Nomenclature	50
3.7.	Remark	50
4.	Repetitive Closed Loop Control of the Multi Column Solvent Gradient Purification ..	51
4.1.	Introduction	51
4.2.	Controller development.....	53
4.3.	Materials and Methods.....	55
4.3.1.	Materials.....	55
4.3.2.	Preparative batch and MCSGP experiments.....	55
4.3.3.	Analytics.....	57
4.3.4.	Controller.....	57
4.4.	Results and Discussion	58
4.4.1.	Purification of Lysozyme	58
4.4.2.	Purification of Fibrinopeptide A human	60
4.5.	Conclusions.....	67
4.6.	Remark	68
5.	Online Control for the Twin-Column Countercurrent Solvent Gradient Unit for Biochromatography	69
5.1.	Introduction	69
5.2.	Controller development.....	72
5.3.	Materials and Methods.....	74
5.3.1.	Modeling and Simulation	74
5.3.2.	Hardware setup	75
5.3.3.	Separation of a protein model mixture.....	75
5.3.4.	Monoclonal Antibody capture from supernatant.....	76
5.4.	Results and Discussion	79
5.4.1.	Closed loop experiments with the protein model mixture	79
5.4.2.	Closed loop experiments for a mAb capture process.....	82
5.5.	Conclusions	87
5.6.	Remark	87
6.	Separation of Lanthanides by Continuous Chromatography.....	88
6.1.	Introduction	88
6.2.	Materials and Methods.....	90
6.2.1.	REE samples and preparation.....	90

6.2.2.	Analytics	91
6.2.3.	Preparative batch separation and MCSGP	91
6.3.	Results and discussion	93
6.3.1.	Preparative batch operation.....	93
6.3.2.	MCSGP operation.....	95
6.3.3.	Comparing the performance of batch and continuous countercurrent (MCSGP) chromatography.....	97
6.4.	Conclusion.....	98
6.5.	Remark.....	98
7.	Concluding remarks	99
8.	Curriculum Vitae.....	101
9.	Figure and Table index	103
9.1.	Figures.....	103
9.2.	Tables	107
10.	References	109

1. Introduction

1.1. Chromatographic separation

Chromatography is a widely used technique for the purification of molecules, ranging from analytical applications up to process scale. The term chromatography comprises a number of distantly related processes, having in common an operating scheme based upon a two phase system [5]. The first phase is called the mobile phase, normally a liquid, gas or supercritical fluid which is flowing through the column. The application in preparative and process scale is limited to liquid and supercritical mobile phases [6-8]; gaseous ones are only applied in analytics. Secondly, a stationary phase or bed is present which build is from solid particles in most cases. In rarer cases, the stationary phase consists of only a single block of solid, e. g. a membrane [9] or a monolith [10, 11] or it might even be replaced by a liquid component [12]. The separation relies on specific interactions of the molecules to be separated with the stationary phase, in most cases; an adsorption mechanism is present, commonly hydrophilic or hydrophobic interactions and ion exchange interactions. Additionally, affinity interactions and pure size exclusion phenomena are exploited.

In typical preparative chromatography, the equilibrated column is first loaded with the feedstock containing the product (P) and impurities which are lumped in two fractions, the ones eluting before the product (called weakly adsorbing impurities, W) and the ones eluting after the product (called strongly adsorbing impurities, S). Following the loading, the column is washed under adsorbing conditions, eluting some flow through impurities and loading buffer components. Afterward, the elution is performed eluting W , P and S in this order. The elution is often performed applying a modifier gradient which is affecting the adsorptive behavior of W , P and S . After eluting all P , the remaining S can be step eluted and the column is cleaned in place (CIP) and equilibrated, ready for the next run. Figure 3.1 shows a typical schematically overview of such a generic chromatographic process.

Mathematical models can be applied to describe the chromatographic elution, a typical model available for the description of the elution is the lumped kinetics model [8]. The partial differential equation describing the behavior of all components in the column is derived from the material balances [13], lumping all non-convective transport phenomena in a dispersion term:

$$\frac{\partial c_i}{\partial t} + \frac{(1-\varepsilon_i)}{\varepsilon_i} \frac{\partial q_i}{\partial t} + \frac{Q_h^n}{A_{col} \varepsilon_i} \frac{\partial c_i}{\partial z} = D_{ax} \frac{\partial^2 c_i}{\partial z^2}, \quad z \in [0, L_{col}], \quad t \in [0, \infty] \quad 1.1$$

With c the concentration in the mobile phase, t the time, ε the total porosity, q the adsorbed concentration, Q_h^n the volumetric flow rate, A_{col} the column inner cross area, z the axial dimension of the column, D_{ax} the axial dispersion coefficient and i the components W , P , S and the modifier concentration. In this equation, the summed terms

from left to right indicate the time evolution of the concentration, the adsorptive interaction, the convective transport and the dispersion. For lumped kinetics, the adsorptive interaction is described as follows:

$$\frac{\partial q_i}{\partial t} = k_i (q_i^* - q_i) \quad 1.2$$

With q the adsorbed concentration, t the time, k the mass transfer coefficient and q^* the equilibrium adsorbing concentration. A typical isotherm describing the equilibrium adsorption behavior for most protein systems is the competitive Langmuir isotherm:

$$q_i^* = \frac{c_i H_i}{1 + \sum_{j=W,P,S} \frac{c_j H_j}{q_j^{sat}}} \quad 1.3$$

With q^* the equilibrium adsorptive concentration, c the corresponding mobile phase concentration, H the henry coefficient being a function of the modifier concentration and q^{sat} the saturation capacity of the stationary phase.

Some of the parameters in previous equations have to be known prior to solve them, namely the axial dispersion coefficient D_{ax} and mass transfer coefficient, k , which can be found through a van Deemter curve, the porosity, ε , and henry coefficient H which can be found from isocratic pulse injections and the saturation capacity q^{sat} which is found of through loading experiments. All these preliminary studies are described in textbooks [14, 15].

1.2. Countercurrent chromatography

Batch chromatography described above is the state of the art technique in most applications of chromatography, however, the productivity of batch chromatography is rather poor making chromatography a very expensive separation only applied if no other separation technique is available. The poor productivity of batch chromatography is partly caused by the yield purity trade-off which occurs when no baseline separation can be achieved. When collecting the product from such a batch elution, it has to be decided whether the overlapping regions are included in the product collecting, resulting in high yield but low purity, or have to be excluded resulting in high purity but low yield. This trade-off is resulting in a pareto front in a yield purity diagram, which cannot be overcome in batch chromatography [16].

A possible way to overcome this problem is countercurrent chromatography which summarizes a number of processes which share a movement of the stationary phase opposite to the mobile phase. The simplest way to explain the countercurrent movement can be shown in the scheme of Figure 1.1. The bed movement is shown as a band conveyor

moving with constant velocity from the right to the left. At a certain time, two animals, a cat and a turtle, are put on the middle section of the conveyor, both of them move towards the right. The cat's velocity is larger than the one of the conveyor, therefore it is finally jumping off the band on the right, while the turtle's speed is below the one of the conveyor resulting in a falloff of this animal on the left.

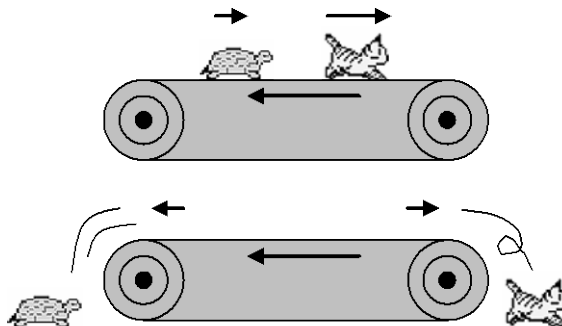


Figure 1.1 Concept study of countercurrent chromatography [16]

Translated to chemistry, the band conveyor becomes the stationary phase, the animals are the two components to be separated and their speed is influenced by the mobile phase movement from the left to the right and their adsorptive behavior. Additionally, a stream continuously feeding new material is required in the middle of the column. A schematic overview is given in Figure 1.2.

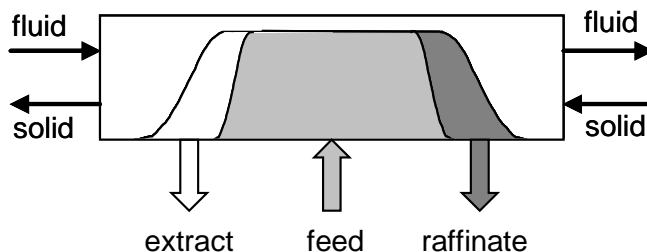


Figure 1.2 Schematic overview of a true moving bed (TMB) chromatography process. Showing the column with fluid stream from the left to the right, solid stream in the opposite direction and the feed in fair grey entering in the middle. The two components in the feed are moving according to their adsorbing behavior to the left or right, being eluted as pure extract and raffinate eventually [16].

The process is called the true moving bed (TMP) and is very limited in application, as the movement of the solid is difficult to be realized. Therefore, the countercurrent movement of the solid is normally discretized applying a number of columns being switched in

countercurrent direction in discrete steps. This process is called the simulated moving bed (SMB) which has been well characterized and applied in a number of industrial processes [17-19].

The SMB in its original setup cannot be applied in the present work, as it is limited to a separation of two components and is unable to incorporate linear modifier gradients. A number of chromatographic methods has been proposed to overcome this problem as steady state recycling [14], modified SMB variants [20] and the multi-column countercurrent solvent gradient purification (MCSGP) process [1], described in detail in this work. All processes have the ability in common to run solvent gradients and separate up to three fractions however they distinguish in their productivity, solvent consumption and complexity. The MCSGP process was first described as a fully continuous process with six columns by Aumann and Morbidelli [1]. Since then, the design and functionality have been further developed. The first step was the reduction of the number of columns to three resulting in a semi continuous process [21] which is covered in detail in chapter 2.2.4. The process has been further optimized resulting in a twin-column MCSGP setup which is described in detail in chapter 5. All MCSGP versions have in common that they can separate the feed into at least three fractions applying a countercurrent movement of the stationary phase and they can operate with all types of chromatographic chemistries and apply modifier gradients. All MCSGP processes are operated, similar to SMB, on a cyclic repetitive base allowing to integrate a cleaning in place step (CIP) and to reach a cyclic repetitive steady state. In this thesis, a number of MCSGP related studies have been executed presented in the following chapters. In a first approach, the three column MCSGP process has been applied for different monoclonal antibody variant separations (chapter 2), followed by the process development for a MCSGP capable of doing multifraction separations (chapter 3) tested with protein systems, the development of two online control strategies for MCSGP based on a direct UV feedback for the three-column unit (chapter 4) and HPLC at-line analysis for the twin-column one (chapter 5), applied in peptide and protein chromatography. Finally, a case study with the twin-column MCSGP for the separation of rare earth elements (REE) is presented (chapter 6).

1.3. PID control

Continuous processes like the MCSGP described above are normally operated for long periods of time, as the start-up of the process lowers the productivity. During the operation time, a number of different process disturbances and uncertainties are present which have to be compensated to guarantee constant product purity. A possibility to encounter this problem is the application of online closed loop control. In contrary to open loop processes, a closed loop system applies a process feedback therefore able to react on disturbances and uncertainties [22].

A typical controller applied very frequently in industry is the proportional, integral and differential controller (PID) [23] defined as follows for a discretized system:

$$u(s) = K \left(e(s) + \frac{1}{I} \sum_{s^*=1}^s e(s^*) + D(e(s) - e(s-1)) \right) \quad 1.4$$

With u the controller output, K , I and D the controller proportional, integral and differential constants, s the actual cycle and e the error defined as the difference between a set value and the feedback. The controller constants have to be set in an empirical way, there are tuning helps available in literature [22, 23], but they only serve as an initial guess and the controller requires some fine tuning afterward which was done in this work according to computer simulations and preliminary experiments.

Figure 1.3 shows a schematical overview of how the controller was implemented in the case of the MCSGP process. The cyclic nature of the MCSGP process was used to define the frequency of the feedback which was forwarded to the control computer once every cycle. Based upon the feedback and an operator influenced set value, the controller was able to manipulate one or multiple process parameters in the following cycle.

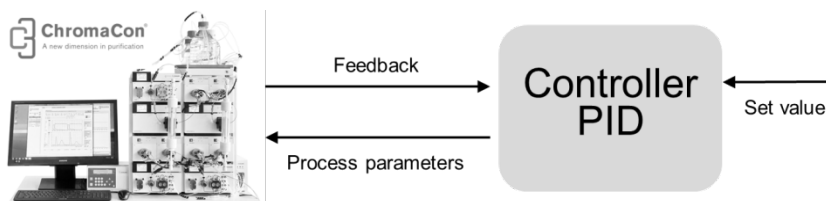


Figure 1.3 Schematic overview of the PID control concept applied for the MCSGP. On the left, the process is shown giving a feedback to the controller on a cyclic basis. The controller on the right calculates according to the feedback and a set value the process parameters for the next cycle.

The feedback and process parameters are chosen for each control routine individually and can be virtually every measurable value for the feedback and every process influencing variable for the parameters. In the current work, two control concepts were tested; the first one was based upon the internal UV chromatogram of the MCSGP process which is readily available and fast to collect. The feedback was limited as this online UV did not include any information on the product quality; therefore the controller was only able to maintain a certain operator chosen point. This process was run on a ChromaCon (Zurich, Switzerland) equipment with a Labview (National Instruments, Austin, USA) based control software, directly included in the process control computer. This control concept is described in detail in chapter 4. The second control concept investigated was based on a more detailed feedback generated by automated at-line HPLC analysis of the product stream collected every cycle. The controller was set up as a decoupled MIMO system able to directly control the product purity. The complete setup consisted of an Äkta (GE Healthcare, Uppsala, Sweden) based MCSGP unit, a 1200 Series analytics (Agilent, Santa Clara, USA) and a control computer. The three software products (controller: MatLab,

MCSGP: Unicorn, Analytics: Chemstation) were interfaced using file communication and a java based robot. Details for this control concept can be found in chapter 5.

2. Increasing the Activity of Monoclonal Antibody Therapeutics by Continuous Chromatography (MCSGP)

2.1. Introduction

2.1.1. mAb variants

Monoclonal antibodies (mAbs) make up for a large fraction of newly developed and approved drugs [24] and are among the biopharmaceutical drugs with the highest production capacities. This is due to the fact that mAbs interact with their antigen target in a stoichiometric ratio of 1:2 at the most, in contrast to other biotherapeutics such as hormones, which activate signal transduction cascades even when present in very small amounts. The overwhelming majority of monoclonal antibody drugs on the market belong to the IgG subclass [25]. The suitability of IgGs as therapeutics depends on their biological activity, pharmacokinetics and tissue targeting [26]. While pharmacokinetics is related mainly to the molecule size, which in the case of mAbs varies around 150 kDa, tissue targeting and biological activity depend strongly on the molecular structure and sequence. The mAb structure typically displays heterogeneity induced by post-translational modifications that take place readily inside the cell during fermentation.

A prominent example for a post-translational modification is glycosylation, which is represented by the attachment of oligosaccharides to Asparagin (Asn) in the Fc part of the mAb molecule. Some mAbs also display glycosylation in the Fab region [27]. Glycosylation is of supreme importance for the mAb activity, more precisely for the capability to elicit antibody-dependent cellular cytotoxicity reactions (ADCC) and complement-dependent cytotoxicity (CDC) [25]. To ensure a human-like glycosylation pattern, nowadays mAbs are produced in mammalian cells. However, changes in fermentation conditions have been reported to impact glycosylation of therapeutic proteins [28-30].

Also environmental parameters such as temperature, pH and residence time influence degradative reactions such as deamidations and isomerizations and decrease the bioactivity of the product [2, 31-33]. It was shown that deamidation progresses even under mild conditions such as during fermentation [31].

Other mAb variants are generated by intracellular and extracellular enzymatic reactions such as C-terminal lysine clipping or proteolytic cleavage of the molecule.

The variant pattern of mAbs is usually analyzed with a number of methods at various stages in product development and as routine analytics in the production process. Among these are mass spectrometry for analysis of the glycosylation pattern [27] and cation-exchange-chromatography (CIEX) and isoelectric focusing (IEF) for the distinction and quantization of charged variants, such as deamidated forms [34, 35].

During product development, the main focus of the analytics is the detection of mAb variants that exhibit low activity or even negative effects and may have to be potentially regarded as impurities. Conditions leading to the formation of the 'impurity-variants' may be examined and avoided. In the routine analytics accompanying production the variants pattern is checked to determine if the product meets the specifications.

The activity of mAbs is determined usually with proprietary cell-based assays. In order to evaluate the activities of single variants, they have to be separated in amounts ranging typically from 10-100 mg. Data comparing the activity of mAb variants is scarcely available in the literature. However, a case has been reported, where one mAb variant has an activity of 140% while another variant has an activity of only 20% compared to the original mixture of the variants which had 100% activity [2].

Despite significant differences in activity, current production processes do not separate mAb variants, which can be attributed also to the widespread use of Protein A chromatography that does not separate mAb variants. Protein A, derived originally from *Staphylococcus aureus* binds to the Fc part of the mAb and is insensitive to the presence of mAb variants. Nevertheless, the product obtained with protein A chromatography is frequently used to set the specification for the mAb variant pattern for the final product since it matches the one generated in the fermentation process.

2.1.2. Purification of mAb variants

Charged mAb variants have rather similar adsorptive properties on cation-exchange materials but even small differences of one charge unit can be exploited to separate them using small-particle analytical ion-exchange stationary phases and gradient chromatography [35]. However, with large-particle preparative chromatographic stationary phases, highly pure mAb variants can only be obtained with low yield, as strong overlapping due to mass transfer limitations can be generally observed [36]. During the fractionation of the product eluate peak the choice has to be made between selecting only the purest fraction with a low yield and collecting a range of fractions with a higher yield but with a larger content of impurities. This drawback of conventional non-affinity chromatography, often referred to as the yield-purity-tradeoff, can be circumvented with the multicolumn countercurrent solvent gradient purification (MCSGP) process that allows for generation of single-variant mAb materials with high purity and yield simultaneously [36].

MCSGP is a continuous multicolumn chromatographic process that is capable of using linear gradients and performing three fraction separations that are very common in biochromatography. This has to be seen in contrast to simulated moving bed chromatography (SMB) that is so far the only established continuous countercurrent chromatographic method in the pharmaceutical industry but is advantageous only for binary separations and isocratic or at most step gradient operations.

The process principle of MCSGP was first described in 2006 [36], followed by the experimental determination procedure for its operating parameters for a six-column

process in 2007 [1]. Afterwards, the concept of separating in time the “batch” state for pure component production and the “interconnected” state for internal side fraction processing was introduced, leading to a reduction of the number of required chromatographic columns from six to three [21]. Applications of this process were investigated using six and three column MCSGP configurations for the purification of a peptide [37] and for the separation of monoclonal antibody *c*-terminal lysine variants [38]. Upgrades to the three-column MCSGP process, namely the introduction of a cleaning-in-place (CIP) section [39] and the introduction of a feeding zone for continuous loading [40, 41], proved to be very advantageous for the increase of purity and productivity, respectively, in mAb capture from clarified cell culture supernatant.

The introduction of a model predictive control concept for the online optimization and control of the MCSGP process was described by Grossmann et al. 2010 based purely on modeling data.

In this study a refinement of mAb variant purification [38] is presented and new aspects are investigated. Firstly, more complex monoclonal antibody therapeutics obtained from the pharmacy are purified with respect to a single mAb variant. Secondly, with activity data available from the literature, the increase in activity of the purified drug is quantified. Furthermore the potential of straightening out fluctuations in mAb isoform concentrations is compared in this work by subjecting MCSGP and batch chromatography processes to feedstocks spiked with different mAb variants.

In the frame of this work three-column and four-column MCSGP processes as presented in Aumann and Morbidelli 2008 and Müller-Späth et al. 2010, respectively, were used. The four-column process consists of a three-column process that is extended by one extra column for loading and washing. A flow scheme and a basic explanation of the four-column process are given in Figure 2.2. For a detailed explanation of the process principles the reader is referred to the literature [1, 21, 36].

The MCSGP process parameters can be determined from batch gradient elutions as described in the literature [1]. The operating parameters determined with this procedure serve as starting values for MCSGP simulations and experimental fine-tuning. The monoclonal antibody separation batch gradient elutions were also used as benchmark for the MCSGP process and to validate the model parameters.

2.2. Materials and methods

2.2.1. Monoclonal antibody products

The following mAb therapeutics were obtained from the pharmacy: Avastin® (Roche, Basel, Switzerland), Herceptin® (Roche, Basel, Switzerland) and Erbitux® (Merck-Serono, Darmstadt, Germany). Avastin® contains the IgG₁ Bevacizumab, Herceptin® contains the IgG₁ Trastuzumab and Erbitux® contains the IgG₁ Cetuximab. An overview of the mAb properties is given in Table 2-1.

Prior to cation exchange chromatography, all mAbs were diluted to a concentration of 0.4 g/L using the binding buffer.

MAB charge heterogeneity was determined by analytical cation exchange gradient chromatography and a nomenclature of the mAb variants was established according to the elution order in the analytics: In the chromatograms, weakly adsorbing variants were named W1, W2 etc., strongly adsorbing variants were named S1, S2 etc., and the main variant, which is the most abundant one, was called *P* as indicated in Figure 2.1. The nomenclature was based on the resolution of the variants by cation exchange chromatography. In some cases, variants that were not clearly distinguishable were lumped with neighboring variants. For the sake of simplicity these variant groups will also be referred to as variants in the following.

For Trastuzumab, shown in the center of Figure 2.1, an analytical cation exchange chromatogram was obtained which matches the one presented in the literature [2] in terms of resolution and peak heights of the variants. The nomenclature from the literature reference is indicated by the letters and numbers in parentheses in Figure 2.1.

In reference [2], table 5, the activities, determined by a cell proliferation assay, were given for the main variants Tra-W3, Tra-*P* and Tra-S1 and were 98%, 141% and 12-30%, respectively. The feed mixture in that case was taken as reference and had an activity of 100%.

Table 2-1: Properties of the mAb used for this study

Brand name	Avastin®	Herceptin®	Erbitux®
mAb	Bevacizumab	Trastuzumab	Cetuximab
Abbreviation	Bev	Tra	Cet
Manufacturer	Roche	Roche	Merck-Serono
Subclass	IgG1	IgG1	IgG1
Type	Humanized	Humanized	Chimeric
Main indication	Colon cancer	Breast cancer	Colon cancer
Cell line	CHO	CHO	SP2/o
Isoelectric point (pI)	pH 8.1-8.4	pH 9	pH 8.2-8.7
Purity with respect to <i>P</i>	64.50%	73.80%	23.90%

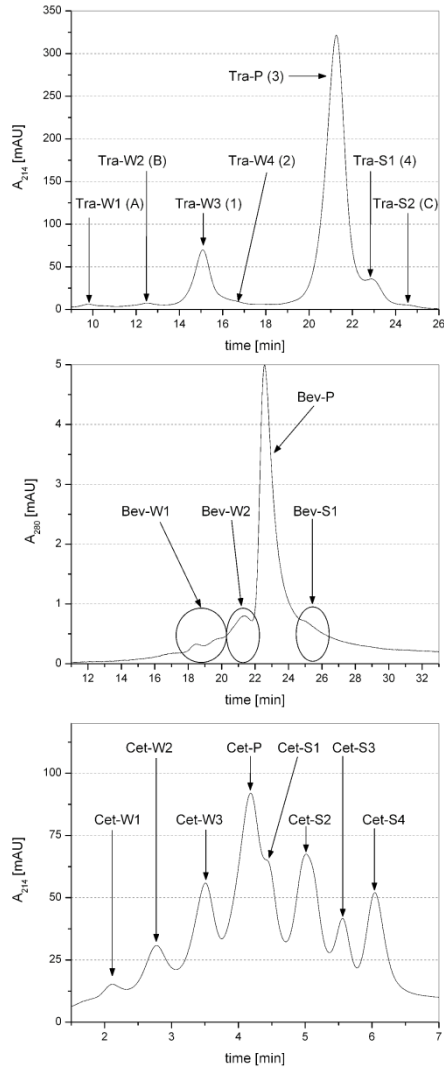


Figure 2.1: Nomenclature of the mAb variants of Bevacizumab 'Bev', top; Trastuzumab 'Tra', center; and Cetuximab 'Cet', bottom. The chromatograms were obtained with cation exchange chromatography as indicated in the analytics section. Symbols in parentheses refer to the nomenclature used in [2].

2.2.2. Analytics

Table 2-2: Parameters for mAb analytics.

Parameter	unit	Bevacizumab	Trastuzumab	Cetuximab
Column type	[-]	Propac wCX-10	CCM103-25	BioPro SP-F 5
Manufacturer	[-]	Dionex	Eprogen	YMC
Length	[mm]	250	250	30
Diameter	[mm]	4	4.6	4.6
Binding buffer	[mmol]	25, Phos.	25, Phos.	25, Phos.
Elution buffer	[mmol]	25, Phos., 250 mM NaCl	25, Phos., 150 mM NaCl	25, Phos., 250 mM NaCl
Buffer pH	[-]	6	7	6
Flow rate	[mL/min]	1.0	1.0	0.5
Gradient start	[%B]	30	5	17
Gradient end	[%B]	50	29	36
Gradient duration	[min]	30	27	9
Approx. mass injected	[ug]	10	30	30
UV	[nm]	220	214	214/280

Purity and concentration of the products obtained in preparative cation exchange chromatography were determined by analytical cation exchange gradient chromatography using phosphate buffers. A Propac wCX-10 column was used to obtain the profile of Bevacizumab. For Trastuzumab analyses a CCM103-25 column from Eprogen was used, which delivered results that were comparable to the ones obtained by [2] using a 4.6 x 250 mm BakerBond CSX column which contains also a silica-based analytical stationary phase. Cetuximab chromatograms were obtained with an YMC BioPro-SP column. Details on the analytics are given in Table 2-2.

The isoelectric points of the mAbs were determined using a Phast system and Phast gels IEF 3-9 (GE Healthcare, Uppsala, Sweden).

2.2.3. Stationary phases, buffers and hardware

Fractogel SO₃ (S) was used for the preparative separation of Bevacizumab variants. The material was packed following to the resin manufacturer's instructions at a linear flow rate of 350 cm/h. The columns used were 0.75 x 10 cm PEEK columns obtained from YMC

(Kyoto, Japan) with titanium 10 μm frits. For Trastuzumab and Cetuximab variant separations, YMC BioPro SP-10 was packed into 0.75 x 15 cm PEEK columns at 540 cm/h with 0.3 M Na_2SO_4 as packing buffer.

Average particle sizes of Fractogel SO_3 (S) and YMC BioPro SP-10 are 30 μm and 10 μm , respectively. The columns were tested after packing using linear gradient elutions of analytical mAb injections. Column properties, buffer and gradient conditions used for preparative batch and continuous chromatography runs are summarized in Table 2-3.

Table 2-3: Conditions for preparative batch and MCSGP experiments and for retention time measurements.

Parameter	unit	Bevacizumab	Trastuzumab	Cetuximab
Column type	[-]	FGSO ₃ (S)	BioPro SP-10	BioPro SP-10
Manufacturer	[-]	Merck	YMC	YMC
Length	[cm]	10	15	15
Diameter	[cm]	0.75	0.75	0.75
Phos. Buffer A	[mmol]	25	25	25
Phos. Buffer B	[mmol]	25	25	25
NaCl buffer A	[mmol]	0	0	0
NaCl buffer B	[mmol]	250	150	250
pH buffer A, B	[-]	6	6.5	6
Flow rate	[mL/min]	1.1	1.2	1.2
Gradient start	[%B]	51	15	16
Gradient start	[%B]	67	25	30
Gradient duration	[min]	30	30	30
Approx. mass injected	[μg]	2300	1500	1600
Detector wavelength	[nm]	220 / 280	214 / 280	214 / 280

The gradient conditions for Bevacizumab and Cetuximab were found through experimental optimization while the conditions for Trastuzumab were determined through simulations using a mathematical model.

Single column experiments for measurements under analytical conditions (retention time, column tests) were performed using an Agilent HP 1100 series (Agilent, Santa Clara, CA, USA) at 25°C. Preparative batch gradient elutions and MCSGP experiments retention time were carried out using ÄKTA basic equipment (pump P-900, UV-900, pH/C-900,

valves PV-go8) (GE Healthcare, Uppsala, Sweden) controlled by Unicorn software. For some experiments, ChromaCon MCSGP equipment was used (ChromaCon, Zurich, Switzerland). The conductivity, pH and UV-absorption were monitored. In order to detect online if the process has reached cyclic steady state one UV-monitor is required.

2.2.4. Four- and three-column MCSGP process

The different process tasks of the four-column MCSGP process are indicated by the numbers in the grey rectangles.

The process is divided into an interconnected state CC, where internal recycling and part of the loading is done (tasks 2, 4, 5b and 6), and into a batch state BL, where product P , strongly adsorbing impurities S and weakly adsorbing impurities W are eluted from the system in a discontinuous manner and another part of the loading is done (tasks 1, 3, 5a, 5c). The columns remain in the interconnected state for the time period t_{CC} and in the batch state for the time period t_{BL} . The columns switch from high to low section numbers in the order 6, 5c, 5b, 5a, 4, 3, 2, 1 and return to section 6 after having completed the task of section 1. Summarizing, the tasks consist of loading (batch and interconnected state, task 5c, 5b), washing (batch state, task 5a), recycling of product overlapping with weakly adsorbing impurities (interconnected state, task 4), product elution (batch state, task 3), recycling of product overlapping with strongly adsorbing impurities (interconnected state, task 2), stripping, CIP, column re-equilibration (batch state, task 1) and reception of the eluate from section 4 (task 6).

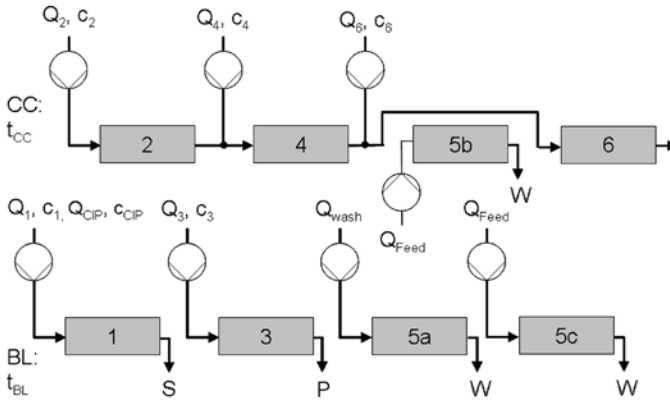


Figure 2.2: Flow scheme of the MCSGP process using four columns. Interconnected state (CC) tasks are indicated with 2, 4, 5b and 6; batch state (BL) tasks are indicated with 1, 3, 5a, 5c. S represents strongly adsorbing components, P the product and W weakly adsorbing components.

Due to the internal recycling of the partially pure side fractions (tasks 2 and 4), the yield-purity tradeoff of batch chromatography can be overcome. As the yield for the desired

purity is increased, also the productivity is raised. Since the four batch and four interconnected state tasks are performed in an alternating manner, the process requires four pumps. In contrast to the process presented in [39], the process used here does not have a section that is dedicated only to column sanitization; however a high salt strip step is incorporated in section 1 after the elution of the strongly adsorbing impurity *S*. In a process where continuous feeding and post-load-washing are not required, for instance if a highly pure and concentrated feed material is applied, the three-column process that requires only three pumps can be used. In the three-column process, sections 5b (feeding) and 5a (washing) are not present and the columns switch in the order 6, 5c, 4, 3, 2, 1 within one cycle.

2.2.5. Modeling

Mathematical modeling was used in this work in order to shorten the process development time and to predict batch and MCSGP performance for the Trastuzumab variant separation. The lumped kinetic model [14, 42], which was used for the simulations in this work, takes into account the slow mass transfer kinetics of large molecules such as mAbs. Chromatograms and fraction analysis values of batch linear gradient elutions were used to validate the lumped kinetic model parameters.

The model comprises a mass balance (equation 2.1), a transport equation (equation 2.2) and an adsorption equilibrium equation (equation 2.3):

$$\frac{\partial c_i}{\partial t} + \frac{1-\varepsilon_i}{\varepsilon_i} \cdot \frac{\partial q_i}{\partial t} + u \cdot \frac{\partial c_i}{\partial z} = u \cdot d_{ax} \frac{\partial^2 c_i}{\partial z^2} \quad 2.1$$

$$\frac{\partial q_i}{\partial t} = k_M \cdot \left(q_i^* - q_i \right) \quad 2.2$$

$$q_i^* = H_i \cdot c_i \quad 2.3$$

Where c_i indicates the concentration of component *i* in the liquid phase, q_i the concentration in the solid phase, q_i^* the equilibrium concentration in the solid phase, ε_i the component-specific porosity, H_i the Henry coefficient, k_M the lumped mass transfer coefficient, u the linear chromatographic flow velocity ($u = Q / (A \cdot \varepsilon_i)$) and d_{ax} the axial dispersion coefficient. The number of components to be modeled is indicated by *n*, which excludes the modifier (salt). A linear driving force with a constant mass transfer coefficient is assumed (equation 2.2). The adsorption of proteins is frequently described with a Langmuir isotherm. However, in this case, due to the limited amount of feed material available for the separation processes, the concentrations were expected to be in the linear range of the isotherm assuming typical saturation capacities for mAbs on CIEX

stationary phases of 60-100 g/L. Therefore the adsorption equilibrium was described with a linear isotherm right from the start (equation 2.3).

Initial and boundary conditions were chosen in agreement with the experimental conditions (e.g. the mAb concentration in the unit was zero at $t=0$). The model equations were numerically solved using a finite difference method with a discretization in space of 150 grid points per column. The modeling was carried out with Intel Visual Fortran software and IMSL library 5.0.

Model parameters for Trastuzumab variants were determined from retention time measurements in single column experiments under adsorbing and non-adsorbing conditions using analytical injections of the feed variant mixture.

For each monoclonal antibody, linear gradients were run on the respective stationary phases (Table 2-5) and the eluate peaks were fractionated. The fractions were analyzed according to the methods shown in Table 2-2 and from the peak areas the concentrations and performance parameters were calculated. For Trastuzumab, the chromatograms and fraction analysis values were used to validate the lumped kinetic model parameters.

2.2.6. Performance parameter definition

The performance parameters yield, purity, load per time, productivity and solvent consumption for the comparison of MCSGP and batch processes performance are defined and summarized in Table 2-4.

Table 2-4: Performance parameters for batch and MCSGP processes. The notation is explained in the nomenclature section

Parameter	Batch process	MCSGP process
Yield	$Y = \frac{m_{p,Product}}{m_{p,Feed}}$ 2.4	$Y = \frac{\dot{m}_{p,Product}}{\dot{m}_{p,Feed}}$ 2.5
Purity	$P = \frac{c_p}{c_{mAb}}$ 2.6	See batch process
Load per time	$L = \frac{m_{mAb,Feed}}{V_{Col}} \cdot \frac{1}{t_{run}}$ 2.7	$L = \frac{\dot{m}_{mAb,Feed}}{V_{Col}}$ 2.8
Productivity	$Prod = L \cdot Y$ 2.9	See batch process
Solvent consumption	$SC = \frac{V_{buff}}{m_{p,Product}}$ 2.10	$SC = \frac{\dot{V}_{buff}}{\dot{m}_{p,product}}$ 2.11

The activity of the mAb products generated by batch and MCSGP chromatography is computed from peak areas and literature values of the activities [2]. Activity data was only available for the Trastuzumab variants Tra-W3 (98%), Tra-P (141%) and Tra-S1 (12-30%). For Tra-S1, the average value of 21% activity was used.

The absolute activity $Act_{abs,i}$ is defined as the sum of the single variant concentrations in one sample, each multiplied by the corresponding specific activity and by the sample volume V_i which, in the case of batch chromatography, corresponds to the feed sample or an eluate fraction. For MCSGP experiments V_i corresponds to the volume injected or eluted within the time span corresponding to the duration of the batch experiment. In both cases, the term is divided by the total stationary phase volume given by the product between the number of columns and the single column volume. In the case of Trastuzumab this leads to:

$$Act_{abs,i} = \frac{(c_{Tra-W3,i} \cdot 98\% + c_{Tra-P,i} \cdot 141\% + c_{Tra-S1,i} \cdot 21\%) \cdot V_i}{n_{col} \cdot V_{col}} \quad 2.12$$

where the absolute activity value, $Act_{abs,i}$ gives a measure of how much activity is “fed” ($Act_{abs,feed}$) or “recovered” ($Act_{abs,eluate}$) from a column of a given size within the time span equivalent to the duration of one batch run. Therefore it is related to the productivity.

An activity yield Y_{act} can be defined by dividing $Act_{abs,eluate}$ by $Act_{abs,feed}$ as follows:

$$Y_{Act} = \frac{Act_{abs,eluate}}{Act_{abs,feed}} \quad 2.13$$

The relative activity of the mAb in one sample is defined as the ratio between a.) the sum of the single variant concentrations in one sample multiplied by the specific activities of the single variants and with the sample volume V_i (numerator) and b.) the sum of the variant masses in one sample (denominator):

$$Act_{rel,i} = \frac{c_{Tra-W3,i} \cdot 98\% + c_{Tra-P,i} \cdot 141\% + c_{Tra-S1,i} \cdot 21\%}{c_{Tra-W3,i} + c_{Tra-P,i} + c_{Tra-S1,i}} \quad 2.14$$

Note that the relative activity $Act_{rel,i}$ is independent of productivity-related parameters such as column volume, time and sample volume V_i .

2.3. Results and discussion

2.3.1. Operation of the batch gradient process

The eluate from each batch gradient run was fractionated and analyzed off-line. The obtained results are shown in Figure 2.3 as a function of time for the three mAbs. For Tra, also simulation results are shown. Already from the online UV signal it can be seen that the YMC BioPro SP material used for Tra and Cet delivers sharper peaks and better separation of mAb variants than the FGSO₃ (S) material used for Bev. This improved resolution comes at the cost of a higher pressure drop of 0.7-0.8 bar/cm at 160 cm/h for YMC BioPro SP versus 0.3-0.4 bar/cm at 150 cm/h for the FGSO₃ (S) material. The capacity of the two resins may differ too, but this is not relevant here since the loads are relatively low. However, offline analysis reveals that all batch chromatograms exhibit a strong overlapping of the mAb variant peaks. The main variant purities decrease strongly towards the peak fronts and tails, emphasizing the yield-purity-tradeoff.

Table 2-5: Performance of experimental MCSGP and batch runs.

	Bevacizumab		
	Yield [%]	Purity [%]	Prod. [g/L/h]
Feed	100	73	n.a.
MCSGP	94	80	0.33
Batch high purity pool	41	80	0.11
Batch high yield pool	88	74	0.23

	Trastuzumab		
	Yield [%]	Purity [%]	Prod. [g/L/h]
Feed	100	75	n.a.
MCSGP	83	89	0.12
Batch high purity pool	21	90	0.03
Batch high yield pool	78	80	0.12

	Cetuximab		
	Yield [%]	Purity [%]	Prod. [g/L/h]
Feed	100	27	n.a.
MCSGP	75	67	0.027
Batch high purity pool	5	49	0.002
Batch high yield pool	64	23	0.021

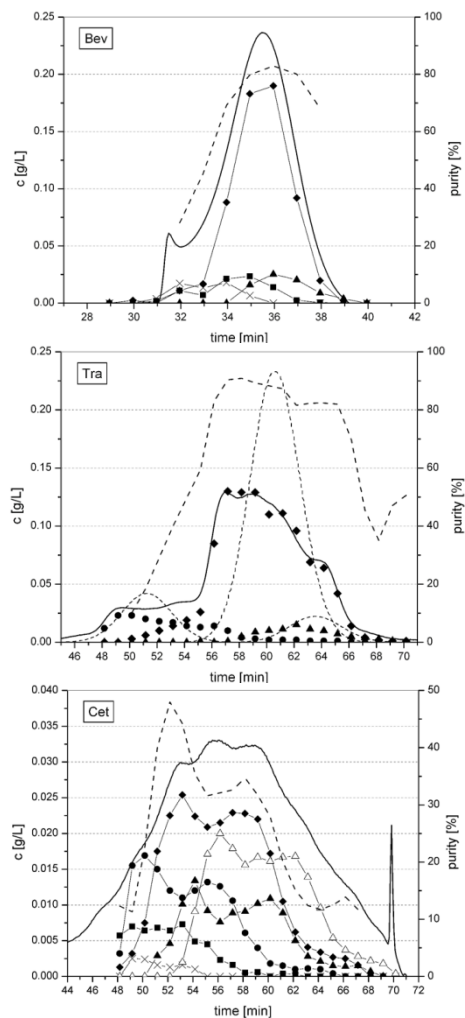


Figure 2.3: Fraction analyses of linear gradient elutions of Bevacizumab (top), Trastuzumab (center) and Cetuximab (bottom). The thick solid line represents the scaled UV-signal at 280 nm, the dashed thick line indicates the purity with respect to the main variant P . The symbols represent the mAb variant concentrations as determined by offline analytics: W_1 (x), W_2 (■), W_3 (●), P (◆), S_1 (▲), S_2 (△). Variants W_1 and W_2 in the case of Trastuzumab and variants S_3 and S_4 in the case of Cetuximab were omitted for the sake of clarity. In the case of Trastuzumab, the simulated variant concentrations are given as thin dashed lines.

It has to be mentioned that for Cet variant separation, a high salt strip with 1M NaCl, following the linear gradient elution on the YMC BioPro SP column was not sufficient to re-establish its performance and the resolution of the variants decreased slightly during repeated separation runs. Thus, in order to compare MCSGP and batch separations for Cet, the first batch run carried out after the final cycle of the MCSGP process was taken as the benchmark batch run. This batch run used one of the columns used in the MCSGP process.

2.3.2. Operation of the MCSGP process

The adopted operating parameters for MCSGP were obtained by experimental fine-tuning (Bevacizumab and Cetuximab) and through simulations (Trastuzumab). The detailed operating conditions for each run are given in Table 2-3: Conditions for preparative batch and MCSGP experiments and for retention time measurements. The UV-signals recorded at the product outlet over time are shown in Figure 2.4 in for each of the mAbs examined. The start-up phase of the MCSGP process with rising product concentrations and yields is typically concluded after three cycles and can clearly be distinguished from the steady state region where the outlet concentration, yield and purity remain constant. During the startup phase the internal profiles of product and impurity variants are built up within the columns. Initially, as the mAb variants accumulate inside the MCSGP unit, the calculated product yield is low. However, the product is not lost since it is internally recycled and it can be recovered during the shutdown of the process.

The shutdown is done by replacing the feed by buffer A and continuing the product collection. It can be noted that the yield is proportional to the product concentration, while the obtained purity is basically constant within the single runs. This behavior is typical in cases where little product displacement is present due to low loadings on the stationary phase. In the experiments presented here, low concentrations had to be used due to the high costs of the feed materials. As mentioned above, two different configurations were used for the MCSGP process: three columns for Tra and Cet and four columns for Bev. In all cases, the concentration values shown in Figure 2.4 represent averages over one or more complete cycles, i.e. three or four switches for the two processes, respectively, or multiples thereof. The collection over one complete cycle ensures that the process performance values are determined as average values. The time required to reach steady state depends on the operating parameters of the MCSGP process and can be tailored. For instance, if the process parameters are chosen such that a large fraction of the injected feed is eluted in the same MCSGP cycle, thus minimizing accumulation inside the unit, cyclic steady state is reached faster than in the runs shown in Figure 2.4.

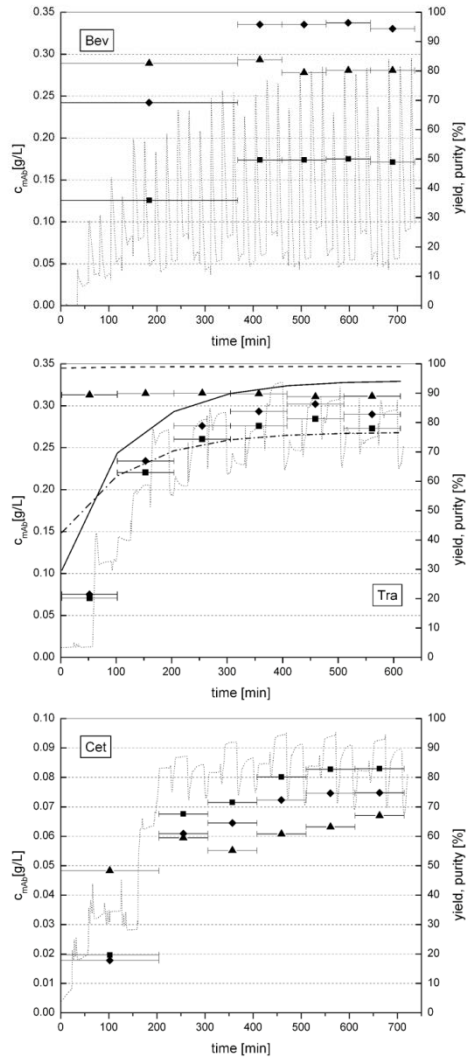


Figure 2.4: MCSGP runs with Bevacizumab (top), Trastuzumab (center) and Cetuximab (bottom). The thin dashed line represents the scaled UV-signal at 280 nm. Purity (▲), yield (◆) and product concentrations (■) were determined by offline analyses. The horizontal bars indicate the sample collection intervals (usually one cycle). For Trastuzumab, the simulation results are also shown in terms of product concentration (-.-.-), yield (—) and purity (---).

2.3.3. Comparison of mAb variant purifications in batch and MCSGP mode

The performance of the empirically optimized batch experiments and the MCSGP runs were compared in terms of yield, purity and productivity. The fine tuning was performed according to available fraction analysis by changing the gradient slope, start and end point. The experimental results of the empirically optimized batch chromatogram are shown in Table 2-5. Due to the yield-purity trade-off inherent to batch chromatography, two yield/purity combinations of batch gradient chromatography are given in the table in order to facilitate the comparison. One combination corresponds to a product pool of maximum yield and the other to a product pool that has the same purity as the one obtained with MCSGP, indicated with “high yield” and “high purity”, respectively. A comparison between batch and MCSGP is justified since the productivities of the batch high yield data and MCSGP are in the same range and the gradient conditions are the same. It has to be noted that the absolute productivity values are rather low which is due to the low feed concentrations used in the experiments. Better productivities are of course expected in both cases for larger loadings [40].

Let us analyze exemplary the results of the Bevacizumab experiments: For a purity of the product variant *P* of 80%, the yield of the batch chromatography product pool is 41%. An increase of the *P*-yield of batch chromatography to 88% can be obtained at the expenses of a decrease in purity to 74% which is close to the feed purity of 73%. However, due to the increased yield, also the productivity increases from 0.11 to 0.23 g/L/h. The point representing the MCSGP process was chosen from the MCSGP pareto curve to reflect the same purity as the batch process (80%), the yield is significantly higher i.e. 94% with a productivity of 0.33 g/L/h. For Trastuzumab and Cetuximab similar trends are observed, with the most significant differences found in the case of Cet. The yield-purity relations of Bev, Tra and Cet for the two processes are illustrated in Figure 2.5.

The robustness of the MCSGP process with respect to varying mAb feed compositions was tested. More specifically, the concentration of certain variants was increased and the impact on the variant pattern of the MCSGP product stream was observed. The variants needed for spiking were obtained by collecting the *W* and *S* outlet streams of the MCSGP (Figure-S 1) operated with regular feed. The feed was then diluted to give the same overall mAb concentration as in the previous experiments with regular feed. The addition of weakly adsorbing variants, which usually contain deamidated mAb forms, simulates a common degradation reaction. In the case of Cet also a feed enriched in strongly adsorbing variants was generated. Analytical chromatograms of the enriched feeds are shown in

Figure 2.6 (left column) together with chromatograms of the regular feeds for comparison. For Bevacizumab the amount of weakly adsorbing variants was increased from 20 to 27%, for Trastuzumab from 14% to 45% and for Cetuximab from 25% to 41%.

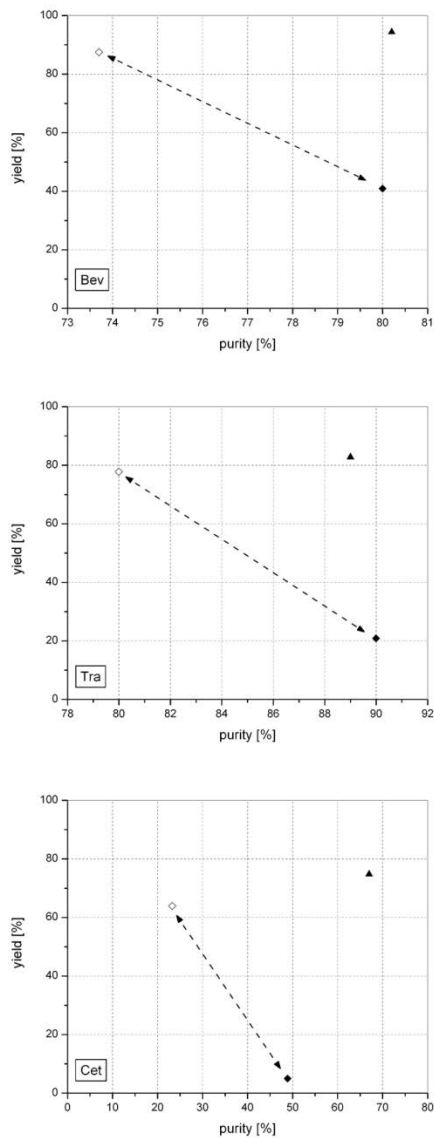


Figure 2.5: Yield-purity relations for batch (◇, ◆) and MCSGP chromatography (▲) of Bevacizumab (top), Trastuzumab (center) and Cetuximab (bottom). The dashed lines with arrows indicate the yield-purity trade-off of batch chromatography.

2.3.4. Robustness to feed variations

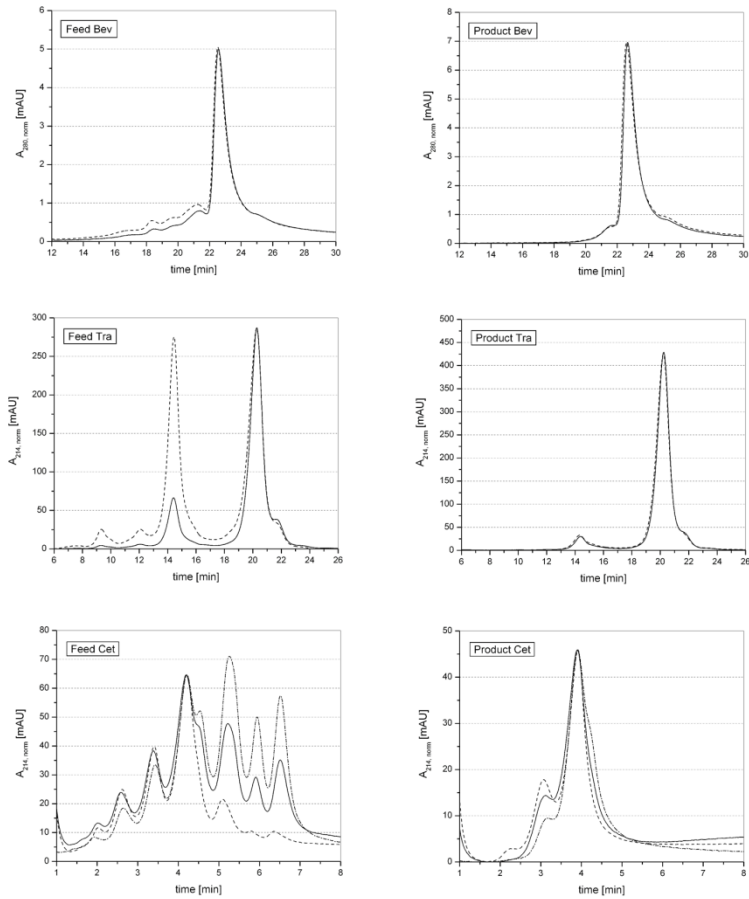


Figure 2.6: Chromatograms of feeds enriched in weakly adsorbing (W) variants (---) together with regular feeds (—) are shown in the left column. Chromatograms of MCSGP-product streams obtained with enriched feeds (---) and regular feeds (—) are shown in the right column. Bev data are displayed at the top, Tra data at the center and Cet data at the bottom. For Cet also the chromatograms based on a feed mixture enriched in strongly adsorbing (S) variants (-.-.-) are shown.

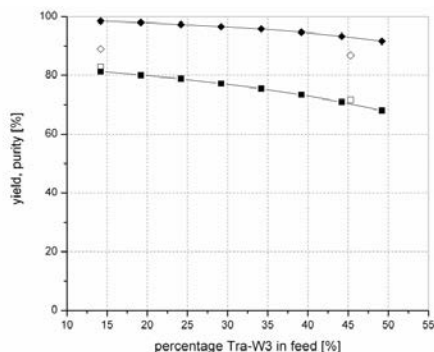


Figure 2.7: Simulated values of purity (◆) and yield (■) for the Trastuzumab *P* variant purified by MCSGP as a function of the W₃-content of the feed mixture. Empty symbols indicate the corresponding experimental data of purity (◇) and yield (□)

The enriched feeds were loaded in separate MCSGP experiments without any modification of the operating conditions. The product chromatograms of MCSGP experiments obtained with the enriched and the regular feed mixtures are shown in the right column of

Figure 2.6. It can be seen that the differences in the outlet chromatograms, when compared with the variations in the feed chromatograms, appear very minor which demonstrates the high robustness of the process against varying feed conditions for the chosen operating parameters. Simulations of MCSGP experiments with varying feed conditions using the lumped kinetic model confirm this observation. In Figure 2.7 values of the product (*P*) purity and yield over the W₃-content for Tra, obtained by simulation, are compared with experimental data from MCSGP. The overall mAb concentration of the feed was kept constant. The prediction of the yield is accurate while for the purity there is an offset. However, in both simulations and experiments, it can be observed that the purity and yield decrease is rather small (< 10% for purity and < 15% for yield) in contrast to the variation of the feed concentration of W₃, which was increased by a factor of 3.3.

2.3.5. Improvement of the bioactivity of Trastuzumab

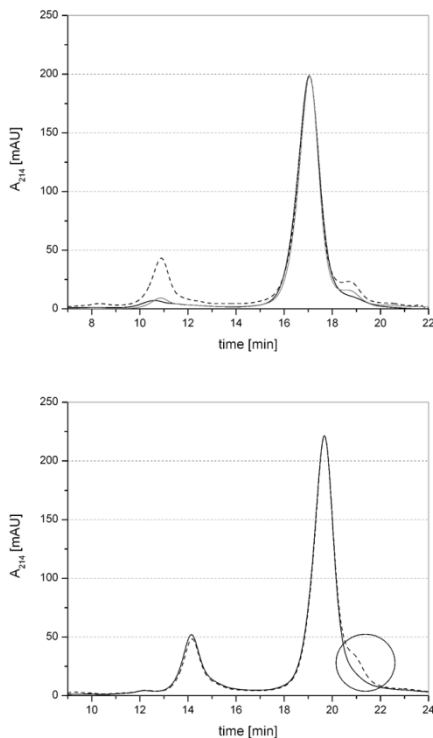


Figure 2.8 Chromatograms of Trastuzumab MCSGP products (—) together with regular feeds (---). In the top part, the results of main variant enrichment (strategy 1) are shown; for comparison a chromatogram of the purest fraction of the empirically optimized batch gradient run is also shown (grey line). The bottom part shows the results of the MCSGP run aimed solely at decreasing the concentration of the S1-variant indicated by the circle (strategy 2).

It has been shown that the single mAb variants distinguished by analytical cation exchange chromatography may significantly differ in specific biological activity [2]. Thus, by properly modifying the mAb variant pattern the activity can be increased. As mentioned above, activity data was available only for the Tra variant mixture and single variants [2]. In the following, the results of activity improvement for Trastuzumab by batch and MCSGP chromatography are shown. Trastuzumab was purified in two separate MCSGP experiments with the aim of firstly enriching the most active variant Tra-P (by removal of W and S variants, strategy 1) and secondly with the aim of reducing as far as possible the content of the least active variant Tra-S1 (strategy 2). The motivation for these two strategies was in the first case to maximize the specific activity by enriching the most

active variant and in the second case to keep the activity yield as high as possible by removing only the least active variant Tra-S₁ (12-30% activity with respect to feed). The latter case essentially aims at a co-purification of the variants Tra-W₃ (98% activity) and Tra-P (141% activity). The resulting analytical chromatograms of the MCSGP product pools for strategy 1 and 2, respectively, are given in Figure 2.8 (top) and Figure 2.8 (bottom). The chromatograms show that in the first case both W₃ and S₁ could be removed to a great extent (Figure 2.8 (top)) while in the second case, W₃ was conserved and mainly S₁, indicated by the circle, was removed (Figure 2.8 (bottom)). The activities and the activity yield of the final mAb products were calculated according to equation 2.12 to 2.14 for the two cases using the literature activity values [2]. The results are given in Table 2-6. In order to compare batch and MCSGP experiments, the yields are compared both for the same product purity and for the same specific activity. In the upper part of Table 2-6, which refers to strategy 1, line 1 corresponds to the feed values and line 2 to MCSGP results. Line 3 corresponds to a pool of batch gradient elution fractions that has the same purity as the MCSGP product (line 2). The batch product corresponding to line 4 has the same specific activity as the MCSGP product. Both batch and continuous chromatography (lines 2-4) are able to increase the specific product activity beyond 130% by enriching the most active variant (strategy 1). However, in batch chromatography this is only possible at the cost of significant losses of the most active variant Tra-P, as indicated by the low Tra-P yield values. The batch product pool delivering Tra-P with the same purity as the MCSGP process (89%) corresponds in fact to a Tra-P yield of 49% (comparison of lines 3 and 2), while the batch product pool delivering Tra-P with an activity equal to the one obtained with MCSGP corresponds to a Tra-P yield of 42%, which have to be compared to the Tra-P yield of MCSGP equal to 83% (comparison of lines 4 and 2). As a consequence with MCSGP, 75% of the absolute feed activity could be recovered, while for batch chromatography only 40-45% was obtained.

Note that, independently of the chromatographic mode, the removal of the less active variants leads to an increase of the specific activity of the final product on the one hand but to a decrease in activity yield on the other hand since even the least active variants do exhibit some non zero activity. In batch chromatography, as a consequence of the low yield of Tra-P, the activity yield is low too. The results of the experiments targeted at removal of only Tra-S₁ (strategy 2) are shown in the lower part of Table 2-6. For comparison the purest batch chromatography fractions were pooled in such a way that the Tra-S₁ content was similar to the one obtained by MCSGP, that is 27.5% (line 7) and 22% (line 6), respectively. A further increase of the batch pool size would lead to a further increased content of S₁. Under these conditions, the batch chromatography yield of Tra-P was 37% (line 7) while that of MCSGP was 85% (line 6). The relative activity for the batch product was 128% and 131% for the MCSGP product. The activity yield of the MCSGP run was 87% with the feed as reference. This relatively large value indicates a high recovery of Tra-W₃ which clearly appears from the chromatogram in Figure 2.8 (bottom). The activity yield of batch chromatography suffered again from the low Tra-P yield and is only 48%.

It has to be noted that the feed reference value for the activity is 100% according to the literature [2]. However, when the relative activity of the feed mixture is calculated using the area percentages of Tra-W₃ (13.6%), Tra-P (73.8%) and Tra-S₁ (8.5%) according to

equation 2.14, the result is a feed mixture activity of 122% assuming an average activity of Tra-S1 of 21% and that the remaining variants have zero activity. Possible explanations may be the large scatter of the cell-based assay or the decrease of activity of one of the more active variants in the presence of a less active variant. Even though for variant mixtures the activities obtained with equation 2.14 may be inaccurate due to this non-linear contribution of some variants, this error should be strongly reduced for purified samples that contain mainly one single variant. On the other hand, these aspects do not affect the possibility of controlling the specific bioactivity by changing the mAb variant profiles discussed in this work.

Table 2-6: Performance of MCSGP and batch runs for strategies 1 and 2. Line 4, marked with an asterisk indicates batch product with the same specific activity as the MCSGP product.

		Tra-S1 content [%]	Tra-P yield [%]	Tra-P purity [%]	Activity, rel. [%]	Activity, yield [%]
Strategy 1						
1	Feed	100	100	74.8	100	100
2	MCSGP	64.2	82.8	89	133	75
3	Batch	73	49.1	89.3	132	45
4	Batch*	35.4	41.8	84.3	133	40
Strategy 2						
5	Feed	100	100	74.8	100	100
6	MCSGP	21.9	84.9	76.2	131	87
7	Batch	27.5	37.1	69.8	128	48

Line 4, marked with an asterisk (*), indicates batch product with the same specific activity as the MCSGP product.

2.4. Conclusion and outlook

Batch and continuous chromatography (MCSGP) using cation-exchange stationary phases were evaluated for mAb variant purification of three commercially available mAbs: Bevacizumab, Trastuzumab and Cetuximab with the aim of improving their specific activity.

Although the results show that mAb variant purification is possible with both batch and continuous chromatography, a comparison of the two processes shows that the MCSGP process provides, for a given purity, significantly higher yields. The simultaneous achievement of high yield and high purity can be attributed to the internal recycling of partially purified side fractions in the continuous process.

Potential advantages of this process include time-savings in the purification of sufficient amounts of single mAb variants for activity assays or pre-clinical studies, as well as improved life-cycle management of the mAb and the possibility of producing drugs with higher specific bioactivity by removal of low-activity variants. Finally, the purification of certain variants offers the opportunity to “straighten out” differences in feed variant compositions to a great extent. This feature may be particularly useful for production processes displaying large product variability in the upstream part or a different variant pattern due to process changes. These aspects are particularly relevant for quality control and regulatory purposes.

2.5. Remark

The work presented in this chapter has been published in:
Müller-Späth T, Krättli M, Aumann L, Ströhlein G, Morbidelli M. 2010. Increasing the Activity of Monoclonal Antibody Therapeutics by Continuous Chromatography (MCSGP). *Biotechnology and Bioengineering* 107(4):652-662. [Full text](#)

3. Multifraction separation in Continuous Chromatography (MCSGP)

3.1. Introduction

Biomolecules, such as recombinant proteins, are steadily gaining importance as therapeutics, leading to increasing demand for adequate purification methods for such molecules [43, 44]. The production of recombinant proteins is traditionally done by cell culture (fermentation), which leads to large amount of impurities such as host cell proteins (HCP), aggregates and DNA fragments in the cell culture harvest. The purity specifications for therapeutics are very strict and therefore it is not surprising that the downstream purification of the desired product is the most expensive part of the process [45]. Most downstream processes for biomolecules are related to chromatographic processes, operated under discontinuous ("batch") conditions [46]. A possible reduction of the cost can be achieved applying continuous chromatography which shows an increase in productivity compared to batch chromatography. The most widely known continuous chromatography process is the simulated moving bed (SMB) [14, 17]. In normal SMB setup, only two fractions can be separated which limits the application to binary separation problems such as chiral separations [47, 48]. SMB chromatography is widely applied for small molecule separations under isocratic conditions with high yield and purity.

For the purification of biomolecules, solvent gradients are most often applied, a feature with is not compatible with classical SMB operation. Additionally, the purification problems require at least three fraction separations, as the raw product contains early and late eluting impurities. For this kind of center cut purification, SMB cannot be applied.

For ternary separations using solvent gradients the multicolumn countercurrent solvent gradient purification (MCSGP) process was developed. The technology was initially designed for three fraction separation and applied linear solvent gradients [1]. The process was described first as a fully continuous process (steady feed supply and steady product elution) applying five [49] and six columns [1]. To save stationary phase material and pumps, various process modifications have been proposed subsequently. A semi continuous process with three columns was introduced [21] where each column fulfills alternating two functions. This setup was expanded to a four column process, in which the additional column can be either used for continuous loading [40] or different types of cleaning in place (CIP) [39]. Recently, a twin-column setup has been developed [50].

The MCSGP process has been applied for different purification problems such as the purification of peptides in reversed phase mode [1], the purification of monoclonal antibody (mAb) charge variants [36, 51] and the purification of mAb from a clarified cell culture supernatant [40], both in cation exchange chromatography. The sensitivity of the process towards parameter changes has been discussed in the literature [36, 37]. To increase the robustness of the process some automatic control strategies have been introduced [52, 53].

In the classical design procedure [1], the MCSGP operating parameters (pump flow rates, gradient concentrations and switching times) are derived from an experimental preparative batch experiment which is considered to be suitable. The batch chromatogram is divided into sections corresponding to the different MCSGP tasks such as elution of the pure product and recycling of overlapping peaks. A detailed description of the MCSGP design can be found in literature [54].

In the frame of this work, the three column MCSGP process [21] is extended to the separation of more than three (overlapping) fractions. In principle, the batch elution described above can be transformed into a continuous process with n fractions applying one additional column for each additional fraction. In process application, the number of columns is limited by the pressure drop over all columns in the interconnected phase. The experimental application is therefore limited to a finite number of fractions. In this work, four fractions have been considered.

The extension of the MCSGP process to collect multiple pure fractions can be of interest for purification problems with more than one desired compound. A typical example is the fractionation of a mAb in its variants. Another one would be the purification of proteins from human blood plasma. The plasma contains a large number of different human proteins of which some were identified as high valued targets for purification. Currently, a cascade of purification steps is necessary to purify these proteins [55].

In this work, the use of MCSGP to collect multiple fractions is demonstrated by separating four proteins from a model mixture. In addition, the two main charge variants of Cetuximab (Erbix[®]) were separated in a single operation using an extended MCSGP process. Cetuximab shows a complex variant pattern exhibiting various variants each of which can be purified with cation exchange chromatography (CIEX) using MCSGP. It is worth noting that the problem of recovering the most dominant variant was already discussed with reference to the three fraction MCSGP process [51].

3.2. The multi fraction MCSGP process

3.2.1. From three to four fraction MCSGP

To explain the four fraction MCSGP process, it is helpful to first consider in detail the process design of a three fraction separation. For the design of a given MCSGP process, the starting point is a batch chromatogram considered “suitable” such as the one schematically shown in Figure 3.1 and referred to in the sequel as the “design batch chromatogram”. The upper part of the figure shows the batch elution chromatogram of a generic three fraction separation, with the desired product P eluting as the middle fraction and W and S as the early and late eluting impurities, respectively. The chromatogram contains parts where only one of the three fractions is eluting, while other regions contain overlapping peak fractions. Therefore in any case, running this process results in a tradeoff between the two extreme situations of either collecting the complete

product peak including some impurities, or collecting only pure product but with a lower yield. In the bottom part of the figure, the corresponding modifier gradient is displayed.

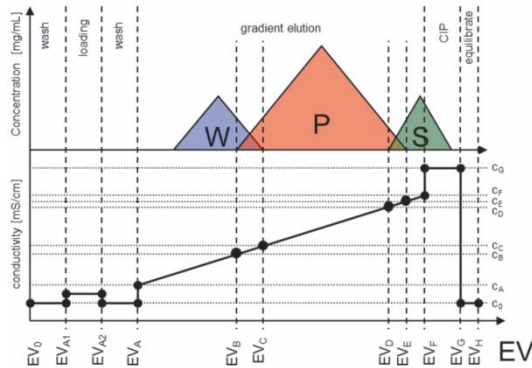


Figure 3.1 Schematic batch elution chromatogram containing three fractions. In the top part of the figure, the schematic elution chromatogram with the target component *P* and the early and late eluting impurities *W* and *S* is shown. On the bottom, the corresponding modifier gradient is displayed.

From the batch elution chromatogram shown in Figure 3.1 as a function of the eluted volume, *EV*, which is considered in the sequel as the “design batch” we want to implement, one can derive the operating conditions of the three fraction MCSGP process. This is done separating the complete elution gradient in six sections. As shown from the left to right in Figure 3.1, these are: The sections corresponding to the tasks of eluting the early eluting impurity *W* (*EV*_A to *EV*_B), the overlapping region of *W* and *P* (*EV*_B to *EV*_C), the pure product *P* (*EV*_C to *EV*_D), the overlapping region of *P* and *S* (*EV*_D to *EV*_E) and finally the late eluting impurities *S* and reequilibration (*EV*_E to *EV*_H). For these six sections, the elution volumes and modifier gradient start and end concentrations can be extracted from the “suitable” batch run. For the MCSGP run, these values are kept unchanged so as to ensure the same elution chromatogram. The six sections are distributed in the MCSGP process on 6 column positions as shown in Figure 3.2. Physically, the number of columns can vary between 3 and 6 as described in the above mentioned literature since not every column position has to be occupied at each point in time [1, 21, 39]. The process operation can be better explained starting from column position 6 in Figure 3.2. There, the entering stream contains all *W* and the overlapping fractions of *W* and *P*. To guarantee retention of all components, the entering stream is mixed with pure adsorbing eluent from pump P6. The stream leaving column position 6 ideally only contains eluent and very weakly or non-adsorbing impurities. In position 5, pure *W* is eluted from the column. This is not done in gradient mode, but in parallel with feeding the column. From position 4 on, the relevant modifier gradient - the elution of product *P* - starts. In position 4, the overlapping regions of *P* and *S* enter the column from position 2, while the overlapping regions of *P* and *W* leave to position 6. The gradient in the column is adjusted to the one from the batch

elution (EV_B to EV_C in Figure 3.1) by pump P4. In position 3, the pure product P is eluted according to the batch chromatogram (EV_C to EV_D). In position 2, the overlapping regions of P and S are eluted according to the batch gradient (EV_D to EV_E). In position 2, all remaining product has left the system and the remaining S is eluted by a step gradient and cleaning in place (CIP) in position 1. Finally, the column is reequilibrated and this completes the so called cycle. It is worth noting that the two positions can be grouped into two types of tasks: recycling in an interconnected flow scheme (referred to as interconnected lane) and batch wise elution (referred to as batch lane). One subsequent interconnected and batch lane are called a switch.

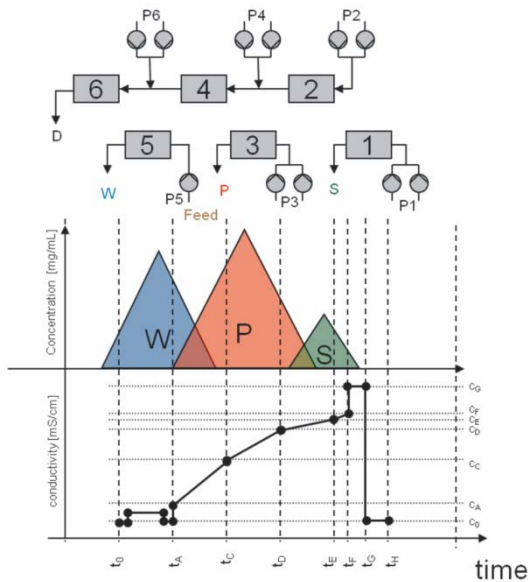


Figure 3.2 Schematic of the three fraction MCSGP process. On top the process flowsheet is shown. In the graphs in the middle and on the bottom, schematic UV and conductivity diagrams are shown, respectively. The vertical, dotted lines indicate section borders. The columns move every switch one position from 6 to 1, fulfilling alternating batch elution (uneven column positions) and interconnected recycling (even column positions) functions.

Let us now proceed to the four fraction separation unit. In this case, an equivalent design procedure can be applied. The MCSGP unit design is starting from the “design batch” experiment as the one shown in Figure 3.3. Similarly to the three fraction process, the batch elution chromatogram contains regions with pure components and others with overlapping components. Contrary to the design batch chromatogram of the three fraction process (Figure 3.1), the elution now contains four species, the early and late

eluting impurities W and S , respectively, and the two species P_1 and P_2 which we consider in the following as valuable components. Accordingly, eight different regions during the batch elution can be identified: Elution of pure early eluting impurities (W), elution of a mixture of W and P_1 , elution of pure product 1 (P_1), elution of overlapping P_1 and P_2 , elution of pure product 2 (P_2), elution of overlapping P_2 and S and finally elution of pure late eluting impurities (S), cleaning and reequilibration of the column.

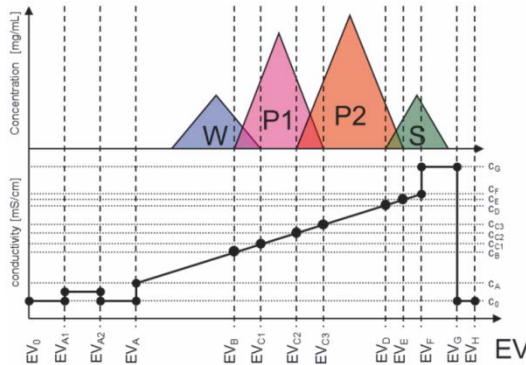


Figure 3.3 Preparative batch chromatogram for the four fraction process. The “design batch” is divided into eight parts corresponding to the eight different tasks in the MCSGP

In order to design now the four fraction MCSGP based upon the “design batch” chromatogram in Figure 3.3, the same strategy is applied as for the three fraction process. First, the column tasks are identified from the “design batch” chromatogram. Contrary to the three fraction MCSGP, the four fraction one carries out eight tasks in total, namely eluting of early eluting impurities (W), recycling of overlapping regions of early eluting impurities and the first product (P_1), collection of the first product (P_1), recycling of overlapping regions between the two products (P_1 and P_2), collection of the second product (P_2), recycling of overlapping regions between the second product (P_2) and late eluting impurities (S) and finally a step including collection of late eluting impurities (S), cleaning in place and equilibration of the column. To translate the “design batch” chromatogram (Figure 3.3) into the four fraction MCSGP process (Figure 3.4), the sequential tasks described above are distributed among the four columns of the MCSGP process. Following the same procedure as for the three fraction MCSGP, the description of the detailed process operation starts at column position 8 in Figure 3.4. Here, the stream containing W and P_1 enters the column, diluted with adsorbing eluent to ensure binding conditions. In position 7, W is eluted while feeding the column. In position 6, the relevant part of the gradient starts with the elution of the overlapping fractions of W and P_1 while the overlapping fractions of P_1 and P_2 enter the column. The internal gradient is adjusted according to the “design batch” chromatogram section (EV_B to EV_{C1} in Figure 3.3) through pump P6. In position 5, P_1 is eluted according to the gradient in EV_{C1} to EV_{C2} . In position 4, the overlapping regions of P_1 and P_2 are eluted from the column while the overlapping

fractions of P_2 and S enter the column. The gradient is adjusted to EV_{C_2} to EV_{C_3} . In position 3, P_2 is eluted according to the gradient in EV_{C_3} to EV_D . In position 2, the overlapping fraction of P_2 and S are eluted from the column with an eluent gradient from EV_D to EV_E . In position 2, the column is freed of product P_2 and the remaining S is eluted by a step gradient in position 1, followed by column reequilibration. It is worth noting that the concept of four fraction MCSGP is very similar to the three fraction one since in both cases alternating interconnected and batch lanes can be identified. Of course, in order to run the four fraction process, 4 or 8 columns are required to either run semi continuous, or fully continuous operation, respectively.

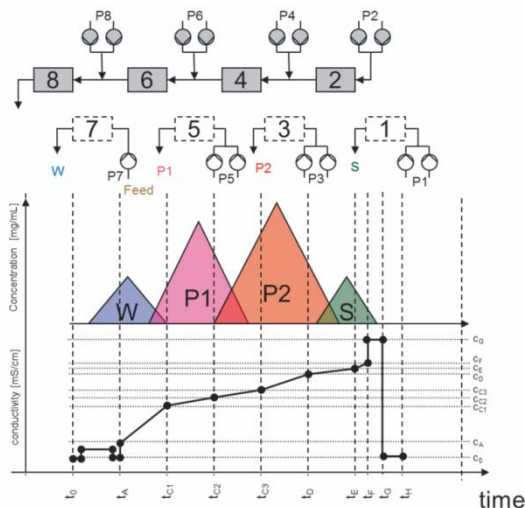


Figure 3.4 Schematic overview of the four fraction MCSGP process. On top the process flowsheet is shown. In the graphs in the middle and on the bottom, schematic UV and conductivity diagram are shown. The vertical, dotted lines indicate column switching. The columns move every switch one position from 8 to 1, fulfilling alternating batch elution (uneven column positions) and interconnected recycling (even column positions) functions.

3.2.2. From four to n- fraction MCSGP with $n > 4$

The extension of the MCSGP process from three to four fraction separations described in the previous section opens up immediately the possibility to extend this same concept to any number of n fractions, with n larger or equal than four. For example, by splitting the “design batch” chromatogram into 10 instead of 8 tasks and introducing two more column positions in the MCSGP process, the purification of an additional stream becomes possible as shown Figure 3.5. Continuing further in this direction, a n fraction MCSGP could be realized by splitting the “design batch” chromatogram into $2 \cdot n$ tasks and

designing a MCSGP process with $2 \cdot n$ column positions, equivalent to n columns in the case of the semi continuous operating mode. Thus summarizing this means starting from the semi continuous three fraction MCSGP which includes 3 columns, one can purify for each additional column one additional fraction which is indicated by the highlighted column position in Figure 3.5. In practice, the addition of further column is of course at some point limited by the pressure drop over all columns during the interconnected phase.

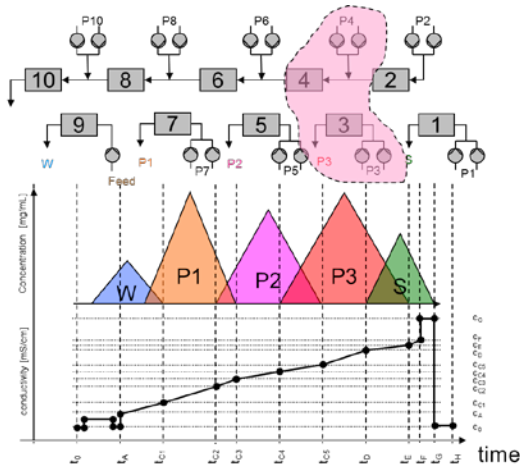


Figure 3.5 Five fraction MCSGP schematic, highlighting in red the hardware additionally required to separate one additional fraction. Adding this highlighted hardware multiple times, the MCSGP can separate as many fractions as columns available.

3.2.3. Design equations

As described above, the selected “design batch” chromatogram (e. g. the one shown in Figure 3.3) is splitted in the eight tasks performed by the four fraction MCSGP process. For each of these in the batch operation mode, the elution volume corresponding to the i -th task, EV_i , as well as the modifier concentration at the beginning and at the end of the task, c_i , are known from the section borders that were set in the “design batch” chromatogram. For each column position, the flow rate through the column is calculated from the corresponding batch elution volume using equations 3.1 to 3.7. For the batch column positions (1, 3, 5, 7) and the first position in the interconnected phase (2), the streams enter the column directly without being mixed with any other stream. On the other hand for each of the tasks in the interconnected operation mode, the elution volumes as well as the modifier concentrations are the result of stream mixing. In particular, the stream entering each column is obtained by mixing the stream exiting the upstream column with

the stream delivered by a gradient pump, represented by P4, P6 and P8 in Figure 3.4. A schematic of this part of the unit is shown in Figure 3.6.

For the interconnected column positions (4, 6 and 8), the feed flow rate to the i -th column, $Q_{i,in}$, is then given by the added flow rate, $Q_{i,add}$ and the outlet flow rate of the previous column in the interconnected operation mode, $Q_{i-2,out}$. In the following, the equations for determining the MCSGP operating parameters for a four fraction separation are reported.

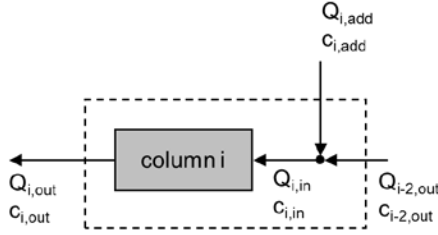


Figure 3.6 Schematic overview of streams around a column and a mixing knot in the MCSGP process.

$$Q_{1,out} = Q_{1,add} = Q_{1,in} = \frac{EV_H - EV_E}{t_{BL}} \quad 3.1$$

$$Q_{2,out} = Q_{2,add} = Q_{2,in} = \frac{EV_E - EV_D}{t_{IC}} \quad 3.2$$

$$Q_{3,out} = Q_{3,add} = Q_{3,in} = \frac{EV_D - EV_{C3}}{t_{BL}} \quad 3.3$$

$$Q_{4,out} = Q_{4,in} = \frac{EV_{C3} - EV_{C2}}{t_{IC}} \quad 3.4$$

$$Q_{4,in} = Q_{2,out} + Q_{4,add}$$

$$Q_{5,out} = Q_{5,add} = Q_{5,in} = \frac{EV_{C2} - EV_{C1}}{t_{BL}} \quad 3.5$$

$$\begin{aligned}
Q_{6,out} &= Q_{6,in} = \frac{EV_{C1} - EV_A}{t_{IC}} \\
Q_{6,in} &= Q_{4,out} + Q_{6,add}
\end{aligned}
\tag{3.6}$$

$$Q_{7,out} = Q_{7,add} = Q_{7,in} = \frac{EV_A - EV_o}{t_{BL}}
\tag{3.7}$$

It is worth noting that in equation 3.7, the inlet flow rate, $Q_{7,in}$, refers to the process feed while $Q_{1,in}$ in equation 3.1 refers to the column cleaning in place (CIP) and reequilibration. It is worth noting that since these quantities do not affect the gradient elution, they might be changed in freely with respect to the “design batch”. From equation 3.1 to equation 3.7, a first constraint for the process design can be derived. In particular, the flow rate has to increase or stay constant along the interconnected columns, but it always has to remain below a certain maximum flow rate, Q_{max} , determined by the column and the packing material backpressure or by the pumps capacity:

$$Q_{2,out} \leq Q_{4,out} \leq Q_{6,out} \leq Q_{8,out} \leq Q_{max}
\tag{3.8}$$

The concentrations of the modifier at the column inlets, $c_{i,in}$, have to be equal to the values in the “design batch” chromatogram at the section borders (Figure 3.3). Thus, for all batch column positions (1, 3, 5, 7), the column inlet modifier concentration $c_{i,in}$ is equal to the modifier concentration from the added pump stream, $c_{i,add}$, as no stream mixing is applied. The concentrations at the beginning and the end of each batch and interconnected operation mode are determined in such a way to reproduce the modifier gradient in the “design batch” chromatogram, whereby the modifier concentrations at the end of a certain phase is equal to the starting value of the following one.

$$\begin{aligned}
c_{2,in} \Big|_{t=0} &= c_D \\
c_{2,in} \Big|_{t=t_{IC}} &= c_E
\end{aligned}
\tag{3.9}$$

$$\begin{aligned}
c_{3,in} \Big|_{t=0} &= c_{C3} \\
c_{3,in} \Big|_{t=t_{BL}} &= c_D
\end{aligned}
\tag{3.10}$$

$$\begin{aligned}
c_{4,in} \Big|_{t=0} &= c_{C2} \\
c_{4,in} \Big|_{t=t_{IC}} &= c_{C3}
\end{aligned}
\tag{3.11}$$

$$\begin{aligned} c_{5,in} \Big|_{t=0} &= c_{C_1} \\ c_{5,in} \Big|_{t=t_{R_2}} &= c_{C_2} \end{aligned} \quad 3.12$$

$$\begin{aligned} c_{6,in} \Big|_{t=0} &= c_A \\ c_{6,in} \Big|_{t=t_{IC}} &= c_{C_1} \end{aligned} \quad 3.13$$

The concentrations $c_{i,in}$ in column positions 1 and 7 are not part of the gradient elution and are therefore determined independently of the “design batch” chromatogram. Position 7 is the feeding step and position 1 the final cleaning, composed of strip, CIP and reequilibration.

For the interconnected phases, an additional material balance over the mixing node is solved so as to define the modifier concentration of the added stream, $c_{i,add}$.

$$\begin{aligned} c_{4,add} \Big|_{t=0} &= \frac{Q_{4,in} c_{4,in} \Big|_{t=0} - Q_{2,out} c_{2,out} \Big|_{t=0}}{Q_{4,add}} \\ c_{4,add} \Big|_{t=t_{IC}} &= \frac{Q_{4,in} c_{4,in} \Big|_{t=t_{IC}} - Q_{2,out} c_{2,out} \Big|_{t=t_{IC}}}{Q_{4,add}} \end{aligned} \quad 3.14$$

$$\begin{aligned} c_{6,add} \Big|_{t=0} &= \frac{Q_{6,in} c_{6,in} \Big|_{t=0} - Q_{4,out} c_{4,out} \Big|_{t=0}}{Q_{6,add}} \\ c_{6,add} \Big|_{t=t_{IC}} &= \frac{Q_{6,in} c_{6,in} \Big|_{t=t_{IC}} - Q_{4,out} c_{4,out} \Big|_{t=t_{IC}}}{Q_{6,add}} \end{aligned} \quad 3.15$$

From equations 3.14 and 3.15, additional constraints arise from the fact that the modifier concentration has to be positive:

$$\begin{aligned} c_{4,add} &\geq 0 \\ c_{6,add} &\geq 0 \end{aligned} \quad 3.16$$

3.3. Materials and methods

3.3.1. Protein model mixture

A model mixture of α -Chymotrypsinogen, Cytochrome C, Lysozyme and Avidin was prepared with a concentration of 1 g/L for each individual protein. The mixture was filtered (45 μ m) and adjusted to pH 6.0 with 1M NaOH. An analytical chromatogram of the

mixture is shown in Figure 3.7. The impurities and isoforms coming with the proteins were not further characterized for purity estimations and lumped together with the closest eluting protein. Purity and concentration of the products obtained in preparative cation exchange chromatography were determined by analytical cation exchange gradient chromatography using phosphate buffers on a 1200 Series (Agilent, Santa Clara, CA). The unit consists of a degasser, a quaternary pump, a thermostated autosampler, a heated column compartment and a DAD detector. The chromatograms of the protein model mixture and Cetuximab were obtained with a YMC BioPro-SP-F. Details on the analytics are given in Table 3-1.

Table 3-1 Parameters for protein standard sytem and Cetuximab analytics.

	unit	Protein model mixture	Cetuximab
Interaction	[-]	Cation exchange	
Resin	[-]	BioPro SP-F	
Manufacturer	[-]	YMC	
Functionalization	[-]	Sulfonyl	
Length	[cm]	3	
Diameter	[cm]	0.46	
Mobile phase A	[-]	25 mM Phosphate, H ₂ O	
Mobile phase B	[-]	25 mM Phosphate, 1 M NaCl, H ₂ O	
pH mobile phase	[-]	6.0	
Flow rate	[mL/min]	0.5	
Gradient start	[%B]	10	16
Gradient end	[%B]	60	32
Gradient duration	[min]	15	9
Detector wavelength	[nm]	280 / 400	280

The product fractions of the preparative experiments were analyzed with analytical cation exchange chromatography on an Agilent 1200 system. An YMC Bio Pro SP-F column with 5 µm non porous particles and dimensions 0.46 x 3.0 cm was used. The parameters for the analytics are summarized in Table 3-1.

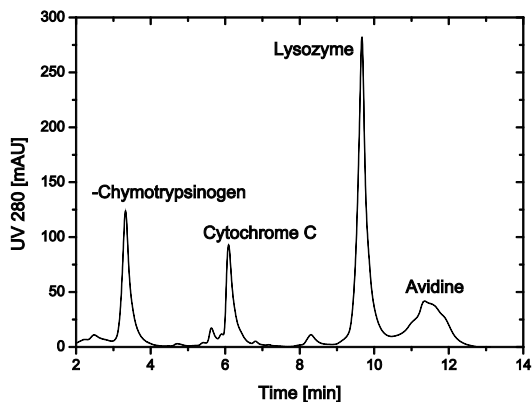


Figure 3.7 Analytical cation exchange chromatogram of the protein model mixture

3.3.2. Monoclonal antibody

Erbix[®] (Merck-Serono, Darmstadt, Germany) containing the IgG₁ Cetuximab was bought from a pharmacy. The chimeric mAb is produced from SP2/o cells and contains at least 8 charge variants with isoelectric points between 8.2 and 8.9. The purification target for this work was arbitrarily selected as one of the two charge variants Cet-3 and Cet-4 which account for 13.8% and 21.2% of the total area, respectively. The mAb charge heterogeneity was determined by analytical cation exchange chromatography as reported in Table 3-1. The variants are numbered according to their elution time as shown in the analytical chromatogram in Figure 3.8. In some cases, variants which were not clearly distinguishable were lumped together and treated as one component.

For preparative experiments on the cation exchange chromatography stationary phase, the mAb was diluted with binding buffer to 0.5 g/L.

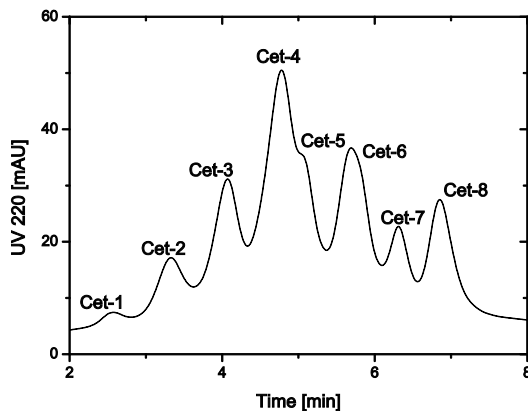


Figure 3.8. Nomenclature of the mAb variants of Cetuximab.

3.3.3. Stationary phases, buffers and hardware

For the model protein separation, cation exchange chromatography was applied. Four identical, prepacked columns (Atoll, Weingarten, Germany) with dimensions 0.5 x 5 cm packed with Fractogel EMD SO₃ (M) (Merck, Darmstadt, Germany) were used.

For the monoclonal antibody, preparative cation exchange chromatography with YMC Bio Pro SP-10 resin was used in 0.75 x 15 cm PEEK columns (YMC, Kyoto, Japan). The resin was packed with a linear velocity of 540 cm/h with Na₂SO₃ as packing buffer. The average particle size of the resin was 10 µm and it was functionalized with sulfonyl groups. The columns were tested after packing for similarity in peak shape and retention time applying linear gradient elutions of analytical mAb injections. The column tests were performed on an Agilent 1100 Series unit (Agilent, Santa Clara, CA) consisting of a degasser, quaternary pump, autosampler, heat exchanger and DAD detector. All preparative batch and MCSGP experiments were performed on a modified ÄKTA Basic equipment (GE Healthcare, Uppsala, Sweden) consisting of 4 two-channel pumps P-900, 8-port switching valves, 2-way buffer valves, 2 online UV-900 and 2 combined pH/Conductivity pH/C-900. The unit was controlled by UNICORN software using a modified software strategy on a standard PC. The setup allows running up to four columns with three gradient and one isocratic pump, as needed for the four fraction process. The parameters of the “design batch” chromatogram as well as the corresponding optimized final MCSGP parameters derived from the “design batch” chromatogram are listed in Table 3-2.

Table 3-2 MCSGP parameters derived from the “design batch” elution chromatogram for the protein model mixture and Cetuximab

Operating variable	Units	Protein model mixture	Cetuximab
Interconnected phase			
Duration	min	6.0	18.0
Flow P2	mL/min	0.17	0.10
Flow P4	mL/min	0	0.10
Flow P6	mL/min	0.72	1.14
Flow P8	mL/min	0.11	0.16
Gradient P2 Start	%	63.9	28.9
Gradient P2 End	%	69.2	29.7
Gradient P4 Start	%	-	25.1
Gradient P4 End	%	-	27.5
Gradient P6 Start	%	1.6	14.1
Gradient P6 End	%	35.2	26.4
Gradient P8 Start	%	0	0
Gradient P8 End	%	0	0
Batch phase			
Duration	min	3.0	12.0
Flow P1	mL/min	1.00	0.70
Flow P3	mL/min	0.77	0.05
Flow P5	mL/min	1.00	0.05
Flow P7	mL/min	0.33	0.32
Gradient P1	-	CIP, Equilibration	
Gradient P3 Start	%	51.6	28.6
Gradient P3 End	%	63.9	28.9
Gradient P5 Start	%	38.3	26.7
Gradient P5 End	%	46.3	27.0

3.4. Results and discussion

3.4.1. Purification of the protein model mixture

The first experimental proof of the multifraction MCSGP separation process described above is discussed in the following with reference to a four component fractionation using the protein model mixture described above. The mixture was loaded on a single preparative column and eluted using a modifier gradient. The elution was fractionated (0.5 mL per fraction) and each fraction analyzed with offline HPLC. The gradient elution was optimized resulting in the final design batch run shown in Figure 3.9. The analyzed fractions show almost pure regions for each one of the four components, although many fractions contain overlapping regions, i.e. mixtures of two components. The basic idea of the MCSGP process is to elute the pure fractions of the “design batch” chromatogram, while recycling internally the overlapping ones.

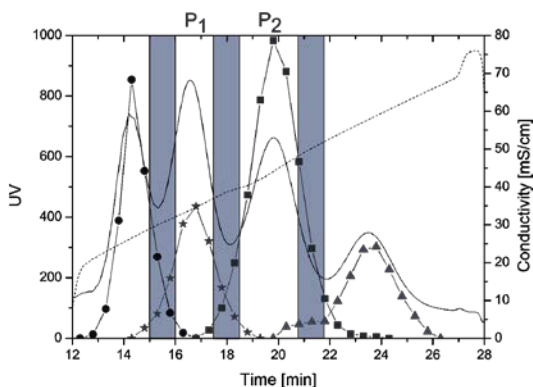


Figure 3.9 “Design batch” chromatogram of the model protein mixture showing online UV (solid line), modifier gradient (dashed line) and fraction analysis for the 4 components (*W*: cycles, *P1*: stars, *P2*: squares, *S*: triangles). Additionally, the recycled fractions for the MCSGP process are indicated by the grey areas. In between the recycled fractions, the collection windows of the two products *P1* and *P2* are indicated.

Figure 3.9 was taken as the “design batch” chromatogram to design the four fraction MCSGP process. The chromatogram regions containing the purest proteins were defined as batch elution windows (1, 3, 5, 7), while the overlapping regions were recycled internally during the interconnected phases (2, 4, 6, 8). The flow rates, gradient points and phase durations were calculated according to the material balance equations 3.1 to 3.16 and the obtained values are summarized in Table 3-2. The MCSGP process was run to cyclic steady state and at each cycle, the outlet streams of *P1* and *P2* were collected and analyzed offline. The obtained values are shown for both products as a function of time in terms of purity and yield in Figure 3.10. The eluting fractions of *W* and *S* were only collected at

steady state. From the data in Figure 3.10 it appears that the process is close to cyclic steady state operation already at cycle 6 on. The yield for both P_1 and P_2 lies constantly above 90% and the mass balance is closed. In the final cycle, P_1 (Cytochrome C) elutes with a yield of 95% and a purity of 94%. The 6% impurities are α Chymotrypsinogen which should elute in stream W . Yield and purity of P_2 (Lysozyme) in cycle 10 lie at 92% and 97%, respectively. The only detectable impurity is S (Avidin), thus indicating that an elongation of the P_2 / S recycling phase would further improve the process performance with respect to these parameters (column position 2).

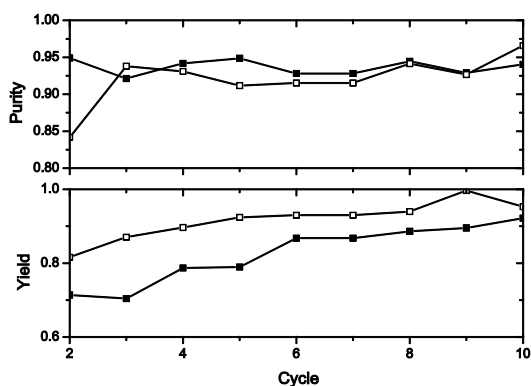


Figure 3.10 Startup of the MCSGP process monitored through the fraction analysis of the center products P_1 (□) and P_2 (■). In the upper part of the figure the purity is shown and in the lower part the yield.

In the final cycle after reaching steady state, all eluting streams were collected and analyzed with offline HPLC. Figure 3.11 shows an overlay of the chromatograms of all eluting streams (i. e. W , P_1 , P_2 and S) compared to the feed chromatogram. It is seen that each eluting stream contains mainly one protein, thereby proving the concept of the four fraction MCSGP operation.

It has to be mentioned that due to the low total load (4 g/L), the concentrations in the eluting streams are lower than the feed concentration. Under process conditions, a higher load would have to be applied in order to increase the productivity and achieve a concentration increase of the protein in each outlet stream.

In order to compare the performance of the “design batch” and the MCSGP process, the corresponding performance has been shown in a yield purity diagram (Figure 3.12). Such diagram can be obtained from the “design batch” chromatogram shown in Figure 3.9. Keeping the given modifier gradient, cuts can be introduced defining the product collection window. Choosing these cuts in such a way that for a given yield the maximal purity is reached, a distinct point on the pareto front of the “design batch” chromatogram

is defined. Repeating this step for various yield values, a pareto front can be drawn as indicated by the dashed line in the purity yield diagram in Figure 3.12. By designing the MCSGP process upon the “design batch” and keeping the same modifier gradient, a comparison between the MCSGP process and the batch pareto can be made. In fact, one could describe a complete pareto curve for the MCSGP process as well, however, normally only a single MCSGP operating point is explored corresponding to a desired product purity. It is worth noting that for the case of the four fraction MCSGP, two yield purity diagrams are required to describe the behavior for the two center products (P_1 and P_2).

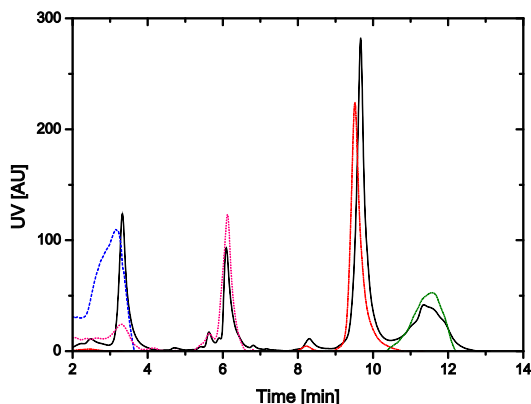


Figure 3.11 Fraction analysis of the feed (black solid line) and the four MCSGP outlet streams (W : blue dashed line, P_1 : pink dotted line, P_2 : red dash dotted line and S : green dash dot dotted line) for the protein model mixture. The y axis is shown in arbitrary units to compare the peaks.

Comparing the batch and MCSGP performances in Figure 3.12, it is seen that the batch operation can only achieve either high yield but moderate purity or high purity but lower yield, while for the MCSGP process such tradeoff is not observed.

In addition, MCSGP is known to provide significantly increased productivity values with respect to batch operation as described in the literature [51]. This holds true also for the four fraction unit. The overall productivity for the model mixture under examination could in fact be increased from 2.9 g/mL_{Column}/hr to 3.1 g/mL_{Column}/hr using the four fraction MCSGP with respect to the “design batch”.

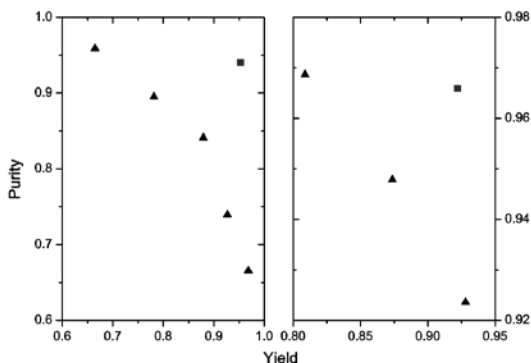


Figure 3.12 Purity versus yield diagram for P_1 (Cytochrome C, left) and P_2 (Lysozyme, right). The squares indicate the MCSGP steady state performance while the triangles indicate points for different cuts of the “design batch” chromatogram thereby forming the pareto curve indicated by the dashed line.

3.4.2. Monoclonal antibody variant separation

The four fraction MCSGP separation unit has been applied to the challenging Cetuximab variants separation process (see Figure 3.8). The variant Cet-4 of Cetuximab has already been isolated successfully in an earlier study [51] using the classical three fraction MCSGP unit. In this work, Cet-4 and its neighboring weakly adsorbing variant Cet-3 were separated from the mixture. Starting from a design batch chromatogram (Figure 3.13), the MCSGP process was designed. It is apparent that this separation was much more challenging than that involving the four proteins model mixture since in this case there is no region of complete separation. Accordingly, some impurities had to be tolerated in both product streams along with Cet-3 and Cet-4. The loads of the design batch run and of the MCSGP process are equal to about 0.3 g antibody per liter column volume, which is low for a preparative process, but justified by its prohibitive cost.

The MCSGP unit was operated for 6 cycles. The streams P_1 and P_2 were collected from the last cycle and the corresponding analytical chromatograms are compared to the one of the feed in Figure 3.14. The purity of P_1 and P_2 with respect to the desired mAb charge variants was 90% and 89%, respectively. These values correspond to purity values of the purest batch fractions which can be extracted from the “design batch” chromatogram as equal to 89% and 90%, respectively. The yield of the MCSGP process was 81% for P_1 and 65% for P_2 .

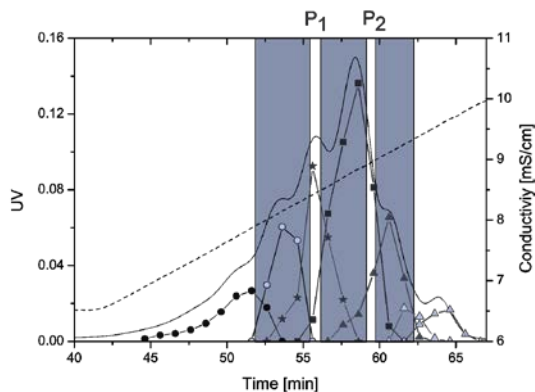


Figure 3.13 “Design batch” chromatogram of Cetuximab, including the online UV signal (solid line), the modifier gradient (dashed line) and the concentrations of the eight variants of Cetuximab: Cet-1(W): filled circles, Cet-2(W): open circles, Cet-3(P₁), stars; Cet-4(P₂), squares; Cet-5 + Cet-6(S), filled triangles; Cet-7 + Cet-8(S), open triangles. The grey areas indicate the recycling fractions selected for the MCSGP operation while in between these, the collection windows for the product streams P₁ and P₂ are indicated.

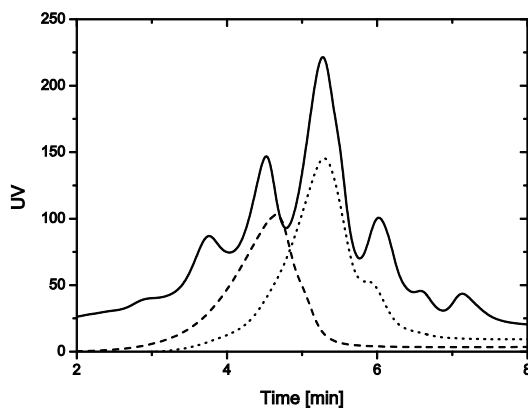


Figure 3.14 Analytical chromatograms of the MCSGP feed stream (solid line) and the product streams P₁ (Cet-3, dashed line) and P₂ (Cet-4, dotted line). The y axis units are normalized, as the concentrations in the three samples are different.

As for the protein model mixture, two purity yield diagrams can be applied to compare the “design batch” and four fraction MCSGP with respect to purity and yield. As described earlier, different cuts for the product collection in the “design batch” chromatogram

(Figure 3.13) are resulting in points corresponding to the pareto curve of the “design batch” in the purity yield diagram represented by the dashed line in Figure 3.15. The MCSGP process derived from this “design batch”, therefore sharing the modifier gradient, is added for comparison and represents a distinct point of a MCSGP pareto. It is seen that the MCSGP process can reach a point above the “design batch” pareto for both product streams meaning it can outperform the “design batch” with the same modifier gradient with respect to yield and purity.

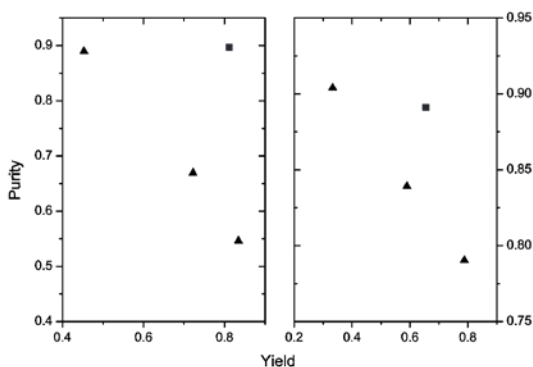


Figure 3.15 Purity yield diagrams for Cet-3 (P1) and Cet-4 (P2) on the left and on the right, respectively. The squares indicate the results for the MCSGP process, the triangles the pareto front derived from the fractionation of the batch elution.

3.5. Conclusion

The MCSGP process originally developed for the gradient separation of three fractions has been extended a number of n larger three fractions using n columns. In principle, the only limitation to the number of fractions n comes from the maximum pressure drop which is obtained when all n columns are connected in series. In practice, it appears unlikely that the MCSGP process will be used to separate more than five fractions.

The multifraction MCSGP unit has been used in this work for the four fraction separation of two protein mixtures. The first one was a model mixture of four proteins: α -Chymotrypsinogen, Cytochrome C, Lysozyme and Avidin. The task of the separation process was to recover all four proteins almost pure. The MCSGP operating conditions were designed based on a preparative “design batch” chromatogram following the literature described in [1]. The performance of the MCSGP unit was compared to the pareto curve in terms of purity versus yield that can be obtained the “design batch” chromatogram which has the same modifier gradient. Of course, in the case of the four fraction separation process two such diagrams are needed, one for each product stream. It was found that the yield could be increased from 67% to 95% for Cytochrome C and from 81% to 92% for Lysozyme in comparison to the “design batch” for the same purity value.

As a second example, the mAb charge variant which is currently sold in the market as Cetuximab was considered. In a previous study [51], the variant pattern of Cetuximab has been identified and the main variant Cet-4 has been purified using the classical three fraction MCSGP. In this work, the two neighboring variants Cet-3 and Cet-4 which are the two most abundant ones have been separated using the four fraction MCSGP. Yields of 81% and 65% with corresponding purities of 90% and 89% were obtained for the two variants, respectively. These values appear quite favorable with respect to the “design batch” operation performance that for the same purity level exhibit yield values of 49% and 34%, respectively.

In conclusion, the above results confirm the possibility to extend the continuous countercurrent operation concept which characterizes the MCSGP process to more than three fractions, while maintaining its significantly improved performance with respect to the batch operation.

3.6. Nomenclature

Symbol	Units	Explanation
$Q_{i,out}$	mL/min	Outlet flow rate of column i
$Q_{i,in}$	mL/min	Flow rate into column section i after mixing
$Q_{i,add}$	mL/min	Flow rate added to mixing knot at column i
Q_{max}	mL/min	Maximum flow rate
$c_{i,in}$	mg/mL	Modifier concentration at column i after mixing
		Modifier concentration at cut point j in the batch elution
c_j	mg/mL	chromatogram
EV_j	mL	Elution volume in batch chromatogram
t_k	min	time of interval K

Subscripts	Range	Explanation
i	1 ... 7	Column position according to MCSGP schematic
j	o ... H	Cuts in batch elution chromatogram
K	IC, BL	Interconnected state, batch state

3.7. Remark

The work presented in this chapter is submitted for publication in the Journal Biotechnology and Bioengineering

4. Repetitive Closed Loop Control of the Multi Column Solvent Gradient Purification

4.1. Introduction

The multi column countercurrent solvent gradient purification technology (MCSGP) is a continuous chromatographic process to separate mixtures into three fractions [1, 37, 49]. In the frame of the present work, a three-column and a four-column MCSGP setup were used [21]. The four-column process derived from the three-column one having an extra column for additional wash and cleaning in place (CIP) steps. Both processes are shown in Figure 4.1. The method shows similarities to the simulated moving bed (SMB) [14] as the column positions are moved countercurrent to the eluent flow, however in the case of MCSGP, a repetitive switch consists of two distinct elements, an interconnected and a batch elution element which form a switch together. The complete turn of a column back to the initial position is called a cycle.

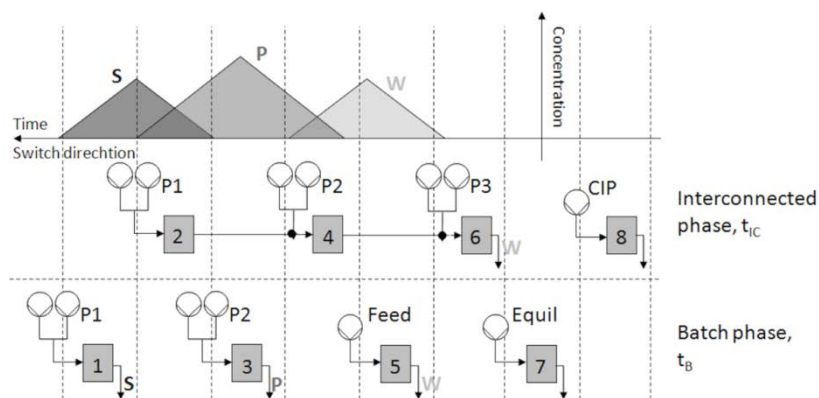


Figure 4.1 Schematic overview of the MCSGP process with three columns (Positions 1 – 6) and four columns with additional cleaning in place (all positions)

The main advantages of the MCSGP process compared to classical batch chromatography are high purity and productivity at once and in comparison to SMB chromatography are the ability to separate three fractions suited for center cut purifications and the applicability of solvent gradients. These advantages make the MCSGP best suited for the purification of biomolecules [36, 39, 51, 56].

For a continuous process like MCSGP, process stability and robustness are particularly important. Even though the MCSGP process is stable in its steady state without control, disturbances in feed quality, environmental parameters and malfunctions of the

hardware can lead to product purity changes and therefore economical losses. To minimize these risks, a controller is applied to the system. A number of different control concepts for continuous chromatography processes, namely SMB have been developed [57-65]. All these works applied a model predictive controller (MPC). This controller provides a fast and accurate control of the process, but as feedback it requires detailed online information about the mixture composition which requires significant effort particularly regarding the analytical part when dealing with biomolecules. More recently, a cycle to cycle repetitive control concept has been developed [66, 67]. Such a repetitive model predictive controller (RMPC) requires less frequent feedback information and can therefore apply more time consuming and more detailed analytical techniques to determine the composition of the outlet streams. For the experimental implementation to a SMB unit, Langel et al. [68] described an at-line HPLC analytics. The RMPC described by Grossmann et al. [66] was applied in a theoretical study to the MCSGP process [53] where it was assumed that a suitable analytical technique was available for measuring online the composition of the outlet streams at the end of each cycle. In the case of crudes of therapeutical proteins this can cause significant problems in practice.

A very simple control strategy can be developed based on the characteristics of the UV chromatogram that can be measured during each cycle. The MCSGP process is in fact typically designed starting from a preparative batch gradient chromatogram which is found to be appropriate for the specific purification problem. The batch gradient elution chromatogram consisting of product, early and late eluting impurities is then reproduced along the MCSGP unit by properly selecting the relevant operating conditions as described in detail by Aumann and Morbidelli [1]. The chromatogram of the batch elution and MCSGP process are then similar, their detailed shape may be a bit different, but the order of peak elution remains the same, and most important, the product elution window defined as the fraction of product elution fulfilling the purity constraints remains similar. The schematic chromatogram shown in Figure 4.1 can therefore be regarded both as a batch elution chromatogram as a function of time as well as the concentration profile along a MCSGP unit.

Accordingly, the design procedure of the MCSGP [1] is based on the concept of first selecting the elution window in the batch chromatogram which satisfies the specifications and then selecting the MCSGP operating conditions so that the same portion of the chromatogram is eluted in the product stream of the MCSGP. In the ideal case of symmetric peak shape and symmetric impurity distribution, the optimal position of the maximum of the product peak is in the middle of the product elution step. Under real conditions, the peak position can vary around this value mainly due to asymmetric distributions of early and late eluting impurities and column overloading. In this case the MCSGP product elution step should be properly shifted to the left or right of the maximum so as to obtain the desired purity level. In the design phase this shift can be determined by considering the batch chromatogram. In any case, it is worth noting that maintaining the position of the product peak constant relative to the MCSGP product elution step results in constant product purity and therefore in stable performance and operation of the unit. This is the objective that is given to the controller developed in this work. The actual peak position is derived from online UV, either by the position of the peak

maximum or its first moment. The switching time t_{ic} is then adjusted by the controller to keep such a peak in the middle of the product collection window. With this approximate but simple concept, even though the controller does not determine the actual mixture composition, the performance of the MCSGP unit can be kept constant with a purity value corresponding to the one found for the selected design batch chromatogram. It is worth noting that this controller has to be regarded as a very effective tool for the operator to properly run the MCSGP unit, but this requires in combination a suitable offline analytics so that the operator can quantitatively check the process purity and yield.

4.2. Controller development

The control concept can be subdivided into a number of steps which are consecutively executed in each control action. The function of each control step is elaborated including UV signal acquiring, UV signal processing, error evaluation and switching time change in the MCSGP process.

In the MCSGP unit used in this work, an online UV signal is recorded at each column outlet. The signals are stored in a matrix with one UV signal per column and a row per collected time. The collection interval is 5 Hz.

At the end of each column switch, the UV signals are processed. As each of the UV detectors has recorded a different quart of the MCSGP process (Figure 4.1), the four UV signals are combined yielding a complete MCSGP chromatogram, E. g. the concentration profiles along the MCSGP unit. If the controller is applied on a switch to switch base, the generated chromatogram is processed further directly. In the case of cycle to cycle control, four switches are recorded and therefore four total MCSGP chromatograms are generated which are ideally identical, but in fact can slightly differ due to differences in column packing or modifier gradients. The raw UV signals are averaged yielding one chromatogram which is further processed. Since we are using a standard PID controller which is a single input single output (SISO) controller, the final chromatogram from either cycle to cycle or switch to switch control has to be reduced to a single feedback time value, t_a . In this work, two different methods for single value reduction are discussed: First moment and peak maximum approach. In the first approach, the whole chromatogram is integrated and the first moment, equivalent to the feedback time, t_a , defined as follows (equation 4.1), is computed.

$$t_a = \frac{\int_0^{t_c+t_b} t UV(t) dt}{\int_0^{t_c+t_b} UV(t) dt} \quad 4.1$$

It is worth mentioning that this method requires the chromatogram to be baseline corrected.

The peak maximum method on the other hand simply requires evaluating the time value at the maximum of the chromatogram. To improve the feedback stability, the fraction of

the chromatogram containing the feeding and CIP steps are excluded from the maximum search, because the feed flow through and CIP agent can cause misleading large UV signals. The feedback time, t_a , resulting from the signal processing is forwarded to the error calculation of the PID controller.

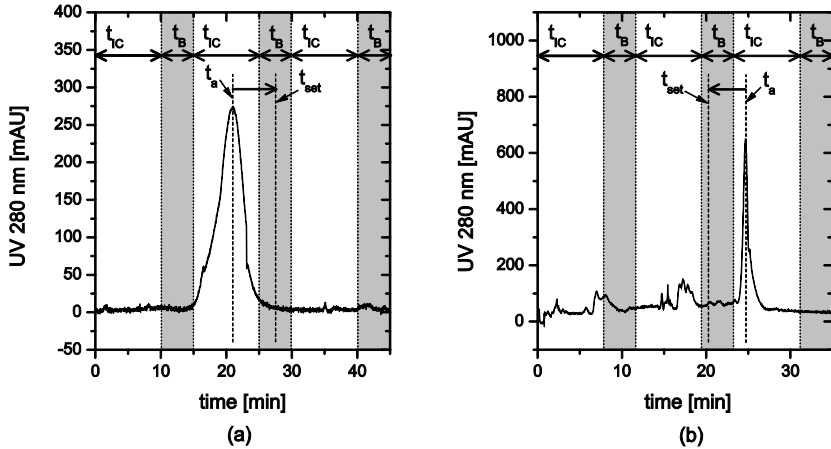


Figure 4.2 Explanation of the controller action. In subfigure (a), a symmetric peak without impurities with the corresponding set value is shown. In subfigure (b), an overloaded signal with early eluting impurities is and the resulting, shifted set value is shown.

The value, t_a , indicates in which position the portion of the UV chromatogram withdrawn as product stream is located along the unit. This value has to be confronted with the location that it should have to guarantee the process performance and the arising error decides the control action which is based on changing the interconnected time, t_{IC} , which linearly affects the position of the chromatogram along the unit. Such an ideal location is determined from the initial and final values of the pool in the selected design batch chromatogram. In the ideal case of symmetric product peak and impurity distribution, t_a should be located in the middle of the batch product pool (Figure 4.2(a)). In general, the ideal location of t_a will be shifted to one or the other extreme so as to reproduce the same profile as in the batch chromatogram and withdraw the desired product pool (Figure 4.2(b)).

The difference by the measured t_a and the set value based on the batch chromatogram provides the error that the controller tries to eliminate by changing the interconnected time, t_{IC} , which linearly affects the position of the UV chromatogram along the unit and therefore the value of t_a . The set value is chosen according to purity information obtained from the batch chromatogram.

4.3. Materials and Methods

4.3.1. Materials

The MCSGP controller was applied for the purification of two biomolecules: Lysozyme (Fluka, Buchs, Switzerland) and Fibrinopeptide A human (Bachem, Bubendorf, Switzerland). Both substances were purchased in solid form and stored at 4 °C. In our lab, the purity for Lysozyme was found to be 87 % and for Fibrinopeptide A human 20 %, respectively measured with analytical HPLC chromatography described in section 3.3. The resulting analytical chromatograms for both feeds are shown in Figure 4.3.

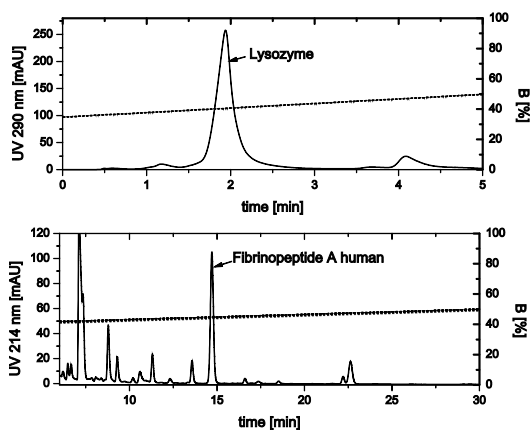


Figure 4.3 Analytical chromatograms for Lysozyme (top) and Fibrinopeptide A human (bottom) crudes. The chromatograms were obtained as indicated in the analytics section (4.3.3)

4.3.2. Preparative batch and MCSGP experiments

For the purification of Lysozyme, cation exchange chromatography (CIEX) was used. Fractogel EMD SO_3 (M) (Merck, Darmstadt, Germany) in prepacked columns (Atoll, Weingarten, Germany) was used as stationary phase. As feeding solution, Lysozyme was dissolved in the adsorbing preparative buffer at a concentration of 0.5 g/L and filtered (45 μm pore size). Fibrinopeptide A human was purified with reversed phase chromatography (RP) applying prepacked columns filled with a C18 functionalized silica resin (Kromasil, Bohus, Sweden). Fibrinopeptide A human was dissolved in a sample solvent (150 g/L Acetonitrile, 20 g/L Acetic acid) at a crude concentration of 3.0 g/L.

The average particle sizes for Fractogel SO_3 (M) and Kromasil-C18 were 50 μm and 10 μm , respectively. Column properties and the mobile phase composition are summarized in Table 4-1.

Table 4-1 Characteristics of the batch and MCSGP purification runs

	unit	Lysozyme	Fibrinopeptide A human
Mode	[-]	Cation exchange	Reversed phase
Resin	[-]	FGSO ₃ (M)	C18
Manufacturer	[-]	Merck	Kromasil
Functionalization	[-]	Sulfonyl	C18
Column length	[cm]	10.0	5.0
Column diameter	[cm]	0.5	0.78
Mobile phase A	[-]	25 mM Phosphate, H ₂ O	50 g/L Acetonitrile, 0.1 % TFA, H ₂ O
Mobile phase B	[-]	25 mM Phosphate, 1 M NaCl, H ₂ O	400 g/L Acetonitrile, 0.1 % TFA, H ₂ O
pH mobile phases	[-]	6.0	Not determined
Flow rate	[mL/min]	1.0	1.4
Gradient start	[%B]	13.8	23.0
Gradient end	[%B]	60.0	35.5
Gradient duration	[min]	30.0	18.0
Load	[mg/mL]	5.0	2.5
UV	[nm]	290	280

The MCSGP process was designed based upon preliminary preparative batch studies described by Aumann and Morbidelli [1]. The final parameters for the batch experiments can be found in Table 4-1. The single column experiments were performed on a HP 1050 (Degasser, pump and VWD detector) (Hewlett Packard, Palo Alto, USA). The batch procedure was translated to the MCSGP process according to Aumann and Morbidelli [1]. The process was not further optimized on purpose so as to have a non ideal start point for the controller and to see if this could be recovered by the controller itself. The MCSGP experiments for both systems were performed on a lab-scale unit from ChromaCon (Zurich, Switzerland). The unit consists of 8 smartline pumps 100 (50 mL/min), 12 WellChrom K-6 (8 run as multiposition valves for column switching, 4 as drain valves), 4 Smartline UV detectors 2500 (Single wavelength, at column outlets) and one pH/C-900 (At 4th column outlet). All parts except the last one listed are manufactured by Knauer (Berlin, Germany), the pH/Conductivity unit was from ÄKTA (GE Healthcare, Uppsala, Sweden). The automation software tailored for the MCSGP was based on LabView (National Instruments, Austin, USA) running on a standard windows PC. As an additional feature in this software, a PID controller was embedded. For cyclic product collection and peak fractionation, a FC203B (Gilson, Middleton, USA) was used at the product outlet.

4.3.3. Analytics

Table 4-2 Summary of analytic conditions

	unit	Lysozyme	Fibrinopeptide A
Mode	[-]	Cation exchange	Reversed phase
Resin	[-]	BioPro SP-F	C18
Manufacturer	[-]	YMC	Kromasil
Functionalization	[-]	Sulfonyl	C18
Length	[cm]	3	25
Diameter	[cm]	0.46	0.46
Mobile phase A	[-]	25 mM Phosphate, H ₂ O	0.1 % TFA, H ₂ O
Mobile phase B	[-]	25 mM Phosphate, 1 M NaCl, H ₂ O	Acetonitrile
pH mobile phase	[-]	6.0	Not determined
Flow rate	[mL/min]	0.5	0.5
Gradient start	[%B]	35.0	40.0
Gradient end	[%B]	50.0	50.0
Gradient duration	[min]	5.0	30.0
UV	[nm]	290	214

All analytics were run on an Agilent 1100 (Agilent, Santa Clara, USA) consisting of a degasser, quaternary pump, autosampler, column oven and a VWD detector. For Lysozyme, the same mobile phase was applied as for the preparative runs. A nonporous BioPRO SP-F column (YMC, Kyoto, Japan) with a particle size of 5 μm was applied. For Fibrinopeptide A human, a C18 column (Kromasil, Bohus, Sweden) with particle size of 3 μm was used. A summary of the parameters for the analytics can be found in Table 4-2. Additionally, in Figure 4.3, analytical chromatograms of both feed solutions are shown.

4.3.4. Controller

The PID controller used in the MCSGP setup is directly embedded in the LabView code of the MCSGP software. In the controller setup, a total of four parameters can be set: Three constants for the controller (K , T_b , T_D) and the controller set point relative to the product elution batch window. This set value was centered in the product elution window for Lysozyme and shifted -100 s for Fibrinopeptide A human, respectively. The values were chosen according to impurities visible in the analytical chromatogram (Figure 4.3). For Lysozyme, the product peak is very pure, while for Fibrinopeptide A human, more early eluting impurities are present and therefore the peak tail has a higher purity. The

controller parameters chosen for Lysozyme and Fibrinopeptide A human are summarized in Table 4-3.

Table 4-3 Controller parameters for MCSGP runs

	unit	Lysozyme	Fibrinopeptide A human
K	$[-]$	-0.5	-0.3
T_I	$[s]$	0.02	0.02
T_D	$[s]$	0.1	0.1

4.4. Results and Discussion

The controller was tested to guide the process startup, to reject external disturbances and to establish long term stability of the process.

4.4.1. Purification of Lysozyme

4.4.1.1. Controller feedback method

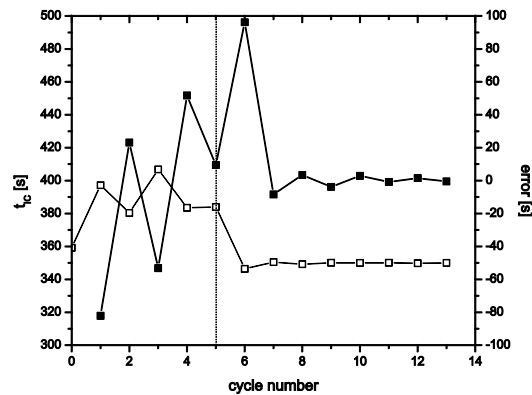


Figure 4.4 Steady state control experiment with Lysozyme. At cycle 5, the data acquisition method for the feedback signal is switched from peak maximum to first moment. The curve with open symbols (\square) indicates the actual interconnected time, the filled symbols (\blacksquare) the actual error, respectively.

For the PID controller, two different methods to process the acquired UV signal can be applied as described above. Maximum and first order moment feedback methods were applied to the case of Lysozyme purification so as to evaluate their strengths and weaknesses (Figure 4.4). The process was started with the maximum feedback method. In the 5th cycle, the data acquisition procedure was switched to the first moment method. In

Figure 4.4, the actual error and the new correspondingly evaluated interconnected time value, t_{IC} , are shown. It is found that the steady state correction is very similar for both methods which is not surprising considering the high purity of the feedstock (Figure 4.3) with very symmetric peaks. It is in fact to be expected that for the ideal case of Gaussian peak shape both methods yield the same result. More surprising is the fact that the first moment is much more stable, while for the peak maximum a significant noise is apparent.

4.4.1.2. Cycle to cycle MCSGP experiment with closed loop controller

The MCSGP experiment described here was started with the closed loop control from the first cycle onward, using the peak first moment as controller feedback signal. The obtained results are shown in Figure 4.5 in terms of the control variable, in particular the interconnected time value, t_{IC} , and the actual controller error. Up to the 6th cycle, we observe the process behavior during startup guided by the controller. It is seen that an initial error of about 50 seconds is corrected by the controller in 6 cycles. During these about 6 cycles, the controller is successfully handling the error caused by the non proper design for the MCSGP initial operating conditions.

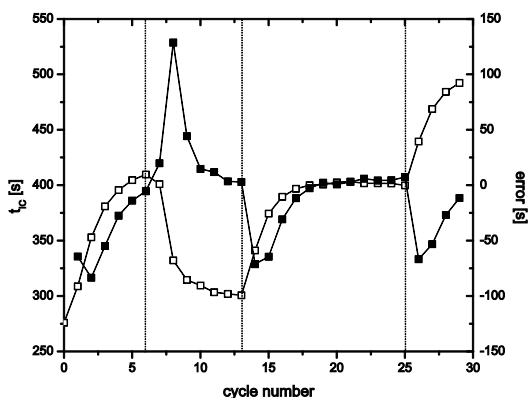


Figure 4.5 Complete MCSGP run with closed loop controller (cycle to cycle) for Lysozyme. The curve with open symbols (□) indicates the actual interconnected time, the filled symbols (■) the actual error. At the times indicated by the vertical, dotted lines, and external disturbances have been introduced.

During cycle 6 an artificial disturbance is introduced in the process. The flow rate of the gradient pump P_1 (Figure 4.1) is changed from 0.25 to 0.30 mL/min during the interconnected phase. The increased flowrate leads to earlier peak elution, to a positive error (Figure 4.5). As a consequence, the controller reduces the interconnected time, t_{IC} , so as to compensate the increased flowrate and pushes the elution peak back to the product collection window at cycle 6 as shown in Figure 4.6. At cycle 13, the flowrate of gradient pump P_1 is changed back to the original value thus simulating a normalization of the

situation. This results in a later peak elution and a negative error value. Thus the controller increases the interconnected time, t_{IC} , back to a higher value so as to drive the error back to zero. Finally, in cycle 25, the gradient endpoint of pump P_1 and thereby the slope is reduced from 60 to 58 % of the stream B (non adsorbing buffer). As a consequence, a later peak elution is expected due to more adsorbing conditions within the MCSGP unit. This is confirmed by the negative value of the error shown in Figure 4.5, cycle 26. The controller reacts to this external perturbation with an increase of the interconnected time, t_{IC} , so as to reduce the error back to zero.

The internal chromatograms of the MCSGP unit during startup (Cycles 1, 3 and 6) obtained by averaging the signals recorded by the UV detectors at all column outlets are superimposed in Figure 4.6. It is seen that during this period, a negative error is corrected by the controller by increasing the interconnected time, t_{IC} . This trend is apparent in the chromatograms shown in Figure 4.6 where it is seen that the position of the peaks first moment moves towards the middle of the product collection window.

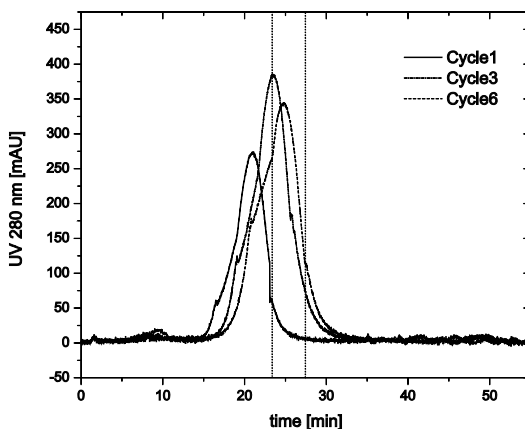


Figure 4.6 Internal profiles averaged from all UV detectors for Lysozyme during MCSGP startup with closed loop controller. The dotted, vertical lines indicate the product collection window of the 6th cycle.

4.4.2. Purification of Fibrinopeptide A human

4.4.2.1. Batch design experiment

In order to identify convenient MCSGP operating conditions, a number of batch experiments were performed. The operating conditions for the preparative design batch run are summarized in Table 4-1. The gradient elution of the selected batch for Fibrinopeptide A human is shown in Figure 4.7. From the chromatogram a large number of early eluting impurities is apparent, some of which cannot be baseline separated from the product under process conditions. This asymmetric distribution of problematic

impurities is taken care of by a proper controller tuning as discussed in detail in the next section.

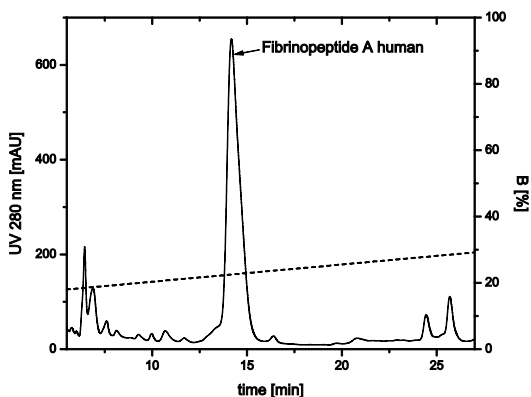


Figure 4.7 Selected batch chromatogram for the design of the MCSGP process for the purification of Fibrinopeptide A human. The dotted straight line shows the gradient to be applied in the MCSGP process.

4.4.2.2. Cycle to cycle MCSGP experiments with closed loop controller

For Fibrinopeptide A human, the controller based on the peak maximum method to process the acquired UV signal was applied. This was necessary because the purity of the feed material was low and the early eluting impurities did not reach steady state during the startup of the process. Therefore, accumulation of early eluting impurities of the left of the product peak occurred with increasing cycle number (Figure 4.8) leading to an unreliable estimation of the first moment of the UV chromatogram.

The MCSGP run with Fibrinopeptide A human starts with operating conditions estimated from the selected batch chromatogram (Figure 4.7) through the method described by Aumann and Morbidelli [1]. The controller was applied to guide the process startup. No external disturbances were performed until cycle 37 to test the long term stability of process and controller. From Figure 4.9 it is found that the process is substantially stable until the first external disturbance is introduced in cycle 37, except from some minor oscillations. This can also be seen by looking at the chromatograms along the MCSGP unit during the process startup (Figure 4.8) where it appears that the highest peak referring to the desired product is not moving significantly between cycles 11 and 15.

For the purification of Fibrinopeptide A human, the first artificial disturbance is introduced at cycle 37. The flow rate of the gradient pump P_2 is reduced in the interconnected phase from 1.60 to 1.40 ml/min. In cycle 53, the pump flow rate is changed back to the original value and simultaneously the feed flow rate is increased from 0.60 to

0.80 ml/min. Finally, at cycle 97 the gradient start point of P_2 in the interconnected phase is reduced from 21.8 to 14.0 % B.

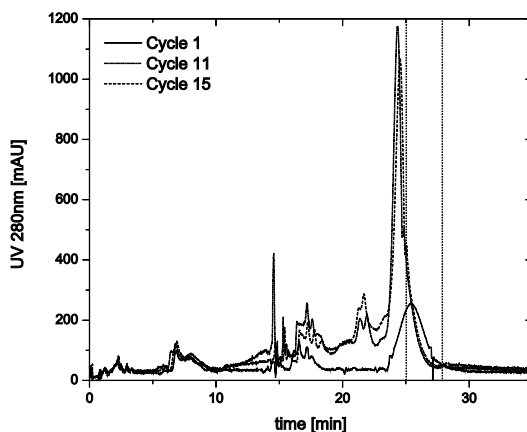


Figure 4.8 Internal profile averaged from all UV detectors for Fibrinopeptide A human during MCSGP startup with closed loop controller. The dotted, vertical lines indicate the product collection window at the 15th cycle.

The first disturbance introduced is expected to lead to a later peak elution, because the flow rate in all columns is reduced. The error in cycle 37 is in fact negative and the controller reacts by increasing the interconnected time, t_{IC} (Figure 4.9). Note that after two cycles, the controller has adjusted the process to a new stable operation point.

The second external disturbance causes the peak to elute too early, thus leading to a negative error. From Figure 4.9, it is seen that the controller changes the interconnected time, t_{IC} , back to the value before the first disturbance at cycle 37. On the other hand, the increase in the feed flow rate could have caused a column overloading leading to peak fronting. The results in Figure 4.9 do not show any such effect and actually the same value of the interconnected time, t_{IC} , before the first distortion was obtained. This is because the load of the column was not close enough to the saturation capacity to show any overloading effects that would have shifted the peak maximum.

The last external disturbance leads to a lower content of buffer B and the resulting stronger adsorbing conditions lead to higher retention times and thus to later peak elution. Accordingly, the interconnected time, t_{IC} , was increased again. It is worth noting that this last control reaction appears less smooth than the previous ones. This is due to the fact that during the same time a second external disturbance was introduced (actually not deliberately) in the process. The isocratic pump P_3 was partly not operating. In particular, one piston of this pump was not or only partly working during cycles 95 and 120. Accordingly, the controller had to handle this problem as well in addition to the

external disturbance. Overall, the run took 72 hours and proves the long term stability of the controller and the whole MCSGP process under various conditions.

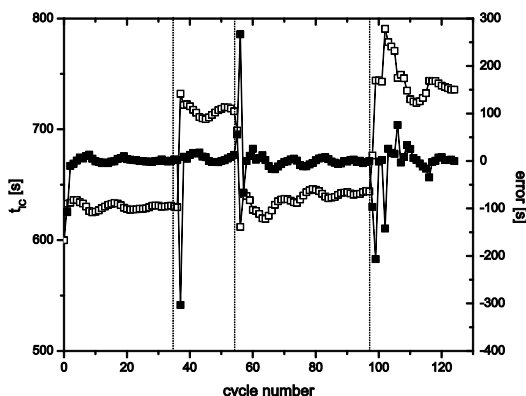


Figure 4.9 Complete MCSGP run with closed loop controller (cycle to cycle) for Fibrinopeptide A human purification. The curve with open symbols (\square) indicates the interconnected time, the filled symbols (\blacksquare) the error. The dotted, vertical lines indicate the time at which an external disturbance is introduced.

The performance of the purification process discussed above was evaluated in terms of purity and yield. The purity of the product fraction of each cycle was determined by offline HPLC analytics as described above. The purity evolution for the purification run discussed above in Figure 4.9 is shown in Figure 4.10.

Up to cycle 36, minor changes in the purity values can be observed indicating that the controller is holding reasonably well stable the steady state conditions. In cycle 37 the first external disturbance leads to a strong change in the product outlet composition. This is due to the shift of the chromatogram to later elution times which causes the elution of more early eluting impurities in the product collection window as shown by the open circles in Figure 4.10. Following the fast controller reaction seen in Figure 4.9, the disturbance in the product purity is recorded in two cycles which would lead only to a minimal increase of impurity content for the entire process. As an alternative, a control error based drain valve could be implemented in order to discard the impure cycles.

At cycle 53 the second external disturbance is introduced. In accordance with the error behavior (Figure 4.9), earlier elution and thereby more lately eluting impurities in the product stream are expected. Instead, the data in Figure 4.10 show that no change in the product stream composition occurs as a consequence of this disturbance. This can be explained with the relatively large selectivity of the product with respect to the late eluting impurities which can be observed in the preparative batch chromatogram (Figure 4.7) and the generally low concentration level of the strong adsorbing impurities.

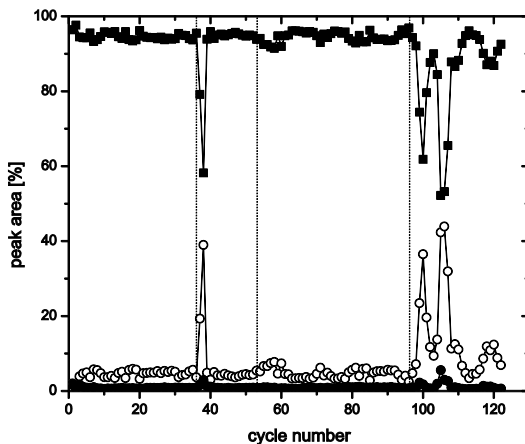


Figure 4.10 Purity trajectory for the cycle to cycle control run with Fibrinopeptide A human. The product stream purity at each cycle was measured using offline HPLC analytics. The curve with filled squares (■) indicate the Fibrinopeptide A human content in the product stream, the one with empty circles (○) the content of early eluting impurities and the one with filled circles (●) the content of late eluting impurities.

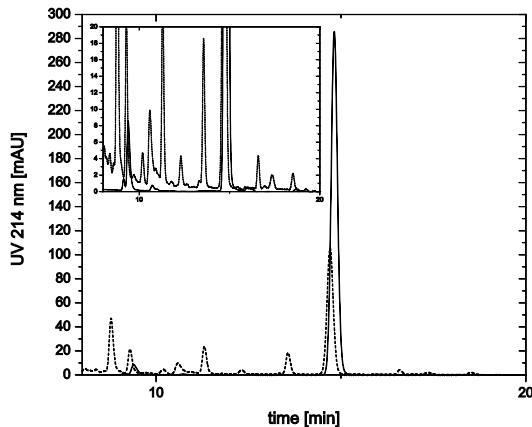


Figure 4.11 Chromatograms of the feed (dashed line) and the product outlet (solid line) at the 36th cycle of the MCSGP run with Fibrinopeptide A human. The main window shows the full chromatograms which the small window in the upper left edge shows a zoom to make the impurities visible. The axis of the zoom has the same units as the main window.

For the last external disturbance arising from buffer B gradient change, a more complicated and longer purity disturbance is observed. This is also due to the simultaneous (unwanted) failure of the pump P_3 described earlier. Despite this additional difficulty which provides a string challenge to the controller, it is seen that the process eventually achieved any way the requested purity level.

On the whole, the steady state purity of the process with the closed loop controller was at 95 % starting from 50 % in the feed. To visualize the reduction of impurities, Figure 4.11 shows the superimposition of the analytical chromatograms of the MCSGP feed material and the product collected at cycle 36. A strong reduction of all impurities is apparent. The concentration of the product is in the same order of magnitude as in the feed. The yield was not evaluated on a cyclic base for this experiment. The steady state yield was determined by manual sample collection and direct HPLC analysis, resulting in a yield >90%.

4.4.2.3. Switch to switch MCSGP experiment with closed loop controller

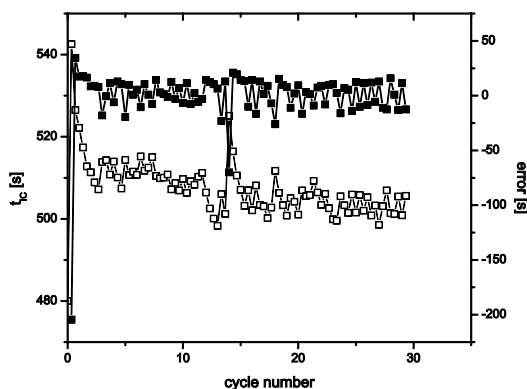


Figure 4.12 MCSGP run from startup with closed loop switch to switch controller for Fibrinopeptide A human. The curve with open symbols (\square) indicates the actual interconnected time and the filled symbols (\blacksquare) the actual error.

A faster sampling time of the controller was applied to the Fibrinopeptide A human purification process. This controller is acting on a switch to switch basis and therefore the considered UV chromatogram is obtained by combining the UV signal of the outlet of each column during a switch. This means that the controller acts four times instead of only once per cycle compared to the cycle to cycle controller. On the other hand the measured UV signal is very sensitive to small differences in the single columns behavior. This effect is instead strongly mitigated by the averaging process over four UV chromatograms in the cycle to cycle controller. In Figure 4.12, the corresponding values of the control variable, in particular the interconnected time, t_{IG} , and the control error are shown for 90 switches starting from suboptimal initial conditions. It appears that the

oscillations are much stronger and last for a longer time compared to the case of the cycle to cycle controller. In addition, the controller is approaching a lower steady state value than in the previous case (Figure 4.9). There are a number of possible explanations for the latter difference in the steady state which obviously cannot be attributed to the controller itself, but rather to the different solvents and buffers used. More interesting for this work is the observation that the switch to switch controller provides a much less stable and tight control of the unit than the cycle to cycle one due to the missing averaging of the UV chromatograms. Each difference in the columns behavior leads to shifts in the peak positions and therefore to noise in the error calculation. This effect overtakes the effect of a four time more frequent control action and we can conclude that the speed of the cycle to cycle controller is more accurate and fast than the switch to switch one. The process inertia present in the cycle to cycle control can dampen the noise generated by differences in columns behavior.

The product fractions of this experiment were collected on a cyclic basis (one fraction every three switches) and analyzed with offline HPLC. The measured compositions are shown in Figure 4.13 as a function of the cycle number. Comparing this result to the one for the cycle to cycle controller (Figure 4.10), it appears that, although reasonable stable, this controller is slower than the cycle to cycle one in driving the process to steady state after start-up

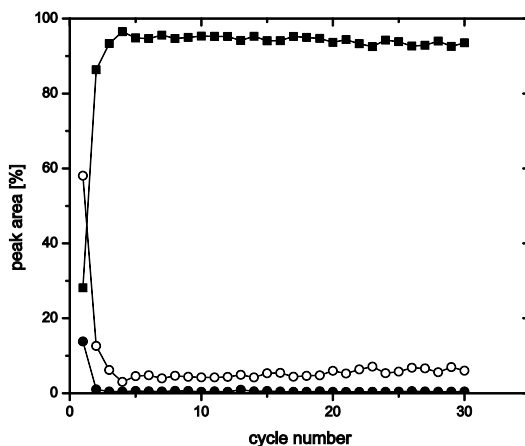


Figure 4.13 Purity Composition of the product stream as a function of the cycle number for the switch to switch controlled Fibrinopeptide A human experiment. The curve with filled squares (■) indicate the Fibrinopeptide A human content in the product stream, the one with empty circles (○) the content of early eluting impurities and the one with filled circles (●) the content of late eluting impurities.

The evolution of the yield for this experiment is summarized in Figure 4.14. As for the purity, the startup takes 3 cycles. As the transient yield is plotted, the value can exceed

100% temporally. Afterward, the yield is stable at >90% which is in the same order of magnitude as the steady state yield for the cycle to cycle controlled experiment.

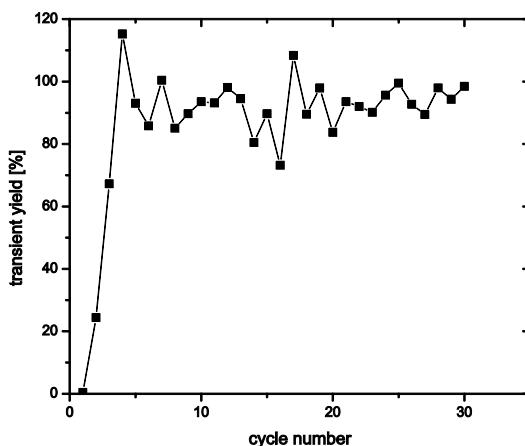


Figure 4.14 Transient yield values as a function of the cycle number for the switch to switch controlled Fibrinopeptide A human experiment

4.5. Conclusions

A simple PID controller, able to guide the start-up and compensate for external disturbances of the MCSGP unit has been developed. The controller does not require any offline analytics and is solely based on the UV signal acquired online at the outlet of each column. This makes the use of the controller very cheap and reliable. The limitation is that it does not guarantee any process performance level, such as purity or yield. Those values do in fact not even enter the controller algorithm. What the controller guarantees is to keep a certain position of the UV chromatogram with respect to the withdrawn window of the product stream. This is developed based on the batch chromatogram selected for the design of the operating conditions of the MCSGP unit and particularly from the distance of the product peak in the UV chromatogram from the start and the end of the product elution pool which satisfies the requested purity.

Two different methods for estimating the position of the UV chromatogram have been considered: One based on the first moment and the second on the peak. Both methods showed limitations and have to be chosen based on the specific process under consideration. Application examples are discussed with reference to a protein and peptide purification process. For both systems, the controller was able to guide the process startup, to keep a stable operation point and to handle external disturbances.

In conclusion, the developed controller provides a very effective tool for an operator to run a MCSGP unit with high reliability, simplicity and efficiency but in combination with a suitable offline analytics to quantify the process performance in term of purity and yield.

4.6. Remark

The work presented in this chapter has been published in:

Krättli M, Ströhlein G, Aumann L, Müller-Späth T, Morbidelli M. 2011 Closed loop control of the multi-column solvent gradient purification process. *Journal of Chromatography A* 1218(50):9028-9036. [Full text](#)

5. Online Control for the Twin-Column Countercurrent Solvent Gradient Unit for Biochromatography

5.1. Introduction

Therapeutical proteins are a fast growing market in the pharmaceutical industry. As the titer of the cell culture supernatant is steadily increasing [44, 45], more efficient purification processes are required. In the case of monoclonal antibodies (mAbs) one of the major groups of therapeutical proteins, affinity chromatography is the state of the art technology for the mAb capture from cell culture supernatants [45, 69]. Affinity chromatography has the advantage of requiring only a simple step gradient batch to recover the mAb with relatively high purity and yield. However, due to the high cost of affinity resins, the cost of the downstream process increases drastically with the titer. An alternative is to use standard non specific chromatography (e. g. ion exchange resins), but in combination with a more efficient process. One process which has been applied for various kinds of therapeutic proteins is the multi-column countercurrent solvent gradient purification (MCSGP) process. This has been described for the first time by Ströhlein et al. [49] and Aumann and Morbidelli [1]. The initial process consisted of at least six columns, was fully continuous, able to separate three fractions, could apply wash and cleaning in place (CIP) steps and could incorporate linear solvent gradients. It is clear that for a platform chromatographic technology applying mostly reversed phase (RP) and ion exchange resins (IEX), gradients, CIP and ternary separation are crucial for the purification of biomolecules. To reduce the fix costs generated by the resin and the required hardware, the MCSGP process has been redesigned several times going from initially six to three or four [21] and eventually to two columns.

A typical schematic of the so-called twin-column MCSGP process is shown in Figure 5.1. The figure shows the principle of operation of the process, showing in the middle the two columns connected by flow streams indicated by arrows. On the left and the right, the portion of the eluting chromatogram treated by each column is sketched vertically, following the process time. The picture shows an entire cycle of the MCSGP which is the complete repeating element of the process. Half a cycle, which is indicated in Figure 5.1 by the blue dashed line, is called a switch. The process can be explained by following one column trough a whole cycle. The column followed is number two starting from phase A, indicated in Figure 5.1. At the beginning of phase A, column two is equilibrated and empty. In a first step, the flow out of column one is entering column 2. The stream contains the overlapping fractions of early eluting impurities *W* and product *P* which are fully retained in column 2. Before entering column 2, this stream is mixed in front of the column with a stream of the pure adsorbing eluent (*E* in Figure 5.1). In phase B, the feed is introduced to column 2 while the purified product *P* is eluted from column 1. In phase C, a second recycling stream (containing the overlapped fraction of product *P* and late eluting impurities *S*) from column 1 is entering column two. At the end of phase C, all recycling

tasks for column 2 are finished and the gradient elution starts. In phase D₁, all pure W is eluted. Phase D₁ ends as the overlapping regions of W and P reach the end of the column, at this point, the switch occurs, meaning that the position of the two columns is exchanged. This means column 1 will now start with recycling and feeding tasks as described above, while column 2 continues with the gradient elution. In phase A₂, the gradient elution from column 2 of the overlapping regions of W and P is performed. As these fractions contain product, they are recycled in column 1 so as not to affect the process yield. Phase B₂ starts when all W is eluted. At this point, pure P is leaving column 2 and then it is collected in the product stream. When the overlapping region between P and S reaches the end of column 2, phase C₂ with the recycling of the eluate from column 2 to column 1 is performed, until all P has left the column. In phase D₂, column 2 is cleaned and reequilibrated. After D₂, the cycle is finished, the column positions are switched back and column 2 starts again from the initial position as described above. Obviously, column 1 follows exactly the same path, just shifted by a switch.

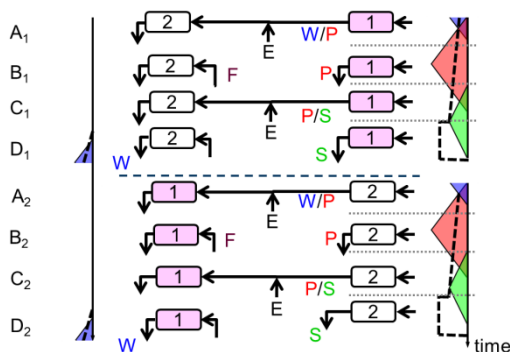


Figure 5.1 Schematic overview of a complete cycle of the twin-column MCSGP process. On the left and the right, the chromatograms of the corresponding column are shown. In the middle, the two columns with connecting streams are shown. F, W, P and S denote the feed, early eluting impurity, the product and late eluting impurity streams, respectively. The capital letters on the left indicate the various phases within switch one and two (See text).

Although no formal comparison of the twin-column MCSGP and the six column setup has been made, it is expected that the twin-column MCSGP behaves similarly as the six column unit, because the countercurrent characteristics of the process are retained. In contrary to the six column MCSGP, the twin column process is not fully continuous, since feeding and product recovery occur only in one phase (B) of the cyclic repeating switches.

MCSGP has been applied to a number of different separation problems in protein and peptide chromatography including mAb supernatant capture and polish [39, 40], mAb charge variant separations [36, 51] and synthetic peptide purification [1, 52].

Since continuous processes like MCSGP are intended to be operated over long time periods, robustness is a critical issue and this requires an efficient online control concept.

The control of continuous chromatographic systems, mainly simulated moving beds (SMB), has been studied extensively [19, 58, 70] in the case of small molecules. The most common control concept studied for SMB is model predictive control (MPC) with optimization. A variety of studies has been performed, both based on computer simulations [57, 59, 64, 70-74] and experiments [58, 60, 63, 67, 75-77]. The so called 'cycle to cycle' MPC concept has received special attention [66, 67, 78]. In this concept, the manipulated variables are changed only at the beginning of each cycle, and are then kept constant during the entire cycle. This on-line controller and optimizer were successfully implemented experimentally, also under high loading conditions which imply a rather nonlinear behavior of the system [79, 80]. Additionally, Langel et al. developed an at-line HPLC analytical system which allows to feed back to the controller the chemical composition of extract and raffinate at the end of each cycle [68].

In case of biomolecules, Grossmann et al. applied the 'cycle to cycle' MPC concept to the MCSGP process in a theoretical study [53]. In particular, a measurement feedback based on automated HPLC analysis of all three outlet streams of the MCSGP process was considered. On the other hand, the first experimental implementation of a controller to the MCSGP process was based on a single proportional, integral, differential (PID) controller acting 'cycle to cycle' basis. Krättli et al. [52] developed such a controller based on a very simple measurement feedback, E. g. the online UV signal of the outlet of the three columns. Contrary to HPLC, this feedback was available without time delay and no additional hardware was required, therefore offering a simple and cheap option. This corresponds of course to a lower performance with respect to MPC, as in this case no online optimization is possible and no direct purity control is possible since the purity of the outlet product streams cannot be measured with a simple UV signal. The purpose of this controller is simply to keep the operation of the MCSGP unit stable and robust, by rejecting possible disturbances.

In this work, a PID based control system is developed which directly controls the impurity content in the product stream. The early and late eluting impurities are controlled independently, thus allowing not only holding an overall purity, but also the purity with respect to a specific chemical species as often required in industrial purification processes. In contrast to Grossmann et al. [53], the feedback was reduced from the HPLC analysis of all three streams to that of only the product stream and the MPC controller was replaced by a PID one. The latter can obviously not provide any online optimization, but is simpler to set-up and can still make the process very robust to disturbances. This is probably a very effective compromise for long running processes with complex, not fully characterized mixtures as it is typical in bio chromatography. The number of feedbacks reduction was necessary due to cost limitations.

5.2. Controller development

Considering the process scheme of the twin- column MCSGP process in Figure 5.1, two characteristics relevant for the controller development should be highlighted. First, the twin- column MCSGP performs the batch chromatogram step by step; that is, the recycling phases are not performed in series with a mixing knot to adjust the gradient like in the equivalent six column unit, but sequentially in time. Therefore, all gradient points and elution volumes of the batch chromatogram can be transferred one to one to the MCSGP without limitations and completely decoupled. With respect to control actions, this means that the size and position of the product elution window (PEW) can be moved freely along the design batch gradient. Second, since the elution of product P is completed at the end of B_2 (Figure 5.1), there is time enough for a sample of P to be analyzed through HPLC during phases C_2 and D_2 . Therefore, at the end of the cycle, the analytical chromatogram of the product stream is available and this contains much more information than the online UV signal used previously [52].

On this basis, a multiple input multiple output (MIMO) PID controller was developed. The controller is starting from the product at-line HPLC analytics which delivers a complete analytical chromatogram of the product stream. This chromatogram is automatically integrated applying the trapezoid rule and the areas assigned to product P , lumped early eluting impurities W and lumped late eluting impurities S . The feedback error e required by the controller is defined as the difference between the measured product purity and the corresponding set value set for each of the two impurities W and S individually, as follows:

$$e_w = \frac{A_w}{A_w + A_p} - set_w \quad 5.1$$

$$e_s = \frac{A_s}{A_s + A_p} - set_s \quad 5.2$$

where A represents the area integrated from the analytical chromatogram (if needed corrected by a suitable correction factor) and the indexes W and S refer to the lumped weak and strong impurities, respectively. The errors given by equations 5.1 and 5.2 are used as feedback in two standard PID controllers [81] which compute the controller outputs $c_{A,n+1}^{mod}$ and $c_{C,n+1}^{mod}$ representing the modifier concentration in the batch chromatogram, at which the product elution window in the subsequent cycle shall start and end, respectively:

$$c_{A,n+1}^{mod} = K_w \left(e_w(n) + \frac{1}{I_w} \sum_{i=1}^n e_w(i) + D_w (e_w(n) - e_w(n-1)) \right) \quad 5.3$$

with $|c_{A,n+1}^{mod}| \leq U_w^{max}$

$$c_{C,n+1}^{mod} = K_W \left(e_s(n) + \frac{1}{I} \sum_{i=1}^n e_s(i) + D_s (e_s(n) - e_s(n-1)) \right) \quad 5.4$$

with $\left| c_{C,n+1}^{mod} \right| \leq u_s^{max}$

where K , I and D are the PID controller parameters and n denotes the current cycle. u^{max} is the maximal allowed step size for the controller output. As shown in Figure 5.2, the action of the W dependent PID only acts on the left PEW side, while the S dependent PID one only on the right PEW side. The outputs from the PID controller are used to calculate the control action through mass balances while keeping constant the modifier concentration gradient with respect to the elution volume:

$$V_{A,PID} = \frac{m_A^{mod}}{c_{A,n+1}^{mod} - c_{A,start}^{mod}} \quad 5.5$$

$$V_{C,PID} = \frac{m_C^{mod}}{c_{C,end}^{mod} - c_{C,n+1}^{mod}} \quad 5.6$$

$$V_{B,PID} = V_{tot} - V_{A,PID} - V_{C,PID} - V_D \quad 5.7$$

where m^{mod} is the modifier gradient slope, c^{mod} the modifier concentration and V the elution volume. The volume variables having PID in the subscript are manipulated by the controller on a cyclic basis. During the entire cycle, the product stream is collected in a mixing vessel and at the end of B_2 , a sample is injected to the at-line HPLC, starting the control process for the next cycle.

The control loop is summarized in Figure 5.2, showing at the top the batch elution chromatogram versus the elution volume. The PEW is collected during the cycle and analyzed via HPLC in the last two phases (C_2 and D_2) of the process. Based on the integrated area from the analytical HPLC chromatogram and the user defined purity requirements of the process, two errors are calculated (Equation 5.1 and 5.2). The errors (e_w and e_s) are forwarded to the PID controllers which compute the initial and end modifier concentration of the PEW (Equations 5.3 and 5.4) and from these the elution volumes $V_{A,PID}$, $V_{B,PID}$ and $V_{C,PID}$ in Figure 5.2 through equations 5.5 to 5.7.

The control parameters for both PID controllers were determined from model based simulations using model separating systems. The obtained set of values is summarized in Table 5-1 and has been found to hold for a relatively large class of systems. These have been kept constant in all applications shown in this work. In addition, the step size of the controller action in terms of Δc^{mod} was limited by the value u^{max} in order to enhance the controller stability.

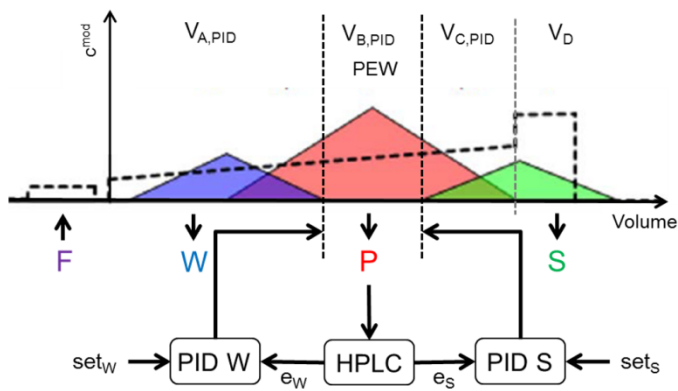


Figure 5.2 Schematic of the MIMO PID controller. At the top, the chromatogram of the MCSGP with the PEW is shown. The eluted *P* is analyzed on a cyclic basis by HPLC producing feedbacks (e_s and e_w) for the two PID controllers. The controller act on the PEW boarder lines via the elution volumes *V* of the MCSGP phases A, B and C: $V_{A,PID}$, $V_{B,PID}$ and $V_{C,PID}$

Table 5-1 Controller constants according to equations 5.3 and 5.4 applied in this work

	PID W	PID S
<i>K</i>	10	10
<i>I</i>	0.1	0.1
<i>D</i>	0.1	0.1
u^{max}	0.3	0.3

5.3. Materials and Methods

5.3.1. Modeling and Simulation

The MCSGP process was modeled applying the lumped kinetic model [14] for each phase and column of the process. This was implemented together with suitable mass balances of the connecting knots of the MCSGP unit as described by Aumann et al. [1]. The FORTRAN based program was implemented in MatLab and various closed loop simulations of the unit were performed to identify the best values for the parameters of the two controllers: *K*, *I*, *D* and u^{max} as reported in Table 5-1.

5.3.2. Hardware setup

The preparative experiments were performed on a Äkta Basic system (GE Healthcare, Uppsala, Sweden) consisting of two gradient pumps *P*-900, four 8-port switching valves, one buffer selection valve for the second pump, two UV-900 detectors and two pH/Conductivity pH/C-900. The detectors were located at the column outlets. The analytics were performed on an Agilent 1200 system (Agilent, Santa Clara, CA, USA) consisting of a degasser, a quaternary pump, temperature controlled autosampler, column oven and a DAD detector.

To allow automated feedback, the analytics and preparative unit were connected via a buffer tank and an automatically refilling sample loop. The injection volume was 20 μ L and the injection was triggered by the preparative system. The control software, data analysis and input commands to the preparative system were handled on a central personal computer running Chemstation (Analytics), UNICORN (Preparative) and MatLab (Controller and Interface) simultaneously.

5.3.3. Separation of a protein model mixture

Three proteins (α -Chymotrypsinogen (*W*), Cytochrome *C* (*P*) and Lysozyme (*S*)) also used as a model system in earlier studies [54] were prepared at a concentration of 0.5 g/L of each protein in a 25 mM phosphate buffer at pH 6.0. To suppress microbiological activity in the feedstock, 0.5 g/L of NaN_3 was added. The separation of these proteins with cation exchange chromatography (CEX) was successfully demonstrated by Aumann et al. [54]. In order to have an efficient composition measurement tool as controller feedback, a fast analytical chromatographic column was set up using a monolithic stationary phase CIM[®] Disk SO_3 from Bia Separations (Villach, Austria). Three disks were piled in the housing leading to a total stationary phase volume of 1 mL at a length of 9 mm. As eluent, a 25 mM phosphate buffer was used with a linear gradient from 0 to 1 M NaCl in 5 minutes at a flow rate of 1 mL/min. Under these conditions, the elution order was α -Chymotrypsinogen, Cytochrome *C* and Lysozyme which is in agreement with literature data [54]. A typical chromatogram is shown in Figure 5.3. To elute Lysozyme completely, the final concentration of modifier was kept constant for 2 min before equilibration. The complete analytical procedure takes seven minutes. The signal was recorded with a UV/Vis DAD detector at 220 and 400 nm wavelengths. The aim of this study is to reduce the amount of both impurities to 10% in the product stream.

The preparative experiments were performed on two prepacked Atoll (Weingarten, Germany) columns of 50 mm length and 5 mm inner diameter. The columns were packed with Fractogel EMD SO_3 (M) (Merck, Darmstadt, Germany). The design of the operating conditions for the twin-column MCSGP unit was performed based on previous batch chromatographic data following the procedure described in the literature [54]. The buffers were the same as for the analytics; the UV chromatograms were recorded at 280 and 400 nm. All operating conditions used for starting the unit in these experimental runs are summarized in Table 5-2, third column.

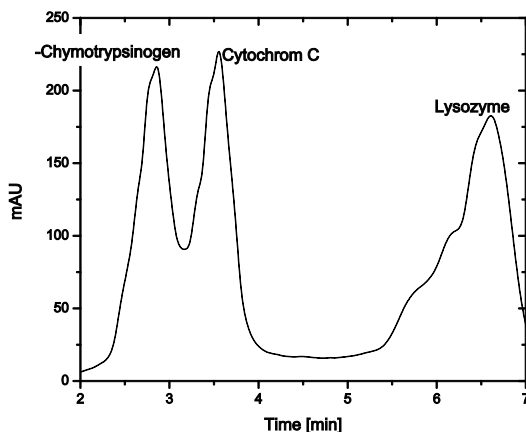


Figure 5.3 Analytical chromatogram of the protein model mixture at 220 nm wavelength

5.3.4. Monoclonal Antibody capture from supernatant

A monoclonal antibody (mAb) clarified cell culture supernatant was purified from aggregated mAbs and mAb fragments. To prepare the feedstock solution, the supernatant was diluted with water until a conductivity of 5 mS/cm and the pH was adjusted to 6.0. The solution was filtered (0.45 μ m) and kept in the fridge to avoid microbiological activity. The mAb concentration in the feedstock was 1 g/L. The analytics of the mixture: mAb, fragments and aggregates was done by size exclusion chromatography (SEC). An Acquity UPLC BEH200 SEC 1.7 μ m column (4.6 x 150 mm) from Waters (Milford, MA, USA) with a pH 7.0 50 mM phosphate and 50 mM sulfate buffer was used at a flow rate of 0.4 mL/min. Each analytic run took 9 minutes. The chromatogram was recorded at 280 nm. A typical chromatogram is shown in Figure 5.4.

For preparative experiments, the same columns were used as for the protein model mixture above. The operating conditions of the twin-column MCSGP were designed based on a batch chromatogram as described by Aumann et al. [1]. The design batch chromatogram was performed on the Äkta system using one CIEX column. The equilibrated column was loaded with 5 mL feed (5 mg_{mAb}/mL_{column}), washed with adsorbing buffer for 3 mL and eluted with a linear gradient from adsorbing buffer to 20% desorbing buffer in 20 minutes. After gradient elution, the column was stripped (Desorbing buffer, 1 mL), cleaned in place (CIP) with 0.5M NaOH (1 mL) and reequilibrated (Adsorbing buffer, 5 mL). The adsorbing and desorbing buffers were the same as for the protein model mixture preparative runs. The chromatogram of the batch elution was recorded with UV at a wavelength of 280 nm. Additionally, the gradient elution was fractionated (1 mL fractions) and analyzed with SEC HPLC. According to this design batch,

the MCSGP process was designed. The so obtained operating conditions used for starting the unit are summarized in Table 5-2, fourth column.

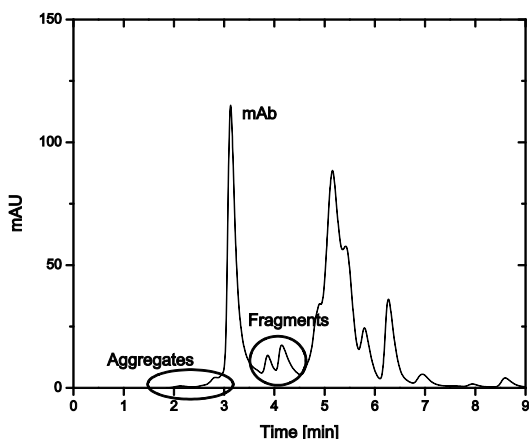


Figure 5.4 Analytical chromatogram of the mAb feed. The relevant impurities: aggregates and fragments are highlighted. All other visible impurities end up in the flow through under process conditions and are therefore not considered in detail. The chromatogram was recorded at 280 nm.

Table 5-2 Operating conditions for all preparative runs in this work. These represent the initial conditions and may be affected by the controller during operation.

	Units	Protein model mixture	mAb
Stationary phase		FG EMD SO3	
Column dimensions	[mm]	5 x 50	
Adsorbing buffer (A)		25 mM Phosphate, pH 6.0	
Desorbing buffer (B)		25 mM Phosphate, pH 6.0, 1 M NaCl	
Design Batch			
Load (Product)	[mg/mL]	1	5
Gradient Start	[%B]	0	0
Gradient End	[%B]	100	20
Duration	[min]	15	20

MCSGP

<i>Phase A</i>			
Duration	[min]	6	0
Flow rate gradient pump	[mL/min]	0.5	-
Flow rate compensation	[mL/min]	0.5	-
Modifier concentration Start	[%B]	29.9	-
Modifier concentration End	[%B]	40	-
<i>Phase B</i>			
Duration	[min]	2	8
Flow rate gradient pump (<i>P</i> elution)	[mL/min]	1	1
Flow rate feeding	[mL/min]	1	0.625
Modifier concentration Start	[%B]	40	8
Modifier concentration End	[%B]	46.5	16
<i>Phase C</i>			
Duration	[min]	8	0
Flow rate gradient pump	[mL/min]	0.25	-
Flow rate compensation	[mL/min]	0.75	-
Modifier concentration Start	[%B]	46.5	-
Modifier concentration End	[%B]	53.3	-
<i>Phase D</i>			
Duration	[min]	5	8
Flow rate equilibrate	[mL/min]	1 (Strip, Equilibrate)	
Flow rate gradient pump	[mL/min]	0.4	1
Modifier concentration Start	[%B]	0	0
Modifier concentration End	[%B]	29.9	8

5.4. Results and Discussion

5.4.1. Closed loop experiments with the protein model mixture

The developed controller was first tested using the three protein model mixture described above. The process was started with empty columns from non-optimized operating conditions and setting the purity values for W and S equal to 0.1. The desired purity of the product would therefore be 0.8, containing equivalent amounts of W and S impurities. The controller was switched on from the first cycle and therefore it guided the start-up until the final steady state. In Figure 5.5, the actual errors e_W and e_S , as defined by equations 5.1 and 5.2, are shown together with the controller output. This is reported in terms of the modifier concentration at the beginning, c_A^{mod} and at the end, c_C^{mod} of the PEW as defined by equations 5.3 and 5.4. It is seen that during the first cycles, the error values rapidly reduce to zero. On the other hand, the PEW increases significantly in width until cycle 12 and after that changes only slightly. The large change in the beginning is due to the fact that in the particular mixture under examination here, the late eluting protein is actually base line separated from the other two (Figure 5.3) which allows a significant widening of the PEW on the side of the weak impurity, E. g. the value c_A^{mod} in Figure 5.5, without affecting the purity in the product stream. Following the process until cycle 25, one can see that the controller keeps the error at zero and the position of the PEW changes only slightly, probably due to disturbances arising from correspondingly small changes in the environmental conditions.

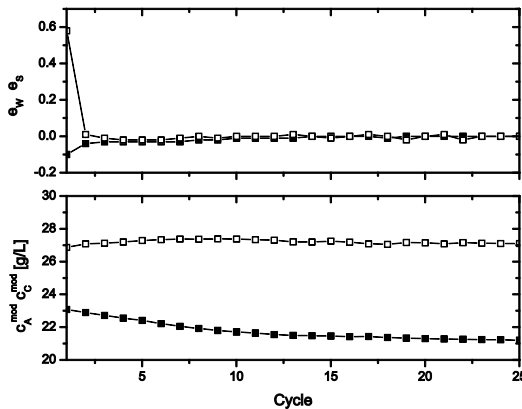


Figure 5.5 Left: Error and controller output trajectories for the protein model mixture showing the process start up. On top, the errors of the W controller (■) and the S controller (□) are shown. On the bottom figure, the controller outputs with the same symbols.

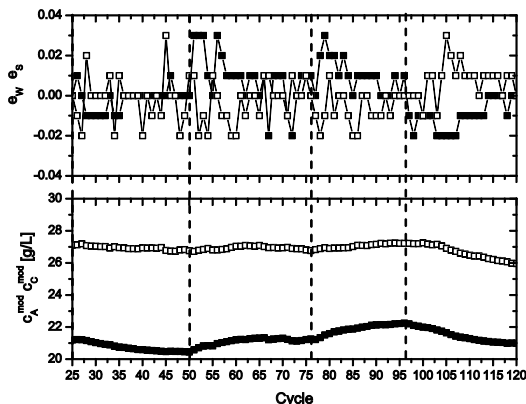


Figure 5.6 Error and controller output trajectories for the protein model mixture showing rejection of disturbances in a gradient pump flow rate in cycles 25, 50, 76 and 97, indicated by dashed lines. On top, the errors of the W controller (■) and the S controller (□) are shown. On the bottom, the controller outputs with the same symbols.

In order to test the controller capability in rejecting disturbances, this experimental run was prolonged beyond the 25th cycle and disturbances were introduced. First, the flow rate in column 2 phase D (Figure 5.1) was changed from 0.4 to 0.5 mL/min at cycle 25 and then changed back to the original value at cycle 50, decreased to 0.3 mL/min at cycle 76 and finally restored to its original value at cycle 97. This flow rate was chosen because it affects the first part of the elution gradient and therefore affects the elution of all components in the system. The obtained results are shown in Figure 5.6. As the flow rate increases the elution shifts to earlier times and consequently, the PEW shifts to lower modifier concentrations. On the other hand, when the flow rate decreases, the elution shifts to higher modifier concentrations and so does the PEW. The same trends are exhibited by the error which remains however always very small in absolute terms.

As a second set of disturbances, the feed composition was changed. While the concentration of the product Cytochrom C was kept constant at 1 g/L, both impurity concentrations were increased from 1 to 1.5 g/L as it appears in the analytical chromatogram of the two feeds (Figure 5.7).

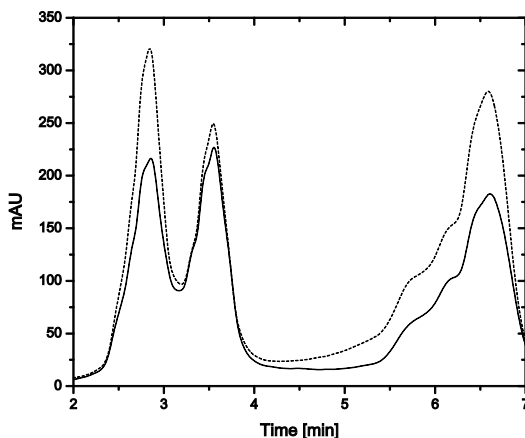


Figure 5.7 Analytical chromatogram of the original protein model mixture feed (solid line) and of the one enriched in the impurities (dashed line)

At cycle 121, the feed vessel was changed and the modified feed was injected into the unit. Due to the larger overlapping between product and impurities caused by the increased concentration of the latter ones, the separation becomes more difficult and therefore the PEW reduces, as shown in Figure 5.8 and consequently, both recycling phases (A and C) increase. The *W* and *S* enriched feed was kept until cycle 150, showing that also with the new feed the controller can lead the unit to steady state. At cycle 150, the unit was switched back to the original feed. The controller reacts properly and restores the previous, larger PEW. It is worth noting that the reaction time after introducing the new *W* / *S* enriched feed was longer than the one after restoring the original feed. This is due to a practical problem contingent on this specific experiment and has no general meaning. In particular, a dead volume was present in the feed tube which was drained manually before the second feed disturbance resulting in the immediate response of the controller which can be seen in Figure 5.8. Overall, the control experiment with the protein model mixture was running 160 cycles which corresponds to 112 hours. During this period, buffer vessels and feed had to be refilled several times. Additionally, the temperature changes in the lab due to day / night rhythm were present. These additional, real disturbances also influenced the controller and led to certain deviations in the operating conditions set by the controller.

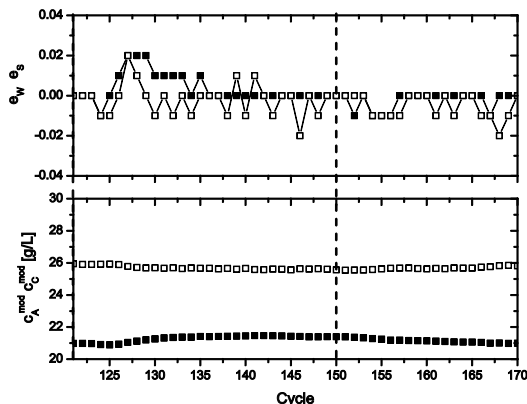


Figure 5.8 Error and controller output trajectories for the protein model mixture showing rejection of disturbances in the feed composition in cycles 121 and 150, indicated by dashed lines in the figure. On top, the errors of the W controller (\blacksquare) and the S controller (\square) are shown. On the bottom, the controller outputs with the same symbols.

5.4.2. Closed loop experiments for a mAb capture process

In the case of the capture process of a mAb from a clarified cell culture supernatant, we present a general procedure that can be used to identify suitable operating conditions for the MCSGP unit with the assistance of the controller and starting from a very general initial condition. In particular the controller is applied to minimize the experimental fine tuning needed to identify the MCSGP operating conditions thus reducing the number of experiments to be performed. This significantly reduces the process development time.

The analytical chromatogram of the mAb feed is shown in Figure 5.4 and two major impurities were identified, most certainly representing mAb fragments and aggregates. In this purification process, the impurities should be both reduced to 5% with respect to the mAb. The MCSGP process design was started according to Aumann et. al. [1, 54] but now including the use of the online controller. As a first step, the mAb supernatant was captured using preparative cation exchange batch chromatography. The supernatant was loaded at a concentration of $5 \text{ mg}_{\text{mAb}}/\text{mL}_{\text{column}}$ and eluted with a linear gradient. The eluted gradient was fractionated and analyzed by SEC HPLC, leading to further gradient optimization. The final selected batch gradient is the one reported in the fourth column of Table 5-2 while the corresponding elution profiles are shown in Figure 5.9. It is seen that the weak impurities W exhibit a nice peak maximum, while the peak for S is very flat and therefore more difficult to be separated from the product.

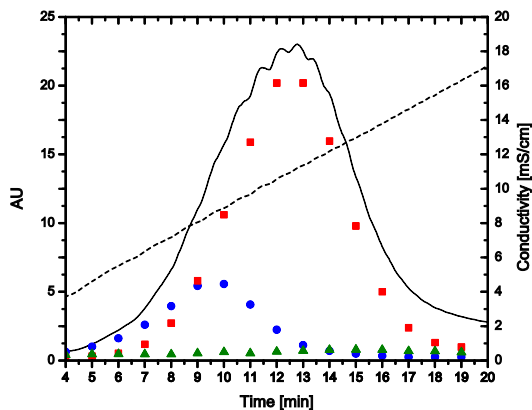


Figure 5.9 Preparative design batch chromatogram for the mAb purification process including the online UV chromatogram (solid black line), fraction analysis (blue circles: W , red squares: P , green triangles: S) on the left y axis in arbitrary units and the modifier gradient (dashed line) on the right y axis.

In order to design the MCSGP process, one has to identify in the batch chromatogram in Figure 5.9 the different MCSGP phases A – D (Figure 5.1). Following Aumann et al [54], the batch chromatogram has to be distributed into five tasks: collecting W , recycling W / P , collecting P , recycling P / S , collecting S . For this, when the online controller is available, the following general simple procedure can be adapted. The chromatogram is cut in only three tasks; one for W (until 8 minutes in Figure 5.9) and one for S withdrawal (from 16 minutes onward in Figure 5.9), and a middle fraction for the production of P . The recycling phases are absent initially and will be introduced later automatically by the controller. In terms of Figure 5.1, this means that only phases B and D are present while phases A and C, representing the recycles, are absent.

Figure 5.10 shows the start-up of the MCSGP unit driven by the controller from the initial conditions described above. It is seen that the controller immediately narrows the PEW, meaning that it is introducing the recycle phases (A and C in Figure 5.1). Consequently, the concentration of the mAb in the product stream increases. After cycle 5, the window size changes only marginally indicating that the process satisfies the purity constraints. This is confirmed by the error, which becomes zero within five cycles. The upper limit of the PEW decreases slightly until the end, similarly to the previous case of the protein model mixture (Figure 5.5). This behavior can be explained by the very flat peak of the S impurity (Figure 5.9), which results in a very small error. Since the S peak is so broad, the upper limit of the PEW has to be shifted quite a bit to smaller values of c_c^{mod} , which with the small error present requires many cycles. However, this does not really affect the control performance; the product purity reaches in fact the desired 90% value after only five cycles and remains there until the end of the process.

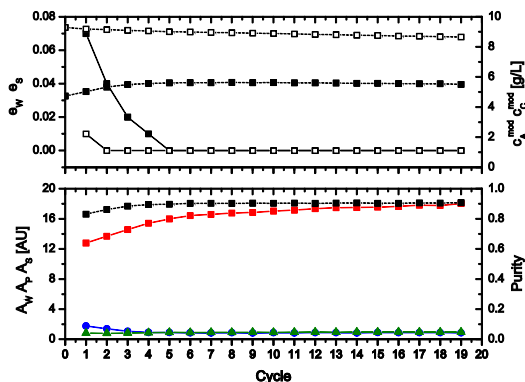


Figure 5.10 The upper diagram shows the actual error (solid lines, filled symbols: W , open symbols: S) on the left axis and the controller outputs (dashed lines, same symbols) on the right axis. In the lower part, the concentrations of the individual components in the product stream (blue circles: W , red squares: P , green triangles: S) are shown on the left axis in terms of the corresponding chromatographic areas and the purity with respect to P (black squares, dashed line) on the right axis

A typical way to compare the performance of the MCSGP process with that of the preparative batch is the yield versus purity diagram shown in Figure 5.11. It is well known that for batch chromatography, the product purity and yield depend on each other resulting in a classical trade off situation [36, 82]. That is caused by the overlapping regions between product and impurities present in the batch chromatogram like the one in Figure 5.9. One has in fact to choose the window along the gradient elution which is collected as product stream. If this window is very wide, all product fractions are collected but also many impurities, resulting in high yield and low purity. Vice versa, a narrow window minimizes the impurity content, but also some product is lost resulting in high purity but low yield. Two such conditions are represented by the closed black squares in Figure 5.11. The MCSGP process is typically able to break this trade-off situation resulting in a product stream with high yield and high purity. The entire time evolution, cycle by cycle, is represented by the red points in Figure 5.11. The MCSGP process starts with a performance represented by a point very close to the pareto curve of the batch process. This is in agreement with the initial condition provided by the general start-up procedure to the MCSGP cycle. This in fact implies no recycle phases and therefore the process does not differ from a batch one. With the changes made by the controller, the recycle phases are introduced and the process performance leaves the batch pareto curve. After 5 cycles, the yield and purity process approaches steady state conditions which correspond to much larger values of both. We expected that the developed MCSGP start-up procedure guided by the controller is able to drive the unit to some sub-optimal conditions represented in Figure 5.11 by one point of the MCSGP pareto. Such a pareto is obviously unknown at this point for the system, but based on general experience on MCSGP one

expects it to be located in the up-right corner of the purity versus yield plot, much above the corresponding batch pareto.

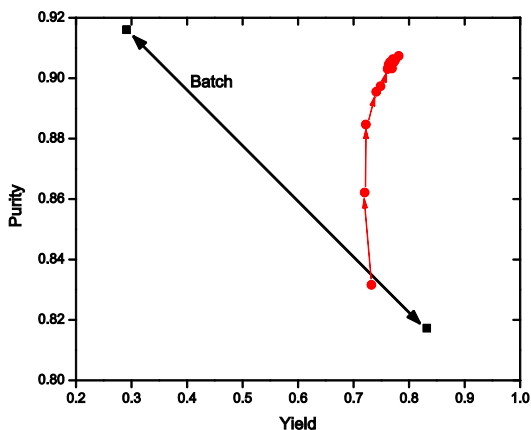


Figure 5.11 Yield versus purity diagram comparing the performance of batch runs (one with high purity and low yield and the other vice versa (black squares)) and the MCSGP run. The process start-up is represented by the red dots connected with arrows indicating the unit time evolution.

To further validate the robustness of the process, the effect of ad-hoc disturbances was tested. Figure 5.12 shows the start-up of the unit with the controller switched on. Steady state operating conditions are reached after about 20 cycles. At cycle 20, a flow rate disturbance was introduced in phase *D* for the first gradient part, reducing the flow rate from 1 mL/min to 0.9 mL/min. The lower flow rate in the first section of the elution chromatogram affects all eluting peaks and therefore the controller shifts the elution window to higher values of the gradient. At cycle 42, a second disturbance was introduced. The fed supernatant was pretreated to remove part of the product mAb. The chromatograms of the original feed and the pretreated one are compared in Figure 5.13. A significant reduction of the product concentration is visible, while the relevant impurity content did not change. Introducing this feed, the PEW was reduced significantly while the recycle streams were increased automatically by the controller. It can be seen that similarly to the previous case, the error in the upper limit took again longer to reach equilibrium, due to the flat peak shape. The process had in fact to be terminated slightly before reaching the new stable operating point due to a malfunction in the process analytics. Nevertheless, it can be seen that the lower boundary of the PEW has reached steady state, while the upper boundary is expected to reach it within a few cycles.

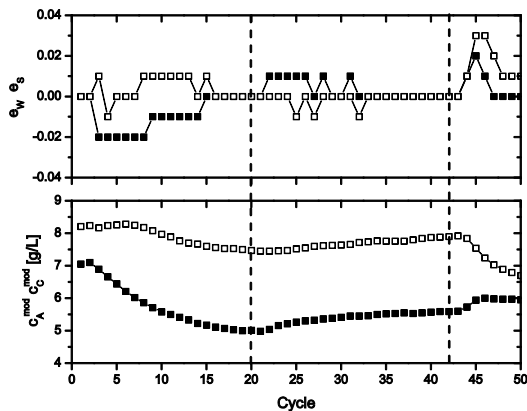


Figure 5.12 Error and controller output trajectories for the mAb supernatant showing the MCSGP unit start-up (until cycle 19), a disturbance in a gradient pump flow rate in cycles 20 and a feed disturbance in cycle 50. The disturbances are indicated by dashed lines in the figure. On top, the errors of the W controller (\blacksquare) and the S controller (\square) are shown. On the bottom figure, the controller outputs with the same symbols.

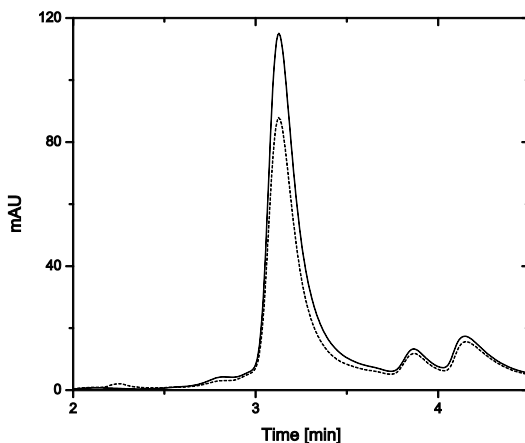


Figure 5.13 Analytical chromatograms of the original mAb supernatant (solid line) and the pretreated supernatant (dashed line) used as second feed to the process.

5.5. Conclusions

A new control concept for the twin-column MCSGP process has been developed. The controller uses atline HPLC as feedback, which allows direct purity measurement of the product stream. The feedback is used in two decoupled PID controllers, which affect the start and endpoint of the product elution window. In combination with suitable mass balances, the developed controller can move the position of the product collection window along the chromatogram without changing the slope of the modifier gradient with respect to the eluted volume. The controller performance was tested with a model mixture of three standard proteins. Both start-up and disturbance rejection capabilities were investigated. The concept of the controller proved to be very stable and reliable, running the protein model separation for 112 hours including disturbances in the pump flow rates and in the feed composition.

The developed controller was also used for a more difficult, real separation that is the capture step of a mAb from a clarified cell culture supernatant with fragments and aggregates as impurities. The desired impurity content was set at 5 % for each of the impurities with respect to the mAb. In this context, a new, general start-up procedure was developed and tested. Initially, the mAb supernatant was captured with a preparative batch chromatography run and the distribution of the impurities was analyzed. The MCSGP was then designed according to Aumann and Morbidelli [1] but now taking advantage of the support of the controller: In particular, the difficult task of setting the recycle rate in the MCSGP process was executed automatically online by the controller without the operator's intervention. It is shown that, following this procedure the MCSGP unit starts from a typical batch chromatography performance and evolves in a few cycles to typical MCSGP performance characterized by higher values of both purity and yield. Also in this case the unit was operated for 20 hours without significant deviation from the set purity values, in spite of several ad-hoc disturbances in the flow rate of a gradient pump and in the feed concentration.

5.6. Remark

The work presented in this chapter is submitted for publication in Journal of Chromatography A

6. Separation of Lanthanides by Continuous Chromatography

6.1. Introduction

The rare earth elements (REEs) are a group of 17 chemical elements sharing similar chemical properties and including the subgroup of the lanthanides in addition to scandium and yttrium. Despite their name, REEs are present in vast amounts in various geological structures around the globe [83]. The main sources for commercial mining of REEs are bastnazite and monazite.

REEs are used in a variety of high tech industries, including applications in the field of optics, magnetism, catalysis, luminescence, superconductors, and batteries [3, 83, 84]. As many of these applications are in a very fast growing phase, it is not surprising that the demand of REEs increased strongly during the last decades [83, 85]. Accordingly, concerns arose that soon the availability of REEs could become the limiting step for the development of new technological areas [3].

The separation and purification of REE compounds turns out to be very difficult due to their very similar chemical and physical properties. For the preparative separation, a number of approaches have been investigated of which the more successful ones were liquid-liquid extraction, liquid-solid extraction and liquid chromatography [83, 86, 87]. Processes based on liquid chromatography were mainly discussed in the first half of the 20th century, but have been abandoned as too cost intensive. Nowadays, industrial processes are based on extraction processes for the separation of the individual REEs [88]. This is also indicated by the large number of publications on newly developed extraction media and processes (e. g. [89-92]). On the other hand, chromatographic separations are being considered again for preparative separation of REEs [4, 93, 94] beside their classical use as analytical techniques (e. g. [95-99]). In particular, the normal phase chromatographic mode [100, 101] and ion exchange (IEX) or ion chromatography [86, 93] have been considered.

In this context, chromatography has actually gained back in term of competitiveness with respect to extraction due to the possibility of collecting multiple pure fractions and developing environmental friendly “green” processes.

In this work, the possibility of using continuous countercurrent chromatography to decrease the purification cost is investigated. In particular, the feasibility of IEX continuous countercurrent chromatography is demonstrated for a model separation of three REEs, namely Lanthanum (La), Cerium (Ce) and Praseodymium (Pr). These three compounds were chosen as they are neighboring in IEX chromatograms, thus representing a “difficult” separation challenge. Additionally, these REEs are currently the ones required in largest amounts for industrial applications [84, 85].

The continuous countercurrent chromatographic process is applied in the following using the multi-column countercurrent solvent gradient purification (MCSGP) unit originally developed for the purification of biomolecules [1, 49, 82, 102]. This process can separate the continuous feed into three fractions and is able to apply solvent gradients including linear gradients. The MCSGP unit was initially designed fully continuous with six columns [1, 37] or semi continuous with three columns [21]. The three column process can be expanded to four columns for continuous feed or additional wash and cleaning in place [39, 51, 52].

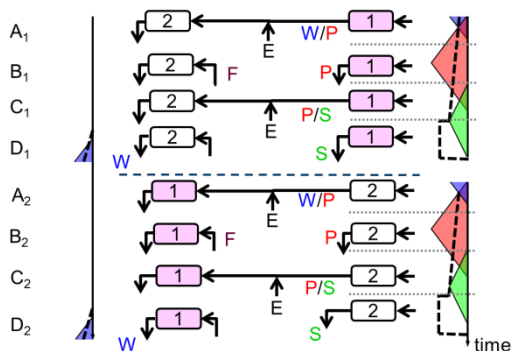


Figure 6.1 Overview of the twin-column MCSGP process. W, P and S indicate the streams of the unit containing the purified REE ions. The time evolves from the top of the figure downward. The two physical columns are numbered and all streams are indicated by arrows. On the left and right of the flow scheme, the internal chromatogram of the neighboring column is shown containing the modifier gradient in dashed line and the three components W, P and S as triangle areas with the same color as in the flow scheme. The blue dashed line indicates the column switch, while the dotted vertical lines indicate the phase changes within a cycle.

In this work, a further simplified version of the MCSGP unit is used, that is one using two columns, referred to as the twin-column MCSGP shown schematically in Figure 6.1. The figure shows the concept of the process, with the columns in the middle of the graph connected by the flows indicated by arrows, and on the left and on the right the schematics of the chromatograms developing in the neighboring columns. The chromatograms are sketched vertically following the process time contain the information on the three species to be separated, indicated as W, P and S with increasing order of adsorptivity (i. e. Pr, Ce and La in this work), and the modifier gradient. The easiest way to explain the process is following one column, starting in A₁. In the beginning of A₁, column 2 is equilibrated and empty; column 1 starts with the elution of the overlapping fraction of W and S. The outlet stream from column 1 is entering column 2. To ensure that the species W and P are retained in column 2, the stream is mixed with pure adsorbing eluent (E) that is not containing any modifier, before entering column 2. In phase B₁, column 1 is eluting the product fraction while fresh feed is introduced in column 2. In

phase C, the overlapping regions of *P* and *S* are eluted from column 1 and are recycled again to column 2, again mixing with pure eluent (*E*) to ensure adsorbing conditions. In phase D, column 1 is eluting the pure *S* fraction. This can be done applying a step gradient to very high modifier concentration; afterward the now empty column is reequilibrated. In parallel, *W* is eluted from column 2 by starting the gradient. These four phases in series (*A*₁ to *D*₁) are called a “switch”. After the switch, the column positions are exchanged and the procedure is repeated. Two switches together form therefore a complete turnover of the columns which is called a “cycle”. In comparison to the original MCSGP process scheme, the two column setup comprises a number of advantages, namely more flexibility due to independent recycling of the fractions *W/P* and *P/S*, lower investment cost due to simpler equipment and easier operating mode with only one gradient and one isocratic pump.

The advantages of MCSGP with respect to other continuous countercurrent chromatographic processes such as simulated moving bed (SMB) are the possibility of implementing a modifier gradient and the capability of performing multifraction (E. g. three in this work) separations. Due to internal recycling of the impure side-fractions, MCSGP can achieve higher product yield and purity than batch chromatography. In the latter purity comes at the cost of yield and vice versa leading to the well-known yield purity trade-off behavior discussed later in more detail. The superior performance of MCSGP in comparison to the equivalent batch process was shown for a number of proteins and peptides [1, 36, 40, 51]. Despite the obtained differences of these molecules compared to REEs in terms of molecular weight and adsorptive properties, in both cases we deal with multicomponent (ternary in the present work) mixtures and solvent gradients are required for the separation. With MCSGP, a mixture of three compounds can be separated with high purity for each compound and therefore the number of unit operations for the REEs separation can potentially be reduced.

6.2. Materials and Methods

6.2.1. REE samples and preparation

All REE samples were obtained as highly pure salts. Praseodymium (III,IV) oxide was obtained from Strem Chemicals (Newburyport, USA) at purity of 99.9 %, Cerium(IV) sulfate was obtained from Sigma-Aldrich (Seelze, Germany) at a purity of 98 % and Lanthanum(III) oxide was obtained from Fluka (Buchs, Switzerland) at a purity of 99.997 %. The individual REE salts were dissolved at a concentration up to 1 g/L in 1 M hydrochloric acid (Fluka). After complete dissolution, the pH was adjusted to 2.0 by addition of conc. NaOH (Sigma-Aldrich) and filtrated over 0.45 µm. The stock solutions were kept in the fridge at 4 °C. All water used for sample and buffer preparation was prepared by a Synergy system (Millipore, Billerica, USA) and filtered over 0.2 µm. The three REE components were chosen as the proof of concept as Ce and La are the highest concentrated species in natural REE samples. Pr was added as the third component as it is the neighboring element in the periodic table and therefore the most difficult one to separate from the first two.

6.2.2. Analytics

All analytics for this work were performed on an Agilent 1100 Series system (Santa Clara, USA) consisting of a degasser, quaternary pump, autosampler, column oven and a multi wavelength UV/Vis detector. To allow for detection of REEs, 25 mM Arsenazo III (Fluka) in 1 M acetic acid (Fluka) was mixed as post column reagent (PCR) with the eluent flow right in front of the detector. The PCR was fed with an isocratic pump from Knauer (Berlin, Germany) at 0.5 mL/min. Absorbance was measured at 658 nm. The isocratic separation of the REE species was performed on a Zorbax Eclipse XDB-C8 (Hewlett Packard, Santa Clara, USA) reversed phase column with temporarily functionalization [96]. The column with inner diameter 0.46 mm and a length of 150 mm was packed with particles of size 3.5 μm . 0.6 M citrate solution at pH 2.5 produced from citric acid (Acros Organics, Geel, Belgium) and sodium hydroxide (Sigma-Aldrich) with 0.01 M n-octylsulfonate (TCI, Tsukuba City, Japan) was used as eluent at a flow rate of 1 mL/min. The analytical separations were performed at 25 °C. A typical chromatogram produced under these conditions is shown in Figure 6.2.

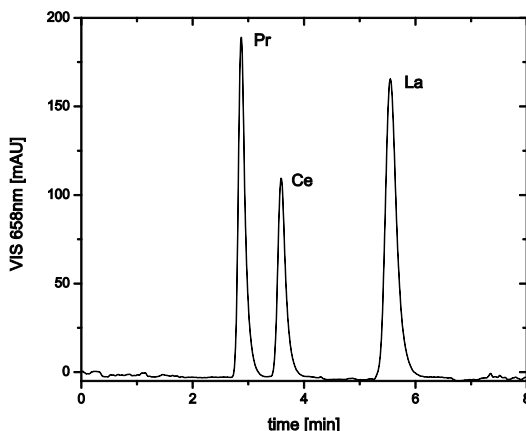


Figure 6.2 Analytical chromatogram of the mixture of Pr, Ce and La

6.2.3. Preparative batch separation and MCSGP

All MCSGP experiments were performed on a lab-scale unit from ChromaCon (Zurich, Switzerland). The unit consists of 4 smartline pumps 100 (50 mL/min), 8 WellChrom K-6 (4 used as multiposition valves for column switching, 3 as drain valves, one as buffer selection valve), 2 Smartline UV detectors 2500 (Single wavelength), at column outlets and one pH/C-900 at the 2nd column outlet. All parts except the last one are manufactured by Knauer (Berlin, Germany) while the pH/Conductivity unit was from ÄKTA (GE Healthcare, Uppsala, Sweden).

For the batch experiments, one detector and two pumps (one for gradient elution and wash, one for feeding) and a fraction collector (FC203B, Gilson, Middleton, USA) were used. The batch experiments were performed starting with feeding the equilibrated column, followed by a wash step with 0.05 M citrate buffer at pH 2.0 and a gradient elution. The elution buffer was based on citrate. Although hydroxybutyric acid solutions as mobile phase provided better performance [103], citrate was chosen as elution buffer because of its low cost, availability and “green character”. As stationary phase, Poros 50HS (Applied Biosystems, Melbourne, Australia) strong cation exchanger resin with mean particle size of 50 µm was used. The resin was packed in 0.5 cm I.D. Tricorn columns (GE healthcare, Uppsala, Sweden) at a volumetric flow rate of 10 mL/min with 0.1 M NaCl solution as packing buffer to a bed height of 10 cm. The columns were tested using analytical injections of REEs.

Table 6-1 MCSGP operating parameters for the four phases defined in Figure 6.1

Variable	Value	Variable	Value
Phase A		Phase B	
Duration	2.0 min	Duration	2.0 min
Flow P1	0.25 mL/min	Flow P1	0.17 mL/min
Flow P2	0.22 mL/min	Flow Feed	0.08 mL/min
Gradient P1 Start	73.3 %	Gradient P1 Start	74.9 %
Gradient P1 End	74.9 %	Gradient P1 End	76.1 %
		Feed	
		concentration	0.13 mg/mL
		Ratio Pr:Ce:La	1:1:1
Phase C		Phase D	
Duration	1.0 min	Duration	14.0 min
Flow P1	0.20 mL/min	Flow P1	0.43 mL/min
Flow P2	0.18 mL/min	Flow Feed	0.50 mL/min
Gradient P1 Start	76.1 %	Gradient P2 Start	50.0 %
Gradient P1 End	76.8 %	Gradient P2 End	73.3 %

In the preparative batch experiments, the capacity of the columns at given conditions was determined and the gradient elution was optimized. The flow through and the elution phases of the chromatography runs were fractionated and then analyzed to guide the identification of suitable operating conditions. In the final batch run selected as the best one, 0.0064 mg of REE were loaded per mL of column volume. After feeding, a wash step

of three column volumes with 25 mM citrate buffer at pH 2.0 was applied followed by the gradient elution. A pH gradient from 3.8 to 5.5 in 7.5 column volumes with 25 mM citrate buffer was applied, and the elution was fractionated for PCR analysis. The flow rate in all steps was 0.5 mL/min. This run was applied as starting point for the MCSGP design as described by Aumann and Morbidelli [1] and is referred to as the “design batch” run in the following.

The MCSGP operating parameters derived from the “design batch” experiment were further fine-tuned to reach the final operating conditions summarized in Table 6-1. The outlet streams *W*, *P*, and *S* indicated in Figure 6.1 of the MCSGP were collected on a cyclic basis and analyzed offline. The process was run until all outlet streams reached steady composition. The columns and buffer applied in the MCSGP were equivalent to the design batch and the specific operating conditions are summarized in Table 6-1.

6.3. Results and discussion

6.3.1. Preparative batch operation

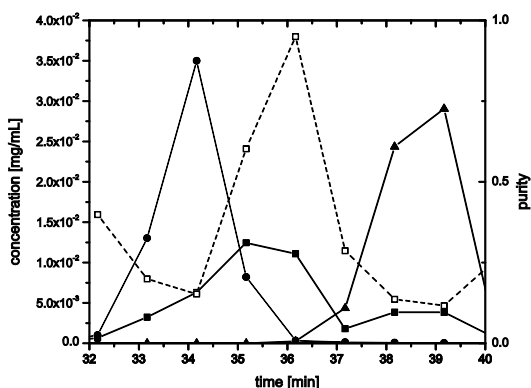


Figure 6.3 Fraction analysis results of the “design batch” showing the concentration of the individual RE species (circles: Pr, squares: Ce, triangles: La) and the purity (dashed line, open squares) with respect to Ce of the collected elution fractions are shown as a function of time. The loaded amount of REE is 0.0064 mg/mL.

The preparative batch chromatographic run used as “design batch” was operated with a total loaded amount of REE equal to 0.0064 mg/mL_{column} as described in the previous section. The feeding flow through, the washing step and the gradient elution were fractionated. The fractions collected during feeding and washing did not contain REE ions, showing that the column loading was below its dynamic binding capacity. During the gradient elution, fractions containing REEs were eluted and analyzed offline through HPLC with PCR leading to the concentration values shown in Figure 6.3. The order of elution

followed the one observed in analytical experiments and was confirmed by experiments published by other authors [97, 101]. Even though the loaded amount of REE material was low, the peaks overlapped significantly leading to very narrow windows in the chromatogram, where highly pure REE species could be obtained. Loading more REEs resulted in incomplete separation with no windows of acceptable purities of the single species. For example, in the case of a load of $0.17 \text{ mg/mL}_{\text{column}}$ shown in Figure 6.4, the center fraction had a maximum purity of only 65% with respect to Ce. It is worth noting that this is not due to column overloading, since the column is still far below its saturation capacity. This is actually due to the too low solubility of the REEs in the citrate buffer. A promising alternative chromatography system has been described by Hansen et al. [4], applying a 1M nitric acid solution as eluent. However, these conditions could not be applied in this work, since our preparative chromatographic equipment does not tolerate such strongly acidic conditions. Nevertheless, the low loading conditions were considered still significant to conduct our study about the reliability of MCSGP for this particular purification process.

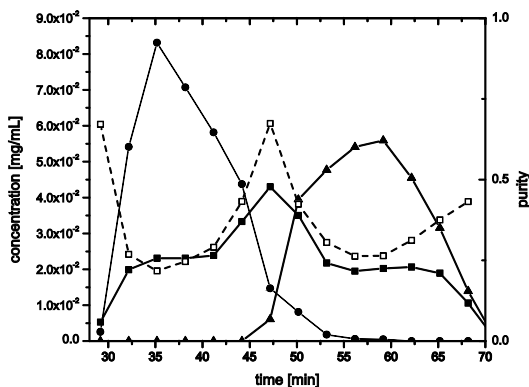


Figure 6.4 Fraction analysis results of a batch elution with higher load (0.17 mg/mL). On the left axis, the individual concentrations (circles: Pr, squares: Ce, triangles: La) and on the right axis the purity with respect to Ce (dashed line, open squares) are shown as a function of time.

In the following the MCSGP operation is designed using the chromatogram shown in Figure 6.3 as the “design batch” experiment. It is worth noting that this corresponds to a preparative process with a maximum purity of 95.0% with respect to Cerium (corresponding to a very narrow central fraction which would lead to a very low yield). Collecting only this fraction as product, the yield for Cerium would in fact be 25.2%. For the batch experiment, the elution was fractionated and the purity and yield of each single fraction determined. Pooling fractions around the peak maximum of Ce and re-analyzing the pools for yield/purity, a so called pareto curve is generated. This curve describes the typical trade-off between product purity and yield in batch chromatography. This trade-

off is due to the fact that product (Ce in this case) and “impurities” (Pr and La in this case) overlap in the preparative chromatogram (Figure 6.3). Under these conditions, one has the choice of collecting the highly pure center fraction of the product peak, resulting in maximum purity, or to collect the complete product peak accepting higher impurity content resulting in maximum yield. These two extreme cases define the limits of the pareto curve, which is a continuous line connecting these two limiting cases in the yield versus purity plot shown in Figure 6.5 and representing the performance of the unit which can be achieved with various operating conditions.

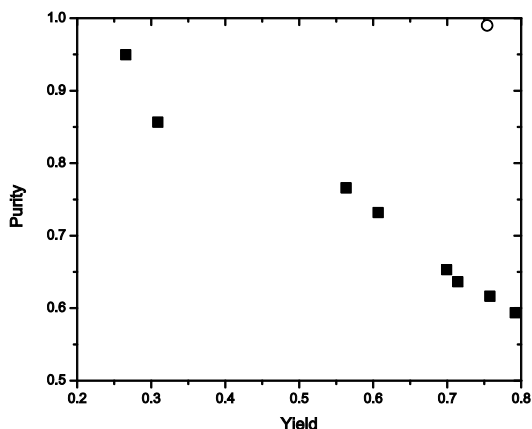


Figure 6.5 Performance comparison with respect to yield and purity of Ce for batch chromatography (■) and MCSGP (○)

6.3.2. MCSGP operation

As discussed above, based on the “design batch” (Figure 6.3), the MCSGP process was designed and operated. The product streams were collected and analyzed. Based on the obtained results the MCSGP was finely tuned leading to the final operating conditions summarized in Table 6-1.

In Figure 6.6, the startup of the final MCSGP process is shown in terms of Ce purity and yield in the product stream of the unit as a function of time. Note that each point corresponds to the average value over one cycle, whose duration is 38 minutes. It is seen that yield and purity build up in time until a steady state value is reached after about three cycles and remain constant from there on. This is due to the fact that during start-up, the internally recycled fraction of the product accumulates.

It is worth noting that the MCSGP process was designed to have not only the center product (E. g. Ce), but also the other two components, E. g. Pr and La, within specified purities. Thus, not only the product stream, but also the side streams *W* and *S* were

collected and analyzed. The comparison among the chromatograms obtained for the feed and all three MCSGP outlet streams is shown in Figure 6.7. It is seen that all outlet streams are virtually pure (Purity of 91.5% for Pr in *W* stream, 99.0% for Ce in *P* and 96.8% for La in *S*), thus proving that the MCSGP process can generate three highly pure streams in a single operation while keeping very high yield.

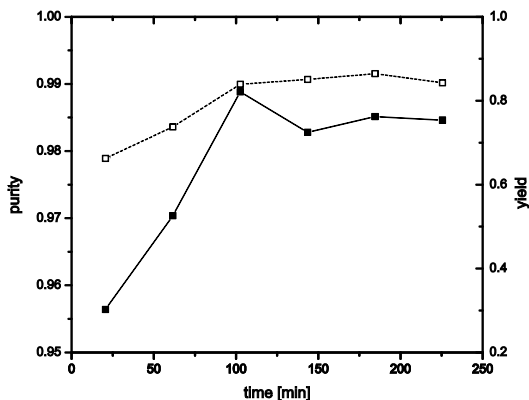


Figure 6.6 Purity (□) and yield (■) values with respect to Ce averaged over an entire cycle as a function of the MCSGP operation time (Cycle time 38 min)

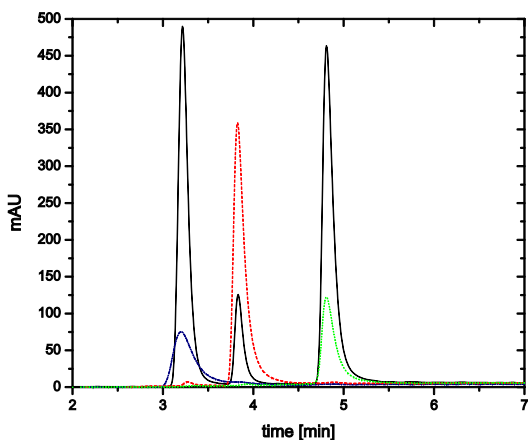


Figure 6.7 Superimposition of the analytical chromatograms of the feed (black solid line) and MCSGP outlet streams (*W*: blue dash dot line, *P*: red dashed line, *S*: green dotted line) at steady state with the operating conditions listed in Table 6-1

The above results indicate that a series of coupled MCSGP units would allow to fractionate a crude, geological sample of REEs into multiple, highly purified streams.

The important limitation which remains at this point relates to the low loading and therefore low productivity of the process. As in the case of the batch process described above, this is due to the low solubility of the REE components in the particular buffer used in this work. It is conceivable that by applying different buffer/solvent conditions could solve this problem.

6.3.3. Comparing the performance of batch and continuous countercurrent (MCSGP) chromatography

The “design batch” experiment and the MCSGP run shown in previous sections can be readily compared in terms of performance, as the loading was approximately the same. In particular, we refer to the Cerium yield versus purity diagram shown in Figure 6.5, where, as discussed above, the pareto curve corresponding to the “design batch” chromatogram is shown. From the MCSGP experiment, a single point in the yield versus purity diagram in Figure 6.5 is obtained representing the product collected during the product elution phase (B) at steady state. It appears that the performance of the MCSGP process is clearly superior to that of the batch process. At equal column loading, the MCSGP can in fact achieve both high purity and high yield in contrast to the trade-off between these two parameters for the batch run. The reason for the better performance of the MCSGP process lies in the internal recycling, which leads to product accumulation in the system and, at steady state, to withdrawn of more concentrated product streams in the same window as in the high purity batch experiment.

The performance parameters for the MCSGP run at steady state and the two extreme points of the pareto curve for the batch runs are compared in Table 6-2. For a better comparison the batch points were chosen in such a way that they are similar to the MCSGP in either purity or yield. Looking at the productivity, the MCSGP provides a productivity increase by a factor 15 together with a yield increase from 26 to 75%, for a fixed purity of more than 95%. On the other hand, when considering the high yield batch run, i. e. about 75%, we observe an about 5 fold increase in productivity with a significant increase in purity from 62 to 99%.

Table 6-2 Comparing the performance parameters of the “batch design” run pools (high purity and high yield pool) with the MCSGP steady state outlet stream

	Yield [%]	Purity [%]	Productivity [g/L/h]
Batch high purity	26.5	95.0	$1.8 \cdot 10^{-3}$
Batch high yield	75.7	61.7	$5.1 \cdot 10^{-3}$
MCSGP	75.4	99.0	$2.6 \cdot 10^{-2}$

6.4. Conclusion

In this work, the application of continuous countercurrent chromatography in the form of MCSGP process to the preparative separation of a REE mixture has been investigated with specific reference to a model ternary mixture of Praseodymium, Cerium and Lanthanum. Starting from a suitably selected “design batch” experiment, the MCSGP process was designed. It was shown that within three cycles, the MCSGP process reached steady state operation and produced three fractions, each containing one of the three chemical species within purity specifications. In comparison to batch chromatography the MCSGP unit provides performances that for a given purity (yield) provide significantly larger yield (purity) and the productivity increases by a factor of up to 15.

The fact that MCSGP provides all three species relatively pure in the three outlet streams allows us thinking of the development of a complete fractionation process for producing REE species. This could include a cascade of MCSGP units starting with dissolved geological samples containing all REE species, but in very different concentrations.

The purity and yield values obtained in the MCSGP run described in this work would be satisfactory for a large scale application. Unfortunately, the productivity of about 1 gram per liter of stationary phase and day is way too small. This is due to the very low loading used in this experiment which is due to the too low solubility of the REEs in the considered buffer. This problem can be overcome through a reformulation of the chromatographic system and in particular of the mobile phase. Indeed it has been shown [97, 103] that going from citrate to HIBA could improve the batch productivity, but the upscaling to an industrial process would be difficult and expensive. A more promising alternative would be a low pH system with nitric or hydrochloric acid as the mobile phase. This approach was already investigated in simulation [4] and showed promising results, but it requires a MCSGP unit made of suitable materials for an experimental proof of concept. Nevertheless, considering the solubility values reported in [104] and knowing the typical performance of the MCSGP process with respect to batch operation [82], a productivity in the order of magnitude of kilograms per liter column volume and day is not unreasonable.

6.5. Remark

The work in this chapter is submitted for publication in the journal of Industrial and Engineering Chemistry Research (IECR).

7. Concluding remarks

In this work, several projects applying and continuing the development of the multi-column countercurrent solvent gradient purification (MCSGP) process have been performed.

The first work described the separation of charge variants from three commercially available monoclonal antibodies (mAb) (Avastin®, Herceptin®, Erbitux®). From literature, the different bio activities for the case of Herceptin® were known [2] and a similar activity pattern can be expected for the other two mAbs. Therefore a purification of the most active variant was performed which could be achieved both with a batch elution process and the MCSGP. However, comparing the productivity, the MCSGP process clearly outperformed the batch separation. In case of Herceptin®, the bio activity of the mAb product could be increased to 130% in comparison to the original mixture at a yield of 0.85, while the batch yield for the same activity increase was 0.24.

The 3 column MCSGP process was expanded with the goal to separate more than three fractions. It has theoretically been shown how to design such a multi fraction separation starting from a batch chromatogram. For each additional fraction, one column has to be added to the setup; therefore theoretically a n -fraction separation is possible. In experimental application, only four fraction separations were performed with model proteins and mAb charge variants, verifying the concept of the four fraction separation.

To stabilize the MCSGP process for long term runs, control concepts based on heuristic PID controller were tested with the process. As a first concept, the online UV of the process was used as feedback directly. This had the advantage that the feedback was readily available and no additional hardware was required. The direct UV controller worked on the maximum of this online UV, keeping it at a certain position of the process. Thereby, the controller was able to keep the process at a stable operating point, during startup and also under disturbed conditions. The drawback of this very simple control concept was the lack of knowledge of the process purity which could not be extracted from the online UV. Therefore, a complete offline tuning had to be performed before applying the controller. The controller was only able to stabilize the process at the operator set conditions. The control concept was successfully applied with two model systems, one based on the protein lysozyme and the other one based on the peptide Fibrinopeptide A human.

In a second approach, a controller still based on PID, was developed which can directly control the product purity. This goal is achieved by changing the feedback to an automated HPLC system able to analyze the product stream more in detail. This more complex feedback, which is much more time consuming and requiring additional hardware, successfully controlled the amount of weak and strong impurities in the product stream. The applied multi input multi output PID control system was experimentally validated with a protein model mixture and a mAb supernatant capture, being able to reject disturbances and guiding the process start-up.

The MCSGP process, which was designed for the purification of biomolecules, was applied to the purification of rare earth elements (REE), which is a very challenging separation as well. As a model separation, three lanthanides (Praseodymium, Cerium and Lanthanum) were separated with complexing chromatography. The MCSGP process could clearly outperform the design batch run, the productivity was increased by factor 15 for the same purity, but the loading had to be kept at a very low value, as the solubility of the metals in citrate was insufficient. TO overcome this limitation, a strong acid based system could be implemented which was implemented with higher loading in batch chromatography [4].

8. Curriculum Vitae

Personal

Martin Krättli

Résumé

Project Manager Downstream Processes for Proteins with Lonza	01.2013 – current
PhD studies in the group of professor Morbidelli, Institute for Chemical and Bioengineering, Department of Chemistry and Applied Biosciences, ETH Zurich Thesis title: ONLINE CONTROL DEVELOPMENT AND PROCESS INTESIFICATION IN CONTINUOUS CHROMATORAPHY (MCSGP)	04.2009 – 11.2012
Research internship with Imperial College Project on ' <i>Modelling of a Solid Looping System for Carbondioxide Capture in Power Plant Flue Gas based on Limestone</i> ' supervised by Prof. C. Pantelides and Prof. N. Shah	10.2008 – 04.2009
Master studies in Chemical and Bioengineering at ETH Zurich Master thesis on ' <i>Crystallization of Acetylsalicylic Acid by Combined Cooling and Antisolvent Addition</i> ', supervised by Prof. M. Mazzotti and C. Lindenberg in cooperation with Novartis Pharma AG (Supervisor Novartis: Dr. J. Brozio) Graduation as: MSc ETH Chem Bio Eng	09.2007 – 08.2008
Bachelor studies in Chemical Engineering at ETH Zurich Graduation as: BSc ETH Chem Eng	09.2004 – 08.2007

Publications

- Krättli M, Ströhlein G, Aumann L, Müller-Späh T, Morbidelli M. 2011 Closed loop control of the multi-column solvent gradient purification process. *Journal of Chromatography A* 1218(50):9028-9036. [Full text](#)
- Brand B, Krättli M, Storti G, Morbidelli M. 2011. Strong cation exchange monoliths for HPLC by Reactive Gelation. *Journal of Separation Science* 34(16-17):2159-2163. [Full text](#)
- Müller-Späh T, Krättli M, Aumann L, Ströhlein G, Morbidelli M. 2010. Increasing the Activity of Monoclonal Antibody Therapeutics by Continuous Chromatography (MCSGP). *Biotechnology and Bioengineering* 107(4):652-662. [Full text](#)

- Lindenberg C, Krättli M, Cornel J, Mazzotti M, Brozio J. 2009. Design and Optimization of a Combined Cooling/Antisolvent Crystallization Process. *Crystal Growth & Design*, 9(2):1124 - 1136. [Full text](#)

Oral and Poster Presentations

- Krättli M, Baur D, Schildbach G, Ströhlein G, Morari M, Morbidelli M. 2011. Cycle to Cycle Model Predictive Control in Continuous Chromatography (MCSGP). *Preparative and Process Chromatography (PREP)*, oral presentation
- Krättli M, Müller-Späth M, Aumann L, Ströhlein G, Morbidelli M. 2011. Continuous countercurrent chromatography (MCSGP) for multi-fraction separations. 7. Doktorandenseminar "Chromatographische Trennprozesse", oral presentation
- Krättli M, Brand B, Müller-Späth T, Aumann L, Morbidelli M. 2010. Monolithic Structures applied in Preparative Chromatography. *Symposium on Preparative and Industrial Chromatography and Allied Techniques (SPICA)*, oral presentation
- Krättli M, Morbidelli M. 2010. Preparative Scale Purification of a Monoclonal Antibody Supernatant with a Strong Cation Exchanger CIM Disk. *Monolith Summer School (MSS)*, poster presentation
- Krättli M, Ströhlein G, Müller-Späth T, Morbidelli M. 2010. Cyclic Control in Protein and Peptide Purification applying Continuous Chromatography (MCSGP). *Preparative and Process Chromatography (PREP)*, oral presentation

Summer schools and training

- Monolith Summer School (MSS), Bia Separations, Portoroz, 2011
- LabView Core 1 training, National Instrument, Ennetbaden, 2010

9. Figure and Table index

9.1. Figures

Figure 1.1 Concept study of countercurrent chromatography [16]	3
Figure 1.2 Schematic overview of a true moving bed (TMB) chromatography process. Showing the column with fluid stream from the left to the right, solid stream in the opposite direction and the feed in fair grey entering in the middle. The two components in the feed are moving according to their adsorbing behavior to the left or right, being eluted as pure extract and raffinate eventually [16].....	3
Figure 1.3 Schematic overview of the PID control concept applied for the MCSGP. On the left, the process is shown giving a feedback to the controller on a cyclic basis. The controller on the right calculates according to the feedback and a set value the process parameters for the next cycle.....	5
Figure 2.1: Nomenclature of the mAb variants of Bevacizumab 'Bev', top; Trastuzumab 'Tra', center; and Cetuximab 'Cet', bottom. The chromatograms were obtained with cation exchange chromatography as indicated in the analytics section. Symbols in parentheses refer to the nomenclature used in [2].....	11
Figure 2.2: Flow scheme of the MCSGP process using four columns. Interconnected state (CC) tasks are indicated with 2, 4, 5b and 6; batch state (BL) tasks are indicated with 1, 3, 5a, 5c. <i>S</i> represents strongly adsorbing components, <i>P</i> the product and <i>W</i> weakly adsorbing components.	14
Figure 2.3: Fraction analyses of linear gradient elutions of Bevacizumab (top), Trastuzumab (center) and Cetuximab (bottom). The thick solid line represents the scaled UV-signal at 280 nm, the dashed thick line indicates the purity with respect to the main variant <i>P</i> . The symbols represent the mAb variant concentrations as determined by offline analytics: <i>W</i> ₁ (x), <i>W</i> ₂ (■), <i>W</i> ₃ (●), <i>P</i> (◆), <i>S</i> ₁ (▲), <i>S</i> ₂ (△). Variants <i>W</i> ₁ and <i>W</i> ₂ in the case of Trastuzumab and variants <i>S</i> ₃ and <i>S</i> ₄ in the case of Cetuximab were omitted for the sake of clarity. In the case of Trastuzumab, the simulated variant concentrations are given as thin dashed lines.	19
Figure 2.4: MCSGP runs with Bevacizumab (top), Trastuzumab (center) and Cetuximab (bottom). The thin dashed line represents the scaled UV-signal at 280 nm. Purity (▲), yield (◆) and product concentrations (■) were determined by offline analyses. The horizontal bars indicate the sample collection intervals (usually one cycle). For Trastuzumab, the simulation results are also shown in terms of product concentration (-.-.-), yield (—) and purity (---).	21
Figure 2.5: Yield-purity relations for batch (◇, ◆) and MCSGP chromatography (▲) of Bevacizumab (top), Trastuzumab (center) and Cetuximab (bottom). The dashed lines with arrows indicate the yield-purity trade-off of batch chromatography.....	23
Figure 2.6: Chromatograms of feeds enriched in weakly adsorbing (<i>W</i>) variants (---) together with regular feeds (—) are shown in the left column. Chromatograms of MCSGP-product streams obtained with enriched feeds (---) and regular feeds (—) are shown in the right column. Bev data are displayed at the top, Tra data at the center and Cet data at the bottom. For Cet also the chromatograms based on a feed mixture enriched in strongly adsorbing (<i>S</i>) variants (-.-.-) are shown.....	24
Figure 2.7: Simulated values of purity (◆) and yield (■) for the Trastuzumab <i>P</i> variant purified by MCSGP as a function of the <i>W</i> ₃ -content of the feed mixture. Empty symbols indicate the corresponding experimental data of purity (◇) and yield (□).....	25
Figure 2.8 Chromatograms of Trastuzumab MCSGP products (—) together with regular feeds (---). In the top part, the results of main variant enrichment (strategy 1) are shown;	

for comparison a chromatogram of the purest fraction of the empirically optimized batch gradient run is also shown (grey line). The bottom part shows the results of the MCSGP run aimed solely at decreasing the concentration of the S1-variant indicated by the circle (strategy 2).....	26
Figure 3.1 Schematic batch elution chromatogram containing three fractions. In the top part of the figure, the schematic elution chromatogram with the target component <i>P</i> and the early and late eluting impurities <i>W</i> and <i>S</i> is shown. On the bottom, the corresponding modifier gradient is displayed.....	32
Figure 3.2 Schematic of the three fraction MCSGP process. On top the process flowsheet is shown. In the graphs in the middle and on the bottom, schematic UV and conductivity diagrams are shown, respectively. The vertical, dotted lines indicate column switchers. The columns move every switch one position from 6 to 1, fulfilling alternating batch elution (uneven column positions) and interconnected recycling (even column positions) functions.	33
Figure 3.3 Preparative batch chromatogram for the four fraction process. The “design batch” is divided into eight parts corresponding to the eight different tasks in the MCSGP	34
Figure 3.4 Schematic overview of the four fraction MCSGP process. On top the process flowsheet is shown. In the graphs in the middle and on the bottom, schematic UV and conductivity diagram are shown. The vertical, dotted lines indicate column switching. The columns move every switch one position from 8 to 1, fulfilling alternating batch elution (uneven column positions) and interconnected recycling (even column positions) functions.	35
Figure 3.5 Five fraction MCSGP schematic, highlighting in red the hardware additionally required to separate one additional fraction. Adding this highlighted hardware multiple times, the MCSGP can separate as many fractions as columns available.	36
Figure 3.6 Schematic overview of streams around a column and a mixing knot in the MCSGP process.....	37
Figure 3.7 Analytical cation exchange chromatogram of the protein model mixture.....	41
Figure 3.8 Nomenclature of the mAb variants of Cetuximab.	42
Figure 3.9 “Design batch” chromatogram of the model protein mixture showing online UV (solid line), modifier gradient (dashed line) and fraction analysis for the 4 components (<i>W</i> : cycles, <i>P</i> ₁ : stars, <i>P</i> ₂ : squares, <i>S</i> : triangles). Additionally, the recycled fractions for the MCSGP process are indicated by the grey areas. In between the recycled fractions, the collection windows of the two products <i>P</i> ₁ and <i>P</i> ₂ are indicated.	44
Figure 3.10 Startup of the MCSGP process monitored through the fraction analysis of the center products <i>P</i> ₁ (□) and <i>P</i> ₂ (■). In the upper part of the figure the purity is shown and in the lower part the yield.	45
Figure 3.11 Fraction analysis of the feed (black solid line) and the four MCSGP outlet streams (<i>W</i> : blue dashed line, <i>P</i> ₁ : pink dotted line, <i>P</i> ₂ : red dash dotted line and <i>S</i> : green dash dot dotted line) for the protein model mixture. The y axis is shown in arbitrary units to compare the peaks.	46
Figure 3.12 Purity versus yield diagram for <i>P</i> ₁ (Cytochrome C, left) and <i>P</i> ₂ (Lysozyme, right). The squares indicate the MCSGP steady state performance while the triangles indicate points for different cuts of the “design batch” chromatogram thereby forming the pareto curve indicated by the dashed line.	47
Figure 3.13 “Design batch” chromatogram of Cetuximab, including the online UV signal (solid line), the modifier gradient (dashed line) and the concentrations of the eight variants of Cetuximab: Cet-1(<i>W</i>): filled circles, Cet-2(<i>W</i>): open circles, Cet-3(<i>P</i> ₁), stars; Cet-4(<i>P</i> ₂), squares; Cet-5 + Cet-6(<i>S</i>), filled triangles; Cet-7 + Cet-8(<i>S</i>), open triangles. The grey areas indicate the recycling fractions selected for the MCSGP operation while in between these, the collection windows for the product streams <i>P</i> ₁ and <i>P</i> ₂ are indicated.	48

Figure 3.14 Analytical chromatograms of the MCSGP feed stream (solid line) and the product streams P_1 (Cet-3, dashed line) and P_2 (Cet-4, dotted line). The y axis units are normalized, as the concentrations in the three samples are different.	48
Figure 3.15 Purity yield diagrams for Cet-3 (P_1) and Cet-4 (P_2) on the left and on the right, respectively. The squares indicate the results for the MCSGP process, the triangles the pareto front derived from the fractionation of the batch elution.	49
Figure 4.1 Schematic overview of the MCSGP process with three columns (Positions 1 – 6) and four columns with additional cleaning in place (all positions)	51
Figure 4.2 Explanation of the controller action. In subfigure (a), a symmetric peak without impurities with the corresponding set value is shown. In subfigure (b), an overloaded signal with early eluting impurities is and the resulting, shifted set value is shown.	54
Figure 4.3 Analytical chromatograms for Lysozyme (top) and Fibrinopeptide A human (bottom) crudes. The chromatograms were obtained as indicated in the analytics section (4.3.3)	55
Figure 4.4 Steady state control experiment with Lysozyme. At cycle 5, the data acquisition method for the feedback signal is switched from peak maximum to first moment. The curve with open symbols (\square) indicates the actual interconnected time, the filled symbols (\blacksquare) the actual error, respectively.	58
Figure 4.5 Complete MCSGP run with closed loop controller (cycle to cycle) for Lysozyme. The curve with open symbols (\square) indicates the actual interconnected time, the filled symbols (\blacksquare) the actual error. At the times indicated by the vertical, dotted lines, and external disturbances have been introduced.....	59
Figure 4.6 Internal profiles averaged from all UV detectors for Lysozyme during MCSGP startup with closed loop controller. The dotted, vertical lines indicate the product collection window of the 6 th cycle.....	60
Figure 4.7 Selected batch chromatogram for the design of the MCSGP process for the purification of Fibrinopeptide A human. The dotted straight line shows the gradient to be applied in the MCSGP process.	61
Figure 4.8 Internal profile averaged from all UV detectors for Fibrinopeptide A human during MCSGP startup with closed loop controller. The dotted, vertical lines indicate the product collection window at the 15 th cycle.	62
Figure 4.9 Complete MCSGP run with closed loop controller (cycle to cycle) for Fibrinopeptide A human purification. The curve with open symbols (\square) indicates the interconnected time, the filled symbols (\blacksquare) the error. The dotted, vertical lines indicate the time at which an external disturbance is introduced.....	63
Figure 4.10 Purity trajectory for the cycle to cycle control run with Fibrinopeptide A human. The product stream purity at each cycle was measured using offline HPLC analytics. The curve with filled squares (\blacksquare) indicate the Fibrinopeptide A human content in the product stream, the one with empty circles (\circ) the content of early eluting impurities and the one with filled circles (\bullet) the content of late eluting impurities.	64
Figure 4.11 Chromatograms of the feed (dashed line) and the product outlet (solid line) at the 36 th cycle of the MCSGP run with Fibrinopeptide A human. The main window shows the full chromatograms which the small window in the upper left edge shows a zoom to make the impurities visible. The axis of the zoom has the same units as the main window.	64
Figure 4.12 MCSGP run from startup with closed loop switch to switch controller for Fibrinopeptide A human. The curve with open symbols (\square) indicates the actual interconnected time and the filled symbols (\blacksquare) the actual error.	65
Figure 4.13 Purity Composition of the product stream as a function of the cycle number for the switch to switch controlled Fibrinopeptide A human experiment. The curve with filled squares (\blacksquare) indicate the Fibrinopeptide A human content in the product stream, the one	

with empty circles (○) the content of early eluting impurities and the one with filled circles (●) the content of late eluting impurities.....	66
Figure 4.14 Transient yield values as a function of the cycle number for the switch to switch controlled Fibrinopeptide A human experiment.....	67
Figure 5.1 Schematic overview of a complete cycle of the twin-column MCSGP process. On the left and the right, the chromatograms of the corresponding column are shown. In the middle, the two columns with connecting streams are shown. F, W, P and S denote the feed, early eluting impurity, the product and late eluting impurity streams, respectively. The capital letters on the left indicate the various phases within switch one and two (See text).....	70
Figure 5.2 Schematic of the MIMO PID controller. At the top, the chromatogram of the MCSGP with the PEW is shown. The eluted P is analyzed on a cyclic basis by HPLC producing feedbacks (e_s and e_w) for the two PID controllers. The controller act on the PEW boarder lines via the elution volumes V of the MCSGP phases A, B and C: $V_{A,PID}$, $V_{B,PID}$ and $V_{C,PID}$	74
Figure 5.3 Analytical chromatogram of the protein model mixture at 220 nm wavelength.....	76
Figure 5.4 Analytical chromatogram of the mAb feed. The relevant impurities: aggregates and fragments are highlighted. All other visible impurities end up in the flow through under process conditions and are therefore not considered in detail. The chromatogram was recorded at 280 nm.....	77
Figure 5.5 Left: Error and controller output trajectories for the protein model mixture showing the process stat up. On top, the errors of the W controller (■) and the S controller (□) are shown. On the bottom figure, the controller outputs with the same symbols.....	79
Figure 5.6 Error and controller output trajectories for the protein model mixture showing rejection of disturbances in a gradient pump flow rate in cycles 25, 50, 76 and 97, indicated by dashed lines. On top, the errors of the W controller (■) and the S controller (□) are shown. On the bottom, the controller outputs with the same symbols.....	80
Figure 5.7 Analytical chromatogram of the original protein model mixture feed (solid line) and of the one enriched in the impurities (dashed line).....	81
Figure 5.8 Error and controller output trajectories for the protein model mixture showing rejection of disturbances in the feed composition in cycles 121 and 150, indicated by dashed lines in the figure. On top, the errors of the W controller (■) and the S controller (□) are shown. On the bottom, the controller outputs with the same symbols.....	82
Figure 5.9 Preparative design batch chromatogram for the mAb purification process including the online UV chromatogram (solid black line), fraction analysis (blue circles: W, red squares: P, green triangles: S) on the left y axis in arbitrary units and the modifier gradient (dashed line) on the right y axis.....	83
Figure 5.10 The upper diagram shows the actual error (solid lines, filled symbols: W, open symbols: S) on the left axis and the controller outputs (dashed lines, same symbols) on the right axis. In the lower part, the concentrations of the individual components in the product stream (blue circles: W, red squares: P, green triangles: S) are shown on the left axis in terms of the corresponding chromatographic areas and the purity with respect to P (black squares, dashed line) on the right axis.....	84
Figure 5.11 Yield versus purity diagram comparing the performance of batch runs (one with high purity and low yield and the other vice versa (black squares)) and the MCSGP run. The process start-up is represented by the red dots connected with arrows indicating the unit time evolution.....	85
Figure 5.12 Error and controller output trajectories for the mAb supernatant showing the MCSGP unit start-up (until cycle 19), a disturbance in a gradient pump flow rate in cycles 20 and a feed disturbance in cycle 50. The disturbances are indicated by dashed lines in	

the figure. On top, the errors of the <i>W</i> controller (■) and the <i>S</i> controller (□) are shown. On the bottom figure, the controller outputs with the same symbols.	86
Figure 5.13 Analytical chromatograms of the original mAb supernatant (solid line) and the pretreated supernatant (dashed line) used as second feed to the process.	86
Figure 6.1 Overview of the twin-column MCSGP process. <i>W</i> , <i>P</i> and <i>S</i> indicate the streams of the unit containing the purified REE ions. The time evolves from the top of the figure downward. The two physical columns are numbered and all streams are indicated by arrows. On the left and right of the flow scheme, the internal chromatogram of the neighboring column is shown containing the modifier gradient in dashed line and the three components <i>W</i> , <i>P</i> and <i>S</i> as triangle areas with the same color as in the flow scheme. The blue dashed line indicates the column switch, while the dotted vertical lines indicate the phase changes within a cycle.....	89
Figure 6.2 Analytical chromatogram of the mixture of <i>Pr</i> , <i>Ce</i> and <i>La</i>	91
Figure 6.3 Fraction analysis results of the “design batch” showing the concentration of the individual RE species (circles: <i>Pr</i> , squares: <i>Ce</i> , triangles: <i>La</i>) and the purity (dashed line, open squares) with respect to <i>Ce</i> of the collected elution fractions are shown as a function of time. The loaded amount of REE is 0.0064 mg/mL.....	93
Figure 6.4 Fraction analysis results of a batch elution with higher load (0.17 mg/mL). On the left axis, the individual concentrations (circles: <i>Pr</i> , squares: <i>Ce</i> , triangles: <i>La</i>) and on the right axis the purity with respect to <i>Ce</i> (dashed line, open squares) are shown as a function of time.....	94
Figure 6.5 Performance comparison with respect to yield and purity of <i>Ce</i> for batch chromatography (■) and MCSGP (○)	95
Figure 6.6 Purity (□) and yield (■) values with respect to <i>Ce</i> averaged over an entire cycle as a function of the MCSGP operation time (Cycle time 38 min)	96
Figure 6.7 Superimposition of the analytical chromatograms of the feed (black solid line) and MCSGP outlet streams (<i>W</i> : blue dash dot line, <i>P</i> : red dashed line, <i>S</i> : green dotted line) at steady state with the operating conditions listed in Table 6-1.....	96

9.2. Tables

Table 2-1: Properties of the mAb used for this study	10
Table 2-2: Parameters for mAb analytics.....	12
Table 2-3: Conditions for preparative batch and MCSGP experiments and for retention time measurements.	13
Table 2-4: Performance parameters for batch and MCSGP processes. The notation is explained in the nomenclature section.....	16
Table 2-5: Performance of experimental MCSGP and batch runs.	18
Table 2-6: Performance of MCSGP and batch runs for strategies 1 and 2. Line 4, marked with an asterisk indicates batch product with the same specific activity as the MCSGP product.	28
Table 3-1 Parameters for protein standard sytem and Cetuximab analytics.....	40
Table 3-2 MCSGP parameters derived from the “design batch” elution chromatogram for the protein model mixture and Cetuximab	43
Table 4-1 Characteristics of the batch and MCSGP purification runs.....	56
Table 4-2 Summary of analytic conditions	57
Table 4-3 Controller parameters for MCSGP runs	58
Table 5-1 Controller constants according to equations 5.3 and 5.4 applied in this work.....	74
Table 5-2 Operating conditions for all preparative runs in this work. These represent the initial conditions and may be affected by the controller during operation.....	77

Table 6-1 MCSGP operating parameters for the four phases defined in Figure 6.1 92

Table 6-2 Comparing the performance parameters of the “batch design” run pools (high
purity and high yield pool) with the MCSGP steady state outlet stream97

10. References

1. Aumann, L. and M. Morbidelli, *A continuous multicolumn countercurrent solvent gradient purification (MCSGP) process*. Biotechnology and Bioengineering, 2007. **98**(5): p. 1043-1055.
2. Harris, R.J., et al., *Identification of multiple sources of charge heterogeneity in a recombinant antibody*. Journal of Chromatography B, 2001. **752**(2): p. 233-245.
3. Hanson, D.J., *Concern Grows over Rare-Earths Supply*. Chemical & Engineering News, 2011. **89**(20): p. 28-29.
4. Max-Hansen, M., et al., *Optimization of preparative chromatographic separation of multiple rare earth elements*. Journal of Chromatography A, 2011. **1218**(51): p. 9155-9161.
5. Cazes, J., *Encyclopedia of chromatography*. 3rd ed. 2010, Boca Raton, FL: CRC Press. 3 Bände.
6. Taylor, L.T., *Supercritical Fluid Chromatography*. Analytical Chemistry, 2010. **82**(12): p. 4925-4935.
7. Guiochon, G. and A. Tarafder, *Fundamental challenges and opportunities for preparative supercritical fluid chromatography*. Journal of Chromatography A, 2011. **1218**(8): p. 1037-1114.
8. Guiochon, G., *Preparative liquid chromatography*. Journal of Chromatography A, 2002. **965**(1-2): p. 129-161.
9. Zhou, J.X. and T. Tressel, *Basic concepts in Q membrane chromatography for large-scale antibody production*. Biotechnology Progress, 2006. **22**(2): p. 341-349.
10. Brand, B., et al., *Strong cation exchange monoliths for HPLC by Reactive Gelation*. Journal of Separation Science, 2011. **34**(16-17): p. 2159-2163.
11. Wang, P.G., *Monolithic chromatography and its modern applications*. The chromsoc separation science series. 2010, St Albans: ILM. 620 S.
12. Hopmann, E., J. Goll, and M. Minceva, *Sequential Centrifugal Partition Chromatography: A New Continuous Chromatographic Technology*. Chemical Engineering & Technology, 2012. **35**(1): p. 72-82.
13. Varma, A. and M. Morbidelli, *Mathematical methods in chemical engineering*. 1997, New York [etc.]: Oxford University Press. XIV, 690 S.
14. Guiochon, G., S.G. Shirazi, and A.M. Katti, *Fundamentals of preparative and nonlinear chromatography*. 1994, Boston [etc.]: Academic Press. XV, 701 S.
15. Schmidt-Traub, H., *Preparative chromatography of fine chemicals and pharmaceutical agents*. 2005, Weinheim: Wiley-VCH. 458 S.
16. Müller-Späth, T., *Purification of monoclonal antibodies by continuous chromatography*, 2009, ETH: Zürich. p. 1 Band.
17. Mazzotti, M., G. Storti, and M. Morbidelli, *Optimal operation of simulated moving bed units for nonlinear chromatographic separations*. Journal of Chromatography A, 1997. **769**(1): p. 3-24.
18. Gomes, P.S. and A.E. Rodrigues, *Simulated Moving Bed Chromatography: From Concept to Proof-of-Concept*. Chemical Engineering & Technology, 2012. **35**(1): p. 17-34.
19. Rajendran, A., G. Paredes, and M. Mazzotti, *Simulated moving bed chromatography for the separation of enantiomers*. Journal of Chromatography A, 2009. **1216**(4): p. 709-738.
20. Silva, R.J.S., et al., *A new multicolumn, open-loop process for center-cut separation by solvent-gradient chromatography*. Journal of Chromatography A, 2010. **1217**(52): p. 8257-8269.

21. Aumann, L. and M. Morbidelli, *A semicontinuous 3-column Countercurrent Solvent Gradient Purification (MCSGP) process*. Biotechnology and Bioengineering, 2008. **99**(3): p. 728-733.
22. Lunze, J., *Regelungstechnik*. [Einzelbände in verschiedenen Auflagen] ed. Springer-Lehrbuch. 1996, Berlin: Springer. 1-2.
23. Visioli, A., *Practical PID control*. Advances in industrial control. 2006, London: Springer. Online-Datei.
24. Walsh, G., *Biopharmaceuticals: recent approvals and likely directions*. Trends in Biotechnology, 2005. **23**(11): p. 553-558.
25. Jefferis, R., *Glycosylation as a strategy to improve antibody-based therapeutics*. Nature Reviews Drug Discovery, 2009. **8**(3): p. 226-234.
26. Sethuraman, N. and T.A. Stadheim, *Challenges in therapeutic glycoprotein production*. Current Opinion in Biotechnology, 2006. **17**(4): p. 341-346.
27. Qian, J., et al., *Structural characterization of N-linked oligosaccharides on monoclonal antibody cetuximab by the combination of orthogonal matrix-assisted laser desorption/ionization hybrid quadrupole-quadrupole time-of-flight tandem mass spectrometry and sequential enzymatic digestion*. Analytical Biochemistry, 2007. **364**(1): p. 8-18.
28. Muthing, J., et al., *Effects of buffering conditions and culture pH on production rates and glycosylation of clinical phase I anti-melanoma mouse IgG3 monoclonal antibody R24*. Biotechnology and Bioengineering, 2003. **83**(3): p. 321-334.
29. Kunkel, J.P., et al., *Comparisons of the glycosylation of a monoclonal antibody produced under nominally identical cell culture conditions in two different bioreactors*. Biotechnology Progress, 2000. **16**(3): p. 462-470.
30. Pluschke, S., et al., *Development and integration of a new animal-component-free process for the production of UK-279,276*, in *Animal Cell Technology Meets Genomics*, F. Godia and M. Fussenegger, Editors. 2005. p. 465-470.
31. Liu, Y.D., R.Z. van Enk, and G.C. Flynn, *Human antibody Fc deamidation in vivo*. Biologicals, 2009. **37**(5): p. 313-322.
32. Vlasak, J., et al., *Identification and characterization of asparagine deamidation in the light chain CDR1 of a humanized IgG1 antibody*. Analytical Biochemistry, 2009. **392**(2): p. 145-154.
33. Yan, B.X., et al., *Succinimide Formation at Asn 55 in the Complementarity Determining Region of a Recombinant Monoclonal Antibody IgG1 Heavy Chain*. Journal of Pharmaceutical Sciences, 2009. **98**(10): p. 3509-3521.
34. Sosic, Z., et al., *Application of imaging capillary IEF for characterization and quantitative analysis of recombinant protein charge heterogeneity*. Electrophoresis, 2008. **29**(21): p. 4368-4376.
35. Weitzhandler, M., et al., *Protein variant separations by cation-exchange chromatography on tentacle-type polymeric stationary phases*. Journal of Chromatography A, 1998. **828**(1-2): p. 365-372.
36. Müller-Späth, T., et al., *Chromatographic separation of three monoclonal antibody variants using multicolumn countercurrent solvent gradient purification (MCSGP)*. Biotechnology and Bioengineering, 2008. **100**(6): p. 1166-1177.
37. Aumann, L., G. Ströhlein, and M. Morbidelli, *Parametric study of a 6-column countercurrent solvent gradient purification (MCSGP) unit*. Biotechnology and Bioengineering, 2007. **98**(5): p. 1029-1042.
38. Müller-Späh, T., et al., *Chromatographic separation of three monoclonal antibody variants using multicolumn countercurrent solvent gradient purification (MCSGP)*. Biotechnology and Bioengineering, 2008. **100**(6): p. 1166-1177.

39. Müller-Späth, T., L. Aumann, and M. Morbidelli, *Role of Cleaning-in-Place in the Purification of mAb Supernatants Using Continuous Cation Exchange Chromatography*. Separation Science and Technology, 2009. **44**(1): p. 1-26.
40. Müller-Späth, T., et al., *Two Step Capture and Purification of IgG(2) Using Multicolumn Countercurrent Solvent Gradient Purification (MCSGP)*. Biotechnology and Bioengineering, 2010. **107**(6): p. 974-984.
41. Glynn, J., et al., *Advances in Monoclonal Antibody Purification*. Biopharm International, 2010: p. 4-+.
42. Miyabe, K. and G. Guiochon, *Determination of the lumped mass transfer rate coefficient by frontal analysis*. Journal of Chromatography A, 2000. **890**(2): p. 211-223.
43. Beck, A., et al., *Strategies and challenges for the next generation of therapeutic antibodies*. Nature Reviews Immunology, 2010. **10**(5): p. 345-352.
44. Birch, J.R. and A.J. Racher, *Antibody production*. Advanced Drug Delivery Reviews, 2006. **58**(5-6): p. 671-685.
45. Roque, A.C.A., C.R. Lowe, and M.A. Taipa, *Antibodies and genetically engineered related molecules: Production and purification*. Biotechnology Progress, 2004. **20**(3): p. 639-654.
46. Shukla, A.A. and J. Thommes, *Recent advances in large-scale production of monoclonal antibodies and related proteins*. Trends in Biotechnology, 2010. **28**(5): p. 253-261.
47. Francotte, E.R. and P. Richert, *Applications of simulated moving-bed chromatography to the separation of the enantiomers of chiral drugs*. Journal of Chromatography A, 1997. **769**(1): p. 101-107.
48. Grill, C.A., L. Miller, and T.Q. Yan, *Resolution of a racemic pharmaceutical intermediate - A comparison of preparative HPLC, steady state recycling, and simulated moving bed*. Journal of Chromatography A, 2004. **1026**(1-2): p. 101-108.
49. Ströhlein, G., et al., *A continuous, counter-current multi-column chromatographic process incorporating modifier gradients for ternary separations*. Journal of Chromatography A, 2006. **1126**(1-2): p. 338-346.
50. Aumann, L. and M. Morbidelli, *METHOD AND DEVICE FOR CHROMATOGRAPHIC PURIFICATION*, E.T.H. ZÜRICH, Editor 2006.
51. Müller-Späth, T., et al., *Increasing the Activity of Monoclonal Antibody Therapeutics by Continuous Chromatography (MCSGP)*. Biotechnology and Bioengineering, 2010. **107**(4): p. 652-662.
52. Krättli, M., et al., *Closed loop control of the multi-column solvent gradient purification process*. Journal of Chromatography A, 2011. **1218**(50): p. 9028-9036.
53. Grossmann, C., et al., *Optimizing model predictive control of the chromatographic multi-column solvent gradient purification (MCSGP) process*. Journal of Process Control, 2010. **20**(5): p. 618-629.
54. Aumann, L., et al., *Empirical design of continuous chromatography (MCSGP process)*. Abstracts of Papers of the American Chemical Society, 2011. **241**.
55. Burnouf, T., *Modern plasma fractionation*. Transfusion Medicine Reviews, 2007. **21**(2): p. 101-117.
56. Aumann, L., et al., *Protein Peptide Purification using the Multicolumn Countercurrent Solvent Gradient Purification (MCSGP) Process*. Biopharm International, 2009. **22**(1): p. 46-+.
57. Engell, S., *Feedback control for optimal process operation*. Journal of Process Control, 2007. **17**(3): p. 203-219.
58. Erdem, G., et al., *Optimizing control of an experimental simulated moving bed unit*. Aiche Journal, 2006. **52**(4): p. 1481-1494.

59. Kloppenburg, E. and E.D. Gilles, *Automatic control of the simulated moving bed process for C-8 aromatics separation using asymptotically exact input/output-linearization*. Journal of Process Control, 1999. **9**(1): p. 41-50.
60. Song, I.H., et al., *Experimental implementation of identification-based optimizing control of a simulated moving bed process*. Journal of Chromatography A, 2006. **1113**(1-2): p. 60-73.
61. Song, I.H., et al., *Optimization-based predictive control of a simulated moving bed process using an identified model*. Chemical Engineering Science, 2006. **61**(18): p. 6165-6179.
62. Song, I.H., et al., *Identification and predictive control of a simulated moving bed process: Purity control*. Chemical Engineering Science, 2006. **61**(6): p. 1973-1986.
63. Schramm, H., S. Gruner, and A. Kienle, *Optimal operation of simulated moving bed chromatographic processes by means of simple feedback control*. Journal of Chromatography A, 2003. **1006**(1-2): p. 3-13.
64. Klatt, K.U., F. Hanisch, and G. Dunnebie, *Model-based control of a simulated moving bed chromatographic process for the separation of fructose and glucose*. Journal of Process Control, 2002. **12**(2): p. 203-219.
65. Alamir, M., F. Ibrahim, and J.P. Corriou, *A flexible nonlinear model predictive control scheme for quality/performance handling in nonlinear SMB chromatography*. Journal of Process Control, 2006. **16**(4): p. 333-344.
66. Grossmann, C., et al., *'Cycle to cycle' optimizing control of simulated moving beds*. Aiche Journal, 2008. **54**(1): p. 194-208.
67. Amanullah, M., et al., *Experimental implementation of automatic 'cycle to cycle' control of a chiral simulated moving bed separation*. Journal of Chromatography A, 2007. **1165**(1-2): p. 100-108.
68. Langel, C., et al., *Implementation of an automated on-line high-performance liquid chromatography monitoring system for 'cycle to cycle' control of simulated moving beds*. Journal of Chromatography A, 2009. **1216**(50): p. 8806-8815.
69. Low, D., R. O'Leary, and N.S. Pujar, *Future of antibody purification*. Journal of Chromatography B-Analytical Technologies in the Biomedical and Life Sciences, 2007. **848**(1): p. 48-63.
70. Wang, C., et al., *Neural network-based identification of SMB chromatographic processes*. Control Engineering Practice, 2003. **11**(8): p. 949-959.
71. Dunnebie, G., et al., *Modeling of Simulated Moving Bed chromatographic processes with regard to process control design*. Computers & Chemical Engineering, 1998. **22**: p. S855-S858.
72. Abel, S., et al., *Optimizing control of simulated moving beds - linear isotherm*. Journal of Chromatography A, 2004. **1033**(2): p. 229-239.
73. Erdem, G., et al., *Automatic control of simulated moving beds*. Industrial & Engineering Chemistry Research, 2004. **43**(2): p. 405-421.
74. Erdem, G., et al., *Automatic control of simulated moving beds II: Nonlinear isotherm*. Industrial & Engineering Chemistry Research, 2004. **43**(14): p. 3895-3907.
75. Toumi, A. and S. Engell, *Optimization-based control of a reactive simulated moving bed process for glucose isomerization*. Chemical Engineering Science, 2004. **59**(18): p. 3777-3792.
76. Abel, S., et al., *Optimizing control of simulated moving beds - experimental implementation*. Journal of Chromatography A, 2005. **1092**(1): p. 2-16.
77. Erdem, G., et al., *Automatic control of simulated moving beds - Experimental verification*. Adsorption-Journal of the International Adsorption Society, 2005. **11**: p. 573-577.

78. Grossmann, C., et al., *Optimizing control of simulated moving bed separations of mixtures subject to the generalized Langmuir isotherm*. Adsorption-Journal of the International Adsorption Society, 2008. **14**(2-3): p. 423-432.
79. Grossmann, C., et al., *Experimental implementation of automatic 'cycle to cycle' control to a nonlinear chiral simulated moving bed separation*. Journal of Chromatography A, 2010. **1217**(13): p. 2013-2021.
80. Langel, C., et al., *Experimental Optimizing Control of the Simulated Moving Bed Separation of Troger's Base Enantiomers*. Industrial & Engineering Chemistry Research, 2010. **49**(23): p. 11996-12003.
81. Franklin, G.F., J.D. Powell, and A. Emami-Naeini, *Feedback control of dynamic systems*. 6th ed. 2010, Upper Saddle River, NJ: Pearson Prentice Hall. 837 S.
82. Müller-Späth, T., et al., *Model simulation and experimental verification of a cation-exchange IgG capture step in batch and continuous chromatography*. Journal of Chromatography A, 2011. **1218**(31): p. 5195-5204.
83. Gupta, C.K. and N. Krishnamurthy, *Extractive Metallurgy of Rare-Earths*. International Materials Reviews, 1992. **37**(5): p. 197-248.
84. Maestro, P. and D. Huguenin, *Industrial Applications of Rare-Earths - Which Way for the End of the Century*. Journal of Alloys and Compounds, 1995. **225**(1-2): p. 520-528.
85. Hurst, C., *China's Rare Earth Elements Industry: What can the West learn*, 2010, Institute for the Analysis of Global Security (IAGS).
86. Gschneidner, K.A. and American Chemical Society Meeting, *Industrial applications of rare earth elements symposium at the second Chemical congress of the North American continent (180th ACS National meeting)*, Las Vegas, Nev., August 25-26, 1980. 1981, Washington, D.C.: American Chemical Society. XI, 297 p.
87. Isshiki, M., *Purification of rare earth metals*. Vacuum, 1996. **47**(6-8): p. 885-887.
88. Gschneidner, K.A., *Handbook on the physics and chemistry of rare earths*. Vol. 39. 2009, Amsterdam: Elsevier. 388 p.
89. Zhu, G.C., R. Chi, and Y.H. Xu, *Separation and recovery of RE and Mn from MN rare earth mud in China*. International Journal of Mineral Processing, 2000. **59**(2): p. 163-174.
90. Nishihama, S., T. Hirai, and I. Komazawa, *Review of advanced liquid-liquid extraction systems for the separation of metal ions by a combination of conversion of the metal species with chemical reaction*. Industrial & Engineering Chemistry Research, 2001. **40**(14): p. 3085-3091.
91. Abreu, R.D. and C.A. Morais, *Purification of rare earth elements from monazite sulphuric acid leach liquor and the production of high-purity ceric oxide*. Minerals Engineering, 2010. **23**(6): p. 536-540.
92. Tian, J., et al., *Extraction of rare earths from the leach liquor of the weathered crust elution-deposited rare earth ore with non-precipitation*. International Journal of Mineral Processing, 2011. **98**(3-4): p. 125-131.
93. Kumar, M., *Recent Trends in Chromatographic Procedures for Separation and Determination of Rare-Earth Elements - a Review*. Analyst, 1994. **119**(9): p. 2013-2024.
94. Ojala, F., et al., *Modelling and optimisation of preparative chromatographic purification of europium*. Journal of Chromatography A, 2012. **1220**: p. 21-25.
95. Rao, T.P. and V.M. Biju, *Trace determination of lanthanides in metallurgical, environmental, and geological samples*. Critical Reviews in Analytical Chemistry, 2000. **30**(2-3): p. 179-220.
96. Santoyo, E. and S.P. Verma, *Determination of lanthanides in synthetic standards by reversed phase high-performance liquid chromatography with the aid of a*

- weighted least-squares regression model - Estimation of method sensitivities and detection limits.* Journal of Chromatography A, 2003. **997**(1-2): p. 171-182.
97. Robards, K., S. Clarke, and E. Patsalides, *Advances in the Analytical Chromatography of the Lanthanides - a Review.* Analyst, 1988. **113**(12): p. 1757-1779.
 98. Nesterenko, P.N. and P. Jones, *Isocratic separation of lanthanides and yttrium by high-performance chelation ion chromatography on iminodiacetic acid bonded to silica.* Journal of Chromatography A, 1998. **804**(1-2): p. 223-231.
 99. Deepika, P., et al., *Separation of lanthanides and actinides on a bistriazinyl pyridine coated reverse phase column.* Radiochimica Acta, 2011. **99**(6): p. 325-334.
 100. Weuster, W. and H. Specker, *Preparative Separation of Lanthanoids by High-Pressure Liquid-Chromatography (Hplc).* Angewandte Chemie-International Edition in English, 1981. **20**(1): p. 132-133.
 101. Post, K. and H. Specker, *Separation of Lanthanides by Column Chromatography at Low-Pressure.* Fresenius Zeitschrift Fur Analytische Chemie, 1981. **306**(2-3): p. 97-99.
 102. Ströhlein, G., et al., *The multicolumn countercurrent solvent gradient purification process.* Biopharm International, 2007: p. 42-48.
 103. Choppin, G.R. and R.J. Silva, *Separation of the Lanthanides by Ion Exchange with Alpha-Hydroxy Isobutyric Acid.* Journal of Inorganic & Nuclear Chemistry, 1956. **3**(2): p. 153-154.
 104. Spedding, F.H. and A.F. Voigt, *Rare Earth Separation by Adsorption and Desorption*, U.S.A.E. Commission, Editor 1951.